

A circulation-based performance atlas of the CMIP5 and 6 models for regional climate studies in the northern hemisphere

Swen Brands^{1,2}

¹MeteoGalicia, Consellería de Medio Ambiente, Territorio y Vivienda - Xunta de Galicia, Santiago de Compostela, Spain

²Tragsatec, Santiago de Compostela, Spain

Correspondence: Swen Brands (swen.brands@gmail.com)

Abstract. Global Climate Models are a keystone of modern climate research. In ~~many-most~~ applications relevant for decision making, ~~and particularly when deriving future projections with the delta-change method,~~ they are assumed to ~~be perfect~~ provide a plausible range of possible future climate states. However, these models have not been originally developed to reproduce the regional-scale climate, which is where information is needed in practice. To overcome this dilemma, two general efforts have

5 been made since their introduction in the late 1960ies. First, the models themselves have been steadily improved in terms of physical and chemical processes, parametrization schemes, resolution and complexity, giving rise to the term “Earth System Model”. Second, the global models’ output has been refined at the regional scale using Limited Area Models or statistical methods in what is known as dynamical or statistical *downscaling*. ~~Both For both~~ approaches, however, ~~are in principle unable~~ it is difficult to correct errors resulting from a wrong representation of the large-scale circulation in the global model. ~~Also,~~

10 ~~dynamical downscaling~~ Dynamical downscaling also has a high computational demand and thus cannot be applied to all available global models in practice. On this background, there is an ongoing debate in the downscaling community on whether to thrive away from the “model democracy” paradigm towards a careful selection strategy based on the global models’ capacity to reproduce key aspects of the observed climate. The present study attempts to be useful for such a selection by providing a performance assessment of the historical global model experiments from CMIP5 and 6 based on recurring regional atmospheric

15 circulation patterns ~~(?)~~ (??). The latest model generation (CMIP6) is found to perform better on average, which can be partly explained by a moderately strong statistical relationship between performance and *horizontal* resolution in the atmosphere. A few models rank favourably over almost the *entire* northern hemisphere extratropics, ~~but the better models tend to be less complex than others. Model selection should therefore not solely rely on model performance but also on model complexity and a discussion is needed on how to combine these two criteria.~~ Internal model variability only has a small influence on the

20 model ranks. Reanalysis uncertainty is an issue in Greenland and the surrounding seas, the southwestern United States and the Gobi desert, but is otherwise ~~negligible.~~ generally negligible. Finally, a relatively simple approach based on the number of climate system components taken into account by the GCMs is proposed as a starting point to introduce model complexity as an additional model selection criterion.

1 Introduction

25 *General Circulation Models* (GCMs) are numerical models capable to simulate the temporal evolution of the global atmosphere or ocean. This is done by integrating the equations describing the conservation laws of physics along time as a function of varying forcing agents, starting with some initial conditions (?). If run in standalone mode, an Atmospheric General Circulation Model (AGCM) is coupled with an indispensable land-surface model (LSM) only, whilst the remaining components of the extended climate system (also called “realms” in the nomenclature of the Earth System Grid Federation), including ocean, 30 sea-ice and vegetation dynamics (depending on the model also atmospheric chemistry, aerosols, ocean biogeochemistry and ~~even~~ ice-sheet dynamics) are read-in from static datasets instead of being simulated online (???). In these “atmosphere-only” experiments, the number of coupled realms is kept at a minimum in order to either isolate the sole atmospheric response to temporal variations in the aforementioned other components (???) or to put all available computational resources into the proper simulation of the atmosphere, e.g. by augmenting the spatial and temporal resolution (?). This kind of experiment is 35 traditionally hosted by the Atmospheric Model Intercomparison Project (AMIP) (?).

In a *Global Climate Model*, interactions and feedbacks between the aforementioned realms are explicitly taken into account by coupling the AGCM and LSM with other component models. In the “ocean-atmosphere” configuration (AOGCM, for Atmosphere-Ocean General Circulation Model), the AGCM plus LSM are coupled with an ocean general circulation model (OGCM) and a sea-ice model. Further model components representing the effects of vegetation, atmospheric chemistry, 40 aerosols, ocean biogeochemistry and ~~even~~ ice-sheet dynamics are then optionally included with the final aim to reach a representation of the climate system as comprehensive as possible with the current level of knowledge and available computational resources. ~~In this context, a model capable to resolve both the terrestrial and oceanic processes affecting the global carbon cycle is commonly referred to as “Earth System Model” (ESM) (?). Hence, while an AOGCM is already complex, an ESM is even more so and thus more prone to~~ However, due to their complexity, coupled climate models are prone to many error 45 sources and model uncertainties, making it difficult to directly compare the simulated climate with the observed one (??).

Since ~~these coupled~~ model experiments are the best known approximation to the real climate system, they constitute the starting point of most climate change impact-, attribution- and mitigation studies. For use in impact studies, the coarse-resolution GCM output is usually downscaled with statistical or numerical models (????) or a combination thereof (?), in order to provide information on the regional to local scale where it can then be used for decision making.

50 Now while downscaling methods are able to imprint the effects of the local climate factors on the coarse resolution GCM, ~~they do not correct~~ the correction of errors inherited from a wrong representation of the large-scale atmospheric circulation (?). ~~Hence, the only~~ is challenging (?). A physically consistent way to circumvent this “circulation error” is choosing a GCM (or group of GCMs) capable to realistically simulate the climatological statistics of the regional-scale circulation. This is why careful GCM selection for long has been the subject of any careful downscaling approach applied in a climate change 55 context (???). However, due to the availability of many GCMs from many different groups, this idea has been partly replaced by the “model democracy” paradigm discussed e.g. in ?, where as many GCMs as possible are applied irrespective of their performance in present-day conditions (?). In the recent past, the importance of careful model selection has been re-emphasized

in the context of bias correction, which can be considered a special case of statistical downscaling (?). It should be also remembered that GCMs by definition were not developed to realistically represent regional-scale climate features (??) and that they have been pressed into this role during the last 3 decades due to the ever increasing demand for climate information on this scale. Hence, finding a GCM capable to reproduce the regional atmospheric circulation in a systematic way, i.e. in many regions of the world, would be anything but expected.

In the present study, a total of ~~116-128~~ historical runs from ~~46-56~~ distinct GCMs (or GCM versions) of the fifth and sixth phase of the Coupled Model Intercomparison Project (CMIP5 and 6) are evaluated in terms of their capability to represent the present-day climatology of the regional atmospheric circulation as represented by the frequency of the 27 circulation types proposed by ?. Based on the proposal in ? that this scheme can in principle be applied within a latitudinal band from 30°N to 70°N, it is here used with a sliding coordinate system (?) running along the grid-boxes of a 2.5° latitude-longitude grid covering the entire Northern Hemisphere mid-latitudes.

In Section 2 and 3, the applied data, methods and software are described. In Section 4, the results of an *overall* model performance analysis including all 27 circulation types are presented. First, ~~the three aforementioned those~~ regions are identified where reanalysis uncertainty might compromise the results of any GCM performance assessment based on a single reanalysis. Then, an atlas of *overall* model performance is provided for each participating model (Sections 4.1 to ~~??~~4.8). The present article file focusses on the evaluation w.r.t. ERA-Interim, complemented by pointing out deviations from the evaluation w.r.t. JRA-55 in the 3 relevant regions in the running text. The *full* atlas of the evaluation against JRA-55 is provided in the supplementary material to this study (see “figs-refjra55” folder therein). In Section 4.9, the atlas is summarized, associations between the models’ performance and their resolution in the atmosphere an ocean are drawn, and the role of *internal* model variability ~~assessed with 70~~ is assessed with 72 additional historical runs from a subgroup of ~~12-13~~ models. Finally, the results of a *specific* model performance evaluation for each circulation type are provided in Section 5, followed by a discussion of the main results and some concluding remarks in Section 6. For the sake of simplicity, the model performance atlas is grouped by the geographical location of the coupled models’ ~~coordinating~~ coordinating institutions, having in mind that most model developments are actually international or even transcontinental collaborating efforts.

2 Applied Data and Usage

The study resides on *6-hourly instantaneous* sea-level pressure (SLP) model data retrieved from the Earth System Grid Federation (ESGF) data portals (e.g. <https://esgf-data.dkrz.de/projects/esgf-dkrz/>), whose Digital Object Identifiers (DOIs) can be obtained following the references in Table 1. These model runs are evaluated against reanalysis data from ECMWF ERA-Interim (?) (<https://apps.ecmwf.int/datasets/data/interim-full-daily/levtype=sfc/>) and Japan Meteorological Agency (JMA) JRA-55 (?) (<https://rda.ucar.edu/datasets/ds628.0/>, DOI:10.5065/D6HH6H41). In a first step, and in order to compare as many distinct models as possible, a single historical run was downloaded for each model for which the aforementioned data were available for the 1979-2005 period. If several historical integrations for a given model version were available, then the first member was chosen. In Section 4.9, it will be shown that the selection of alternative members from a given ensemble does *not* lead to

substantial changes in the results. Out of the ~~25-31~~ models used in CMIP6, ~~20-26~~ were run with the “f1”, four with the “f2” and one with the “f3” forcing datasets (?) (see Table 1). Not only version *pairs* from CMIP5 to CMIP6 are considered, but also model versions either not having a predecessor in CMIP5 or a successor in CMIP6. In the most favourable case, two versions of a given model are available for both CMIP5 and 6: A higher-resolution ~~configuration-setup~~ considering fewer realms (the
95 AOGCM configuration), complemented by a ~~lower-resolution-more complex~~ setup including more ~~realms, ideally reaching the status of an ESM.~~

~~component models, usually run with a lower resolution than the AOGCM version.~~

An overview of the ~~46-56~~ applied model versions is provide in Table 1. The table provides information about the component AGCMs and OGCMs, their horizontal and vertical resolution, ~~details about the considered runs and the reference publications.~~
100 ~~The models’ degree of complexity, here defined by the number of considered realms, is also indicated. “AOGCM” refers to the basic coupling configuration covering atmosphere, land-surface, ocean and sea-ice dynamics only. As a trade-off between a fully comprehensive ESM, as described e.g. in ? for the case of MRI-ESM, and the considerations of other model developers, a model is here declared an ESM if both the terrestrial and oceanic biogeochemical processes relevant for the carbon cycle are calculated online instead of being read-in from external files, which is in line with the proposal made in ?. Assignment to either~~
105 ~~of the two groups was made on the basis of the reference articles and the metadata provided the model output files. The “source” attribute present in these files contains the specifications of the individual model components. This attribute was extracted for each model and permanently stored at . Since many models are ahead of the basic AOGCM configuration but yet cannot be considered ESMs because terrestrial and/or ocean biogeochemistry processes are missing, these additional components are added to the base category “AOGCM” (plus either “tbge” or “obge”, respectively). Likewise, if a given model is more complex~~
110 ~~than the basic ESM configuration because atmospheric (photo)chemistry, aerosols and/or ice sheet dynamics are also taken into account, this is also indicated (ESM plus “chem”, “aero” and/or “icesheet”, respectively). Note that a model’s complexity is not solely defined by the number of considered realms but also the by the variety of coupled processes. For these coupling details, the interested reader is referred to the reference articles listed in Table 1~~ run specifications and complexity estimates as described in Section 3.3.

115 For ~~12-13~~ selected models (ACCESS-ESM1, CNRM-CM6-1, HadGEM2-ES, EC-Earth3, IPSI-CM5A-LR, IPSL-CM6A-LR, MIROC-ES2L, MPI-ESM1-2-LR, MPI-ESM1-2-HR, MRI-ESM2, NorESM2-LM, NorESM2-MM, NESM3), a total of ~~70-72~~ additional historical integrations (between 1 and 17 additional runs per model) were retrieved from the respective ensembles in order to assess the effects of internal model variability. By definition of the experimental protocol followed in CMIP, ensemble spread relies on initialization from distinct starting dates of the corresponding pre-industrial control runs (~~or~~ or similar,
120 shorter runs as e.g. indicated in ?) —, i.e. on “initial conditions uncertainty” (?).

3 Methods

3.1 Lamb Weather Types

The classification scheme used here is based on H.H. Lamb's practical experience when grouping daily instantaneous SLP maps for the British Isles and interpreting their relationships with the regional weather (?). His subjective classification scheme contained 27 classes and was brought to an automated and objective approach by ? in what is known as the "Lamb Circulation Types" or "Lamb Weather Types" (LWTs) approach (??).

The spatial extension of the 16-point coordinate system defining this classification is 30 longitudes \times 20 latitudes with longitudinal and latitudinal increments of 10° and 5°, respectively (see Figure 1 for an example over the Iberian Peninsula). The following numbers are place-holders of instantaneous SLP values (in hPa) at the corresponding location p (from West to East and North to South):

p01 p02

p03 p04 p05 p06

p07 p08 p09 p10

p11 p12 p13 p14

p15 p16

, and the variables needed for classification are defined as follows:

$$\text{Westerly flow } (W) = \frac{1}{2}(p_{12} + p_{13}) - \frac{1}{2}(p_{04} + p_{05}) \quad (1)$$

$$\text{Southerly flow } (S) = a \left[\frac{1}{4}(p_{05} + 2 \times p_{09} + p_{13}) - \frac{1}{4}(p_{04} + 2 \times p_{08} + p_{12}) \right] \quad (2)$$

$$\text{Resulting flow } (F) = (S^2 + W^2)^{1/2} \quad (3)$$

$$\begin{aligned} \text{Westerly shear vorticity } (ZW) = & b \left[\frac{1}{2}(p_{15} + p_{16}) - \frac{1}{2}(p_{08} + p_{09}) \right] \\ & - c \left[\frac{1}{2}(p_{08} + p_{09}) - \frac{1}{2}(p_{01} + p_{02}) \right] \end{aligned} \quad (4)$$

$$\begin{aligned}
\text{Southerly shear vorticity } (ZS) = d \left[\frac{1}{4}(p06 + 2 \times p10 + p14) \right. \\
\left. - \frac{1}{4}(p05 + 2 \times p09 + p13) \right. \\
\left. - \frac{1}{4}(p04 + 2 \times p08 + p12) \right. \\
\left. + \frac{1}{2}(p03 + 2 \times p07 + p11) \right]
\end{aligned}
\tag{5}$$

145 where $a = 1/\cos(\phi)$, $b = \sin(\phi)/\sin(\phi - \delta\phi)$, $c = \sin(\phi)/\sin(\phi + \delta\phi)$ and $d = 0.5(\cos(\phi)^2)$; ϕ is the central latitude and $\delta\phi$ is the latitudinal distance.

The 27 classes are then defined following ? and ?:

1. The direction of flow is $\tan^{-1}(W/S)$. Add 180° if W is positive. The appropriate direction is calculated on an eight-point compass allowing 45° per sector. Thus, as an example, a westerly flow would occur between 247.5° and 292.5° .
- 150 2. If $|Z|$ is less than F , then the flow is essentially straight and corresponds to one of the 8 purely directional types defined by Lamb: Northeast (NE), East (E), SE, S, SW, W, NW, N.
3. If $|Z|$ is greater than $2F$, then the pattern is either strongly cyclonic (for $Z > 0$) or anticyclonic (for $Z < 0$), which corresponds to Lamb's pure cyclonic (PC) or anticyclonic type (PA), respectively.
4. If $|Z|$ lies between F and $2F$, then the flow is partly directional and either cyclonic or anticyclonic, corresponding
155 to Lamb's *hybrid* types. There are 8 directional-*anticyclonic* types (Anticyclonic Northeast (ANE), Anticyclonic East (AE), ASE, AS, ASW, AW, ANW, AN) and another 8 directional-*cyclonic* types (Cyclonic Northeast (CNE), Cyclonic East (CE), CSE, CS, CSW, CW, CWN, CN).
5. If F is less than 6 and $|Z|$ is less than 6, there is light indeterminate flow corresponding to Lamb's unclassified type U . The choice of 6 is dependent on the grid spacing and would need tuning if used with a finer grid resolution.

160 An illustrative example for the results obtained from this scheme is provided in Figure 1 for the case of the central Iberian Peninsula. Shown is the coordinate system and the composite SLP maps for a subset of 14 LWTs, as well as the respective relative occurrence frequencies, taken from ? (courtesy to John Wiley and Sons, Inc.).

Particularly since the ~~1990s~~1990ies, this classification scheme has been used in many other regions of the NH mid-latitudes (????). Since the LWTs are closely related to the local-scale variability of virtually all meteorological- and many other envi-
165 ronmental variables (??), they constitute an *overarching* concept to verify GCM performance in present climate conditions and have been used so in a number of studies (??).

Here, for each model run and the ERA-Interim or JRA-55 reanalysis, the 6-hourly instantaneous SLP data from 01/01/1979 to 31/12/2005 are bi-linearly interpolated to a regular latitude-longitude grid with a resolution of 2.5° . Then, the Lamb classification scheme is applied for each time instance and grid-box, using a sliding coordinate system whose centre is displaced from one grid-box to another in a loop recurring all latitudes and longitudes of the aforementioned grid within a band from 35° to 70° N. Note that the geographical domain is cut at 35° N (and not at 30°) because the various available reanalyses are known to produce comparatively large differences in their estimates for the “true” atmosphere when approaching the tropics (??). Also, since some models do not apply the Gregorian calendar but work with 365 or even 360 days per year, *relative* instead of absolute LWT frequencies are considered. Further, since HadGEM2-CC and HadGEM2-ES lack SLP data for December 2005, this month is equally dropped from ERA-Interim or JRA-55 when compared with these models.

As mentioned above, the LWT approach has been successfully applied for many climatic regimes of the NH, including the extremely continental climate of central Asia (?), which confirms the proposal made in ? that the method in principle can be applied in a latitudinal band from 30° to 70° N. Here, a criterion is introduced to explicitly test this assumption. Namely, it is established that ~~LWTs cannot~~ the LWT method should not be used at a given grid-box if the relative frequency for any of the 27 types is lower than 0.1% percent (i.e. ~~15~~1.5 annual occurrences on average). Note that, already in its original formulation for the British Isles, some LWTs were found to occur with relative frequencies as small as 0.47% (?). This is why the 0.1% threshold seems reasonable in the present study. If at a given grid-box this criterion is not met in the LWT catalogue derived from ERA-Interim or alternatively JRA-55, then this grid-box does not participate in the evaluation.

3.2 Applied GCM performance measures

To measure GCM performance, the Mean Absolute Error (MAE) of the $n = 27$ relative LWT frequencies obtained from a given model (m) w.r.t. to those obtained from the reanalysis (o) are calculated at a given grid-box:

$$MAE = \frac{1}{n} \sum_{i=1}^n |m_i - o_i| \quad (6)$$

The MAE is then used to rank the ~~46~~56 distinct models at this grid-box. The lower the MAE, the lower the rank and the better the model. After repeating this method for each grid-box of the NH, both the MAE values and ranks are plotted for each individual model on a polar stereographic projection.

In addition to the MAE measuring *overall* performance, the *specific* model performance for each LWT is also assessed. This is done because, by definition of the MAE, errors occurring in the more frequent LWTs are penalized more than those occurring in the rare LWTs. Hence, a low MAE might mask errors in the least frequent LWTs. For a LWT-specific evaluation, the simulated frequency map for a given LWT and model are compared with the corresponding map from the reanalysis by means of the Taylor Diagram (?). This diagram compares the spatial correspondence of the simulated and observed (or “quasi-observed” since *reanalysis* data are used) frequency patterns by means of 3 complementary statistics. These are the Pearson

correlation coefficient (r), the standard deviation ratio ($ratio = \sigma_m/\sigma_o$), with σ_m and σ_o being the ~~the~~ standard deviation of modelled and observed frequency patterns, and the normalized ~~centred~~ centered root mean-square error (CRMSE):

$$CRMSE = \frac{\sqrt{\frac{1}{n} \sum_{i=1}^n (cm_i - co_i)^2}}{\sigma_o} \quad (7)$$

200 , with $n = 2016$ grid-boxes covering the NH mid-latitudes and cm and co the modelled and observed frequency patterns after subtracting their own mean value (i.e. both the minuend and subtrahend are anomaly fields, “c” refers to centred). Normalization enables for comparison with other studies using the same method.

3.3 Model complexity estimate

205 In addition to the model performance assessment, a simple approach is followed to estimate the complexity of the numerous coupled model configurations considered here. The approach is based on the idea that this complexity is proportional to the number of interactively resolved climate system components. Apart from the atmosphere, land-surface, ocean and sea-ice models making up the minimum configuration of an AOGCM, the following 6 realms are taken into account: 1. Vegetation properties, 2. Terrestrial carbon-cycle processes, 3. Aerosols, 4. Atmospheric Chemistry, 5. Ocean biogeochemistry and 6. Ice sheet dynamics. In this order, an integer is assigned to each component depending on whether it is not taken into account at all (0), interactive in the sense of feeding back on at least one another realm (2), or anything in between (1) including prescription from external files, semi-interactive approaches or components simulated online but without any feedback on other components.

215 As an example, MRI-ESM’s complexity code is 122220, indicating prescribed vegetation properties, interactive representations of the terrestrial carbon-cycle, aerosols, atmospheric chemistry and ocean biogeochemistry, and no representation of ice sheet dynamics. For each model version, an initial “best-guess” complexity code was derived from the respective reference article(s) and “source attributes” within the netCDF files derived from the ESGF data portals. This code was then sent by e-mail to the respective modeling group for confirmation or correction. The sum of the integer code is here taken as an estimator for model complexity. An integer sum ≥ 6 will be referred to as a “more complex” model and a sum < 6 as a “less complex” model, respectively. In the light of various available definitions for the term “Earth System Model” (??), this is a flexible approach used as a starting point for further specifications in the future. The obtained complexity codes are provided in Table 1, column 7. Since the approach might be modified in the future, the interested reader is invited to consult the up-to-date version available at https://github.com/SwenBrands/gcm-metadata-for-cmip/blob/main/get_historical_metadata.py. The Python function hosted there also provides the full names of all component models, including the coupling software, resolution details of the AGCM and OGCM components and other relevant model metadata.

225 Note that a model’s complexity is not solely defined by the number of considered realms but also by the variety of coupled processes, coupling frequency and treatment of the forcing datasets. For further details, the interested reader is referred to the reference articles listed in Table 1. The aforementioned source attributes were extracted from the model output files and permanently stored at <https://doi.org/10.5281/zenodo.4452080>.

3.4 Applied Python packages

230 The coding to the present study relies on the Python v2.7.13 packages *xarray* v0.9.1 written by ? (<https://doi.org/10.5281/zenodo.264282>), *NumPy* v1.11.3 written by ? (<https://github.com/numpy/numpy>), *Pandas* v0.19.2 written by ? (<https://doi.org/10.5281/zenodo.3509134>) and *SciPy* v0.18.11 written by ? (<https://doi.org/10.5281/zenodo.154391>); here used for i/o tasks and statistical analyses. The *Matplotlib* v2.0.0 package written by ? (<https://doi.org/10.5281/zenodo.248351>), as well as the Basemap v1.0.7 toolkit (<https://github.com/matplotlib/basemap>) are applied for plotting and the functions written by ? (<https://doi.org/10.5281/zenodo.3715535>) for generating Taylor diagrams.

4 Overall model performance results

In Figure 2, the MAE of JRA-55 w.r.t. ERA-Interim is mapped (panel a), complemented by the corresponding rank within the multi-model ensemble plus JRA-55 (panel b). In the ideal case, the MAE for JRA-55 is lower than for any of the ~~46-56~~ CMIP models, which means that the alternative reanalysis ranks first and that a change in the reference reanalysis does not influence the model ranking. This result is indeed obtained for a large fraction of the NH. However, in the Gobi desert, in Greenland and the surrounding seas, and particularly in the southwestern United States of America, substantial differences are found between the two reanalyses. Since different reanalyses from roughly the same generation are in principle equally representative of the “truth” (?), the models are here evaluated twice in order to obtain a robust picture of their performance. In the present article file, the evaluation results w.r.t. to ERA-Interim are mapped and deviations from the evaluation against JRA-55 in the 3 relevant regions are pointed out in the text. In the remaining regions, reanalysis uncertainty plays a minor role. Nevertheless, for the sake of completeness, the ~~interested reader can see in the~~ full atlas of the JRA-55-based evaluation ~~in~~ was added to the supplementary material to this study. For a quick overview of the results, Table 1 indicates whether a given model closer agrees with ERA-Interim or JRA-55 in the 3 sensitive regions. In the following, this is referred to as “reanalysis affinity”.

250 Figure 2 also shows that the LWT usage criterion defined in Section 3.1 is met almost everywhere in the domain, except in the high-mountain areas of central Asia (grey areas within the performance maps indicate that the criterion is not met). This region is governed by the monsoon rather than the turnover of dynamic low- and high pressure systems the LWT approach was developed for. It is thus justified to use the approach over such a large domain.

Grouped by their geographical origin, Sections 4.1 to ~~?? describe how the~~ 4.8 describes the composition of the ~~56~~ participating coupled models ~~are composed~~ in terms of their atmosphere, land-surface ~~and ocean models (and others)~~, ocean and sea-ice models in order to make clear whether there are shared components between nominally different models that might explain common error structures. The names of all other component models are documented at https://github.com/SwenBrands/gcm-metadata-for-cmip/blob/main/get_historical_metadata.py. Then, the regional error and ranking details are provided. In Section 4.9, these results are summarized in a single boxplot and put into relation with the resolution setup of the atmosphere and ocean component models. The role of internal model variability is also assessed there.

[A complete list of all participating component models is provided at https://github.com/SwenBrands/gcm-metadata-for-cmip/blob/main/get_historical_metadata.py.](https://github.com/SwenBrands/gcm-metadata-for-cmip/blob/main/get_historical_metadata.py)

The first result common to all models is the spatial structure of the absolute error expressed by the MAE. Namely, the models tend to perform better over ocean areas than over land and perform poorest over high-mountain areas, particularly in central Asia. Further regional details are documented in the following sections.

4.1 Model contributions from the United Kingdom and Australia

All components of the Hadley Centre Global Environment Model version 2 (HadGEM2) have been developed independently by the *Met Office Hadley Centre* during the last decades. Atmospheric, land-surface and ocean dynamics are represented by the HadGAM2, MOSES2 and HadGOM2 models, respectively. Both [the terrestrial model versions comprise interactive vegetation properties, land carbon](#) and ocean carbon ~~eyes are taken into account by the two HadGEM2 versions considered here (CC and ES), which only differ by the inclusion of gas-phase chemistry in the therefore slightly more complete ES version cycle processes and aerosols. The ES version also includes an interactive atmospheric chemistry which, in turn, is prescribed in the CC configuration, making it slightly less complex~~ (?). This centre's model contributions to CMIP6 are following the concept of seamless prediction (?), in which lessons learned from short-term numerical weather forecasting are exploited for the improvement of longer-term predictions/projections up to climatic time-scales, using a "unified" or "joint" model for all purposes (?). For atmosphere and land-surface processes, these are the Unified Model Global Atmosphere 7 (UM-GA7) AGCM and the Joint UK Land Environment Simulator (JULES) (?). However, the specific CMIP6 model version considered here (HadGEM3-GC31-MM) is a very high-resolution AOGCM configuration ~~with the ocean biogeochemistry module turned off (?). Unlike comprising only one further interactive component (aerosols). In comparison with~~ HadGEM2-ES and CC, HadGEM3-GC31-MM is therefore ~~not considered an ESM~~ less complex.

With nearly identical error and ranking patterns associated with the aforementioned almost identical configuration, already the two model versions used in CMIP5 (HadGEM2-CC and ES) yield a good to very good performance which, for the European sector, is in line with ? and ?. Only a close look reveals slightly lower errors for the ES version, particularly in a region extending from western France to the Ural mountains (see Figure 3). Both CMIP5 versions are outperformed by HadGEM3-GC31-MM. While HadGEM2-CC and ES rank very well in Europe and the central North Pacific only, HadGEM3-GC31-MM does so in virtually all regions of the NH mid-latitudes except in central Asia. It is undoubtedly one of the best models considered here. ~~However, unlike its CMIP5 predecessors, it is not an ESM.~~

While CSIRO-MK (~~not assessed here~~ [see supplementary material and Figure 11 below](#)) was an independently developed ~~model~~ GCM of the Australian research community (?), the *Community Climate and Earth System Simulator* (ACCESS) depends to a large degree on the aforementioned models from the Met Office Hadley Centre. ACCESS1.0, the starting point for the new Australian ~~ESM~~ coupled model configurations, makes use of the same atmosphere and land-surface components as HadGEM2 (see above), but is run in ~~AOGCM mode only. As such, it~~ a less complex configuration. It is considered the "control" configuration of all further developments ~~towards the ESM configuration~~ made by the Australian ~~research community~~ modelling group (?). ACCESS1.3 is the first step into this direction. Instead of HadGAM2, it uses a slightly modified version

295 of the Met Office Global Atmosphere 1.0 (GA1) AGCM, coupled with the CABLE1.8 land surface model developed by CSIRO. ACCESS-CM2 is the AOGCM version used in CMIP6, relying on the UM10.6-GA7.1 AGCM (also used in HadGEM3-GC31-MM) ~~coupled with and the~~ CABLE2.5 coupler (?). ACCESS-CM2, however, was run with a lower horizontal resolution in the atmosphere than HadGEM3-GC31-MM. ~~ESM status is finally attained by~~ Whereas the 3 aforementioned ACCESS versions only have interactive aerosols on top of the four AOGCM components, ACCESS-ESM1.5 ~~; at the expense of using somewhat~~ additionally includes interactive land and ocean carbon cycle processes and prescribed vegetation properties. It uses slightly 300 older AGCM and LSM versions (UM7.3-GA1 and CABLE2.4) than ~~in~~ ACCESS-CM2 ~~; probably in order to free computational resources for and makes use of~~ the ocean biogeochemistry model WOMBAT (?). ~~With GFDL-MOM and CICE, all~~ All ACCESS models use the same ocean and sea-ice models (GFDL-MOM and CICE), which differ from those used in the HadGEM model family. The OASIS coupler (?) is ~~again~~ applied by both model families.

305 Within the ACCESS model family, version 1.0 performs best (see Figure 3). The corresponding error and ranking patterns are virtually identical to HadGEM2-ES and HadGEM2-CC, which is due to the same AGCM used in these three models (HadGAM2). The 3 more independent versions of ACCESS (1.3, CM2 and ESM1.5) roughly share the same error pattern, which differs from ACCESS1.0 in some regions. While the 3 independent developments perform worse in the North Atlantic and western North Pacific, they do better in the eastern North Pacific off the coast of Japan and, in case of ACCESS-CM2, 310 also in the high mountain areas of central Asia and ~~the Mediterranean over the~~ Mediterranean Sea. In the latter two regions, the performance of ACCESS-CM2 is comparable to HadGEM3-GC31-MM. Overall, version 1.0 performs best within the ACCESS model family.

The two HadGEM2 versions and also ACCESS1.3 compare better with JRA-55 in the southwestern U.S. but thrive towards ERA-Interim in the seas around Greenland and in the Gobi desert. HadGEM3-GC31-MM, ACCESS1.0, ACCESS-CM2 and 315 ACCESS-ESM1.5 have similar reanalysis affinities, except for thriving towards JRA-55 in the seas around Greenland and for showing virtually no sensitivity in the Gobi desert in case of ~~the~~ ACCESS-ESM1.5 (compare Figure 3 with the “figs-refjra55/maps/rank” folder in the supplementary material).

4.2 Model contributions from North America

~~Figure 4 shows the respective results for the models developed in North America. Each of the four model families are built upon independent and long-standing research lines.~~

 320

~~From model version~~ The Geophysical Fluid Dynamics Laboratory Climate Models 3 and 4 (GFDL-CM3 and CM4) are composed of in-house atmosphere, land-surface, ocean and sea-ice models and comprise interactive vegetation properties, aerosols and atmospheric chemistry (??). GFDL-CM4 also includes simple land and ocean carbon cycle representations which, however, do not feed back on other climate system components. From CM3 to CM4 ~~; the Geophysical Fluid Dynamics~~ 325 ~~Laboratory~~ (GFDL) ~~has updated and considerably increased the resolution of its in-house AGCM and OGCM (??) —except for the number of vertical levels~~ a considerable resolution increase was undertaken, except for a reduction in the AGCM, ~~which was reduced from CM3 to CM4—’s vertical levels~~, and this actually pays off in terms of model performance (see Figure 4). While GFDL-CM3 only ranks well in an area ranging from the Great Plains to the central North Pacific, GFDL-CM4 yields

balanced results over the entire NH and is one of the best models considered here. Notably, GFDL-CM4 also performs well
330 over central Asia and in an area ranging from the Black Sea to the Middle East, which is where most of the other models
perform less favourable. Note also that GFDL's Modular Ocean Model (MOM) is the standard OGCM in all ACCESS models
and is also ~~being used in BCC-CSM2-MR~~ used in the BCC-CSM model versions (see Table 1 for details).

~~The All Goddard Institute of Space Studies model versions used in CMIP5 are AOGCMs including the effects of atmospheric
chemistry and aerosols considered here are AOGCMs with prescribed vegetation properties, aerosols and atmospheric chemistry.~~
335 The two versions are identical except for the ocean component: HYCOM was used in GISS-E2-H and Russel Ocean in GISS-
E2-R (?). Russel Ocean was then developed to GISS Ocean v1 for use in GISS-E2.1-G (?), the CMIP6 model version assessed
here ~~;~~ ~~which however was run without the aforementioned chemistry and aerosol modules~~ (note that the 6-hourly SLP data for
the more complex model versions contributing to CMIP6 were not available from the ESGF data portals). All these versions
comprise a relatively modest resolution for the atmosphere and ocean and no refinement was undertaken from CMIP5 to 6.
340 However, many parametrization schemes were improved. GISS-E2.1-G generally ranks better than its predecessors, except in
eastern Siberia and China, where very good ranks are obtained by the two CMIP5 versions (see Figure 4). The small differ-
ences between the results for GISS-E2-H and R might stem from internal model variability (see also Section 4.9) ~~or indeed~~
~~and~~ from the use of two distinct OGCMs. Unfortunately, all ~~versions of the GISS model~~ GISS-E2 model versions considered
here are plagued by pronounced performance differences from one region to another, meaning that they are less balanced than
345 e.g. GFDL-CM4.

The *National Center for Atmospheric Research* (NCAR) Community Climate System Model 4 (CCSM4) is composed of the
Community Atmosphere and Land Models (CAM and CLM), the Parallel Ocean Program (POP) and the Los Alamos Sea Ice
Model (CICE), combined with the CPL7 coupler (??). The ~~CMIP5 experiment model version~~ considered here was ~~run with a~~
~~classical AOGCM configuration used in CMIP5 and includes interactive vegetation properties and land carbon cycle processes,~~
350 ~~whereas aerosols are prescribed.~~ During the course of the last decade, CCSM4 has been further developed ~~to~~ into CESM1
and 2 (??) which, due to data availability issues, can unfortunately not be assessed here (the respective data for CESM2 are
available, but only for 15 out of the 27 years considered here). However, CMCC-CM2 and NorESM2 are almost entirely made
up by components from CESM1 and 2, respectively, and should thus be also indicative for the performance of the latter (see
~~Sections 4.6 and 4.7). Similar data availability problems apply to CanESM5 (?), the latest ESM generation contributed by the~~
355 ~~Canadian Centre for Climate Modeling and Analysis (CCCma). Hence, only CanESM2 (?) —the Section 4.8).~~

The Canadian Earth System Model version 2 (CanESM2) is composed of the CanAM4 AGCM, the CLASS2.7 land surface
model, the CanOM4 OGCM and the CanSIM1 sea-ice model (?). It contributed to CMIP5 ~~antecessor~~ ~~can be assessed~~
~~here and comprises interactive vegetations properties, land and ocean carbon cycle processes and aerosols, whilst ice sheet area
is prescribed.~~

360 Results indicate a comparatively poor performance for both CCSM4 and CanESM2. Exceptions are found along the North
American west coast and the Labrador Sea, where both models perform well; in the central to eastern subtropical Pacific and
in northwestern Russia plus Finland, where CCSM4 performs well; and in Quebec, Scandinavia and eastern Siberian, where

CanESM2 ranks well (see Figure 4). As for the GISS models, both CCSM4 and CanESM2 are also plagued by large regional performance differences.

365 Regarding the models' reanalysis affinity, GFDL-CM3 thrives towards ERA-Interim in the seas around Greenland and towards JRA-55 in the Gobi desert, while being almost insensitive to reanalysis choice in the southwestern United States (compare Figure 4 with the "figs-refjra55/maps/rank" folder in the supplementary material to this article). GFDL-CM4 has similar reanalysis affinities, but largely improves (by up to 20 ranks) in the southwestern United States when evaluated against JRA-55. Results for GISS-E2-H and GISS-E2-R are slightly closer to ERA-Interim in the southwestern U.S. and otherwise
370 virtually insensitive to reanalysis choice. GISS-E2-1-G is virtually insensitive in all 3 regions. CanESM2 ranks consistently better if compared with JRA-55, with a stunning improvement of up to 30 ranks in the southwestern United States, and CCSM4 slightly thrives towards ERA-Interim in all 3 regions.

4.3 Model contributions from France

The CMIP5 contributions from the *Centre National de Recherches Météorologique (CNRM)* and *Institut Pierre-Simon Laplace (IPSL)* use the same OGCM and coupler, i.e. the Nucleus for European Modelling of the Ocean model (NEMO) (??) and OASIS, but differ in their remaining components. CNRM-CM5 comprises the ARPEGE AGCM, ISBA land-surface model and GELATO sea-ice model (?) whereas IPSL makes use of LMDZ, ORCHIDEE and LIM, respectively (?). For CNRM-CM6-1, these components were updated ~~and an atmospheric chemistry model was implemented in addition (?). Note that aH(?)~~. All CNRM model versions considered here are AOGCMs with prescribed aerosols and atmospheric chemistry, except
380 ~~CNRM-ESM2-1 (?)are AOGCMs (plus interactive atmospheric chemistry in CNRM-CM6-1 and CNRM-CM6-1-HR) whereas all model versions from IPSL are considered ESMs (see Table 1). Consequently, the CNRM models could be generally run with a much finer resolution in the atmosphere and ocean than the more complex IPSL models, which additionally comprises interactive component models for vegetation properties, terrestrial carbon cycle processes, aerosols, stratospheric chemistry and ocean biogeochemistry. Along with HadGEM2-ES, CNRM-ESM2-1 is thus the most complex model configuration considered~~
385 here, following the criteria described in Section 3.3.

Within the CNRM model family, CNRM-CM5 is found to perform very well except in the central North Pacific, the southern USA and in a subpolar belt extending from Baffinland in the West to western Russia in the East (see Figure 5). This includes a good performance over the Rocky Mountains and central Asia. From CNRM-CM5 to CNRM-CM6-1, performance gains are obtained in the central North Pacific, the southern USA, Scandinavia and western Russia which, however, are compensated
390 by performance losses in the entire eastern North Atlantic and in an area covering Manchuria, Korea and Japan. A similar picture is obtained for CNRM-ESM2-1, whereas a performance *loss* is observed for for CNRM-CM6-1-HR. This is surprising since, in addition to improved parametrization schemes, the model resolution in the atmosphere and ocean was particularly increased in the latter model version. Under these circumstances, CNRM-CM6-1-HR is actually the only model suffering clear performance *losses* from CMIP5 to 6. The reasons for this are unknown and should be assessed in future studies.

395 ~~While missing in all CNRM model versions except CNRM-ESM2-1, the ocean carbon cycle was an integral part of the IPSL model already~~ All IPSL-CM model versions participating in CMIP5 and 6 comprise interactive vegetation properties and

terrestrial carbon cycle processes, as well as prescribed aerosols and atmospheric chemistry. Ocean biogeochemistry processes are simulated online, but do not feed-back on other components of the climate system. A simple representation of ice sheet dynamics was included to IPSL-CM6A-LR (??), but is absent in IPSL-CM5A-LR and MR (?). The two model versions used in CMIP5 (?) and the associated computational costs likely might have forced this group to run their model versions have been run with a modest horizontal resolution in the atmosphere (LMDZ) and ocean (NEMO). This changed for the better with in IPSL-CM6A-LR, where a more competitive resolution was applied and all component models were improved(??). The result is a considerable performance increase from CMIP5 to CMIP6. Whereas both IPSL-CM5A-LR and IPSL-CM5A-MR perform poorly, IPSL-CM6A-LR does much better virtually anywhere in the NH, a results that is virtually finding that is insensitive to the effects of internal model variability arising from initial conditions uncertainty (see Section 4.9).

The quite different results between the CNRM and IPSL models indicate that the common ocean component (NEMO) only marginally affects the simulated atmospheric circulation as defined here. All CNRM models, and also IPSL-CM6A-LR, thrive towards Interim in the southwestern U.S. and towards JRA-55 in the seas around Greenland and the Gobi desert. IPSL-CM5A-LR and MR are virtually insensitive to reanalysis choice (compare Figure 5 with the “figs-refjra55/maps/rank” folder in the supplementary material).

4.4 Model contributions from China, Taiwan and JapanIndia

The Beijing Climate Center Climate System Model (BCC-CSM version 1.1 (BCC-CSM1.1) comprises the BCC-AGCM3 BCC-AGCM2.1 AOGCM, originating from CAM3 and developed independently thereafter (?), the completely independent BCC-AVIM1.0 land-surface model BCC-AVIM developed by the Chinese Academy of Science (?) and GFDL’s MOM and MOM4-L40 ocean model and GFDL’s Sea Ice Simulator (SIS). For BCC-CSM2-MR, the standard coupled model version used in CMIP6 (?), the latest updates of the in-house models are used in conjunction with the CMIP5 versions of MOM and SIS (v4 and 2 respectively). The two model versions are composed of interactive vegetation properties, terrestrial and oceanic carbon cycle processes, while aerosols and atmospheric chemistry are prescribed. The MAE and ranking patterns of BCC-CSM1.1 and BCC-CSM2-MR are quite similar to those obtained from NCAR’s CCSM2 (compare Figure 6 and 34), which is likely due to the common origin of their AGCMs, meaning that BCC-CSM2-MR is the two BCC-CSM versions are likewise found to perform comparatively poor in most regions of the NH. The similarity between both model families is astonishing since they only share the origin of their atmospheric component but rely on different land-surface, ocean and sea-ice models. This in turn means that the latter two components do not noticeably affect the simulated atmospheric circulation as defined here, which is in line with the large differences found for the French models in spite of using the same ocean model (see Section 4.3).

The Flexible Global Ocean-Atmosphere-Land System Model, Grid-point version 2 (FGOALS-g2) comprises an independently developed AGCM and OGCM (GAMIL2 and LICOM2), as well as CLM3 and CICE4-LASG for the land surface and sea-ice dynamics, respectively (?), all components being coupled with CPL6. Vegetation properties and aerosols are prescribed in this model configuration. For FGOALS-g3, the model version contributing to CMIP6, the AGCM was updated to GAMIL3, including convective momentum transport, stratocumulus clouds, anthropogenic aerosol effects and an improved boundary layer scheme as new features (?). The OGCM and coupler were also updated (to LICOM3 and CPL7) and a modified version

of CLM4.5 (called CAS-LSM) is used as land surface model, whereas the sea-ice model is practically identical to that used in the g2 version. In the g3 version, vegetation properties, terrestrial carbon cycle processes and aerosols are prescribed. While FGOALS-g2 is one of the worst performing models considered here, FGOALS-g3 performs considerably better, particularly over the northwestern and central North Atlantic Ocean, western North America and the North Pacific Ocean (see Figure 6).

435 The Nanjing University of Information Science and Technology Earth System Model version 3 (NESM3) is a new CMIP participant and is entirely built upon component models from other institutions (?). Namely, the AGCM, land-surface model, coupling software and even the atmospheric resolution are adopted from MPI-ESM1.2-LR (see Section 4.6) whereas NEMO3.4 and CICE4.1 are taken from IPSL and NCAR respectively (?). As a resultsVegetation properties and terrestrial carbon cycle processes are interactive, aerosols are prescribed. Due to the use of the same AGCM, the error and ranking patterns for NESM3
440 are similar to those obtained for MPI-ESM1.2-LR (compare Figure 6 with Figure 78). Exceptions are found over the central and western North Pacific, where NESM3 performs poorer than MPI-ESM1.2-LR, and also over the eastern North Pacific, where NESM3 performs better. The similarity to MPI-ESM1.2-LR again points to the fact that ~~LWT frequency is the simulated LWT frequencies are~~ determined by the AGCM rather than other component models.

The Taiwan Earth System Model version 1 (TaiESM1) is run by the Research Center for Environmental Changes, Academia Sinica in Taipei. It is essentially identical to NCAR's Community Earth System Model version 1.2.2, including new physical and chemical parametrization schemes in its atmospheric component CAM5 (?). TaiESM1 comprises interactive vegetation properties, terrestrial carbon cycle processes and aerosols. The model's performance is generally very good, except over northern Russia, northeastern North America and the adjacent northwestern Atlantic Ocean, and the error and ranking patterns are roughly similar to SAM0-UNICAN (see Figure 6), another CESM1 derivative, with TaiESM1 performing much better over
445 Europe.

The Indian Institute of Tropical Meteorology Earth System Model (IITM-ESM) includes the National Centers of Environmental Prediction Global Forecast System (NCEP GFS) AGCM, the MOM4p1 OGCM, Noah LSM for land surface processes and SIS sea-ice dynamics (?). Vegetation properties and aerosols are prescribed and ocean biogeochemistry processes interactive. The results for IITM-ESM reveal large regional performance differences. The model ranks well in the central North Atlantic Ocean, Mediterranean Sea, the U.S. west coast and subtropical western North Pacific, but performs poorly in most of the remaining regions.
455

The results for BCC-CSM1.1, BCC-CSM2-MR and NESM3 are virtually insensitive to reanalysis uncertainty. To the southwest of Lake Baikal, both FGOALS-g2 and g3 are in closer agreement with JRA-55 than with ERA-Interim (compare Figure 6 with the "figs-refjra55/maps/rank" folder in the supplementary material). Over southwestern North America, however, FGOALS-g3 yields higher ranks if compared with ERA-Interim. TaiESM1 compares more closely with ERA-Interim over the southwestern U.S. and the subtropical North Atlantic Ocean. The effects of reanalysis uncertainty on the results for IITM-ESM are generally small, except over the southern U.S., where JRA-55 yields better results, and in the seas surrounding Greenland, where the model agrees more closely with ERA-Interim.
460

4.5 Model contributions from Japan and Korea

465 The Model for Interdisciplinary Research on Climate (MIROC) relies on long-standing research efforts of the Japanese re-
search community led by the *Center for Climate System Research (CCSR)*, the *National Institute for Environmental Studies*
(NIES) and the *Japan Agency for Marine-Earth Science and Technology (JAMSTEC)*. It comprises the *Frontier Research*
Center for Global Change (FRCGC) AGCM and CCSR's *Ocean Component Model (COCO)*, as well as an own land-surface
470 (MATSIRO) and sea-ice model. MIROC5 and 6 ~~are considered AOGCMs (??) whereas comprise interactive aerosols and~~
~~prescribed vegetation properties (??).~~ MIROC-ESM and MIROC-ESL2L are ~~ESMs including atmospheric chemistry more~~
~~complex configurations additionally including interactive terrestrial and ocean carbon cycle processes, as well as interactive~~
~~vegetation properties in the case of MIROC-ESM (??).~~ Results indicate a systematic performance increase from MIROC5 to
MIROC6 in the presence of large performance differences from one region to another (see Figure 6). Both models perform very
well for over the Mediterranean, northwestern North America and East Asia but do a poor job in northeastern North Amer-
475 ica and northern Eurasia. MIROC6 outperforms MIROC5 in the entire North Pacific basin including Japan, Korea and western
North America and is also better in the central North Atlantic. On the contrary, MIROC5 only does better in southwestern North
America. The performance of the two ESM more complex model versions is considerably lower, both ranking unfavourably
within the ensemble if compared to the remaining GCM versions considered here.

Unarguably one of the most comprehensive representations of the Earth System is provided by *Japan's Meteorological*
480 *Research Institute (MRI)*. Already in the CMIP5 version of their ESM the model version used in CMIP5 (MRI-ESM1) , an
atmospheric (photo)chemistry model coupled, an aerosol model and even a simple ice sheet scheme was included in addition
to the land and ocean carbon cycle schemes necessary to form an ESM comprises interactive terrestrial and ocean carbon cycle
processes, aerosols, atmospheric photochemistry, as well as prescribed vegetation properties (?). MRI-ESM2 is less complex
485 since terrestrial and ocean carbon cycle processes are no longer interactive but prescribed from external files (?). The coupling
applied in the MRI models is also more comprehensive than in most other models (?). Noteworthy, each model component
and also the coupler have been originally developed by MRI. The comparatively high model resolution traditionally applied
in this model family was further improved from MRI-ESM1 to MRI-ESM2 (?) by adding vertical layers, particularly in the
atmosphere (see Table 1). Especially when taking into account their complexity, both MRI models perform well in comparison
with other models To the north of approximately 50°N, both model versions perform very well, except for Greenland and the
490 surrounding seas in MRI-ESM1. Model performance decreases to the south of this line, particularly in the central to western
Pacific basin including western North America, the subtropical North Atlantic to the west of the Strait of Gibraltar, and the
regions around Greenland and the Caspian Sea. It is in these “weak” regions where the largest performance gains are obtained
from MRI-ESM1 to MRI-ESM2. As a results, in a zonal belt extending from approximately 50°N to 75°N, MRI-ESM2 is one
of the best performing models considered here.

495 In the southwestern The Korea Institute of Ocean Science and Technology Earth System Model (KIOST-ESM) comprises
modified versions of GFDL-AM2.0 and CLM4 for atmospheric and land-surface dynamics, as well as GFDL-MOM5 and
GFDL-SIS for ocean and sea-ice dynamics (?). The model has an interactive representation of the vegetation properties and
terrestrial carbon cycle processes and works with prescribed aerosols. It's error and ranking patterns are similar to that obtained
from GFDL-CM3 (using GFDL-AM3) meaning that the models share those regions where they perform least favourable

500 (i.e. the western U.S., the Mediterranean Basin, Manchuria and the central North Pacific Ocean). However, KIOST-ESM consistently performs weaker.

The *Seoul National University Atmosphere Model version 0 with a Unified Convection Scheme* (SAM0-UNICON) contributes for the first time in CMIP6 (?). Its component models are identical to CESM1 in its AOGCM configuration including aerosols (?), with the special feature of using a large number of alternative parametrization schemes involving convection, stratiform clouds, aerosols, radiation, surface fluxes and planetary boundary layer dynamics (?). Vegetation properties are resolved interactively, terrestrial carbon cycle processes and aerosols are prescribed. In spite of its conceptional similarity to CMCC-CM2-SR5 and ~~around Greenland, the MRI models surprisingly~~ NorESM2, the error pattern is different in SAM0-UNICON (compare Figure 7 with Figure 10), which might be due to the different ocean models (POP is used instead of NEMO or MICOM, see Table 1), or precisely due to the effects of the particular parametrization schemes mentioned above. Although the error magnitude of SAM0-UNICON is similar to CMCC-CM-SR5, SAM0-UNICON exhibits weaker regional performance differences, making it the more balanced model out of the two. In most regions of the NH, SAM0-UNICON yields better results than NorESM2-LM but is outperformed by NorESM2-MM.

The MRI models generally agree closer with ERA-Interim than with the JRA-55 reanalysis, which is surprising since JRA-55 was also developed at JMA (compare Figure 6-7 with the “figs-refjra55/maps/rank” folder in the supplementary material). For the MIROC family, a heterogeneous picture is obtained. While MIROC5 and MIROC-ESM clearly thrive towards ERA-Interim and JRA-55, respectively, MIROC6 is closer to JRA-55 in the southwestern U.S. and closer to ERA-Interim in the Gobi desert and around Greenland. The results for MIROC-ES2L, ~~and also for BCC-CSM2-MR and NESM3,~~ are virtually insensitive to reanalysis uncertainty. In the 3 main regions of reanalysis uncertainty, SAM0-UNICON is in closer agreement with ERA-Interim than with JRA-55. For KIOST-ESM it’s the other way around. Over the central U.S. and Gobi desert, this model more closely resembles JRA-55.

4.6 Model contributions from Germany and ~~Italy~~Russia

The *Max-Planck Institute Earth System Model* (MPI-ESM) is another example for the ~~synthesis-success~~ of long-standing research efforts from many research institutes around the world, coordinated by the Max-Planck Institute for Meteorology (MPI-M) in Germany, with all component models developed independently. It comprises the ECHAM, JSBACH, ~~MPIOM and HAMMOCC models representing the~~ and MPIOM models representing atmosphere, land-surface and terrestrial biosphere processes, ~~as well as~~ ocean and sea-ice dynamics (???). All model configurations interactively resolve vegetation properties as well as ~~ocean biogeochemistry, respectively, which~~ terrestrial and ocean carbon cycle processes, the latter represented by the HAMMOCC model; and are coupled with the OASIS software(???). ~~Since atmospheric chemistry and aerosols are missing in all model versions except.~~ Aerosols are additionally prescribed in MPI-ESM1.2-HAM, these are generally less complex than e.g. ~~the MRI model configurations mentioned above, but nevertheless include the carbon cycle and are thus considered ESMS-LR and HR.~~ The “working horse” used for generating large ensembles and long control runs is the “LR” version applied in both MPI-ESM-LR and MPI-ESM1.2-LR (for CMIP5 and 6, respectively). In this configuration, ECHAM (version 6 and 6.3) is run with a horizontal resolution of 1.9° (T63) and 47 layers in the vertical, and MPIOM with a 1.5° resolution near the equator

and 40 levels in the vertical. In MPI-ESM-MR, the number of vertical layers in the atmosphere is doubled and the horizontal
535 resolution in the ocean augmented to 0.4° near the equator. In MPI-ESM1.2, several atmospheric parametrization schemes
have been improved and/or corrected, including radiation, aerosol, clouds, convection and turbulence, and the land-surface
and ocean biogeochemistry processes have been made more comprehensive. ~~In MPI-ESM1.2-LR the distribution of vegetation
and landuse changes are simulated online, whereas they are prescribed in MPI-ESM1.2-HR, meaning that this high-resolution
version is on the limit to be considered an ESM.~~ Since the carbon-cycle has not been run to equilibrium ~~either,~~ with MPI-
540 ESM1.2-HR, this model version is considered unstable by its development team ~~?(?)~~. For MPI-ESM1.2-HAM, an aerosols and
sulphur chemistry module, developed by a consortium led by the *Leibniz Institute for Tropospheric Research*, are coupled with
~~ECAM6~~ ECHAM6.3 in a configuration that otherwise is identical to MPI-ESM1.2-LR (?). Similarly, *Alfred Wegener Institute's*
AWI-ESM-1.1-LR makes use of their in-house ocean and sea-ice model FESOM but otherwise is identical to MPI-ESM1.2-LR
(?).

545 Results show that the vertical resolution increase in the atmosphere undertaken from MPI-ESM-LR to MR (the CMIP5
versions) sharpens the regional performance differences rather than contributing to an improvement (see Figure 78). When
switching from MPI-ESM-LR to MPI-ESM1.2-LR, i.e. from CMIP5 to 6 with constant resolution, the performance ~~on the
one hand increases for Europe but on the other~~ increases over Europe but decreases in most of the remaining regions. Notably,
MPI-ESM-LR's good to very good performance in a zonal belt ranging from the eastern subtropical North Pacific to the eastern
550 subtropical Atlantic is lost in MPI-ESM1.2-LR. This picture worsens for MPI-ESM1.2-HAM and AWI-ESM-1.1-LR ~~worsen
this picture and,~~ which, even more so than MPI-ESM-MR, are characterized by large regional performance differences and
particularly unfavourable results over almost the entire North Pacific basin. However, *systematic* performance gains are ob-
tained by MPI-ESM1.2-HR, indicating that a horizontal rather than vertical resolution increase in the atmosphere conducts to a
better performance in this model family (recall that the sole *vertical* resolution increase from MPI-ESM-LR to MPI-ESM-MR
555 worsens the results). In the "HR" configuration, MPI-ESM1.2 is one of the best performing ~~ESMs within the ensemble~~ models
considered here.

The ~~Centro Euro-Mediterraneo per i Cambiamenti Climatici (CMCC) models are mainly built upon component models from
MPI, NCAR and IPSL. For CMCC-CM, ECHAM5 is used in conjunction with SILVA, a land-vegetation model developed in
Italy (?), and OPA8.2 (note that later OPA versions were integrated into the NEMO framework) plus LIM for atmosphere,
560 land-surface, ocean and sea-ice dynamics, respectively. The very high horizontal resolution in atmosphere (T159) is achieved
at the expense of a low horizontal resolution in the ocean and comparatively few vertical layers in both realms. Note that the
carbon cycle is not represented in this model version (?). For the core model contributing to CMIP6 (CMCC-CM2), CMCC
substituted all of the aforementioned components except the OGCM by the those available from CESM1 (?). For the model
version considered here (CMCC-CM2-SR5), CAM5.3 is run in conjunction with CLM4.5, taking into account components
565 of the Institute of Numerical Mathematics, Russian Academy of Sciences model INM-CM4 were all developed by scientists
working in Russia (?). This model comprises interactive vegetation properties and terrestrial carbon cycle processes. ~~For ocean
and sea-ice dynamics, NEMO3.6 (i.e. OPA's successor) and CICE are applied (?). The coupler changed from OASISv3 to
CPLv7 (??). Since ocean biogeochemistry processes are missing, none of the two model versions considered here reach ESM~~~~

status. Due to the completely distinct model setups, the error and ranking patterns substantially change from, as well as a simple
570 ocean carbon model, including atmosphere-ocean fluxes, total dissolved carbon advection by oceanic currents and a prescribed
biological pump (Evgeny Volodin, personal communication). INM-CM4 contributed to CMIP5 to 6 for this model family.
While CMCC-CM performs relatively weak in northern Canada, Scandinavia and northwestern Russia, CMCC-CM2-SR5
does so in the and an updated version (INM-CM4-8) is currently participating in CMIP6, but the 6-hourly SLP data is not
575 available for this version so that it had to be excluded here. The resolution setup of INM-CM4 is comparable to other CMIP5
models, except for the very few vertical layers used in the atmosphere (see Table 1). As shown in Figure 8, INM-CM4 performs
well in the eastern North Atlantic, particularly to the west of the Strait of Gibraltar. In the remaining regions, very good ranks
are obtained by both models. Notably, CMCC-CM2-SR5 is one of the few models performing well in the central Asian high
mountain ranges and also in the Rocky Mountains (except in Alaska). In most of northern Europe and the Gulf of Alaska,
regularly over northern China and Korea and poorly over the remaining regions it is likewise one of the best models considered
580 here. Note that this model, due to identical model components for all realms except the ocean, is a good estimator for the
performance of CESM1, which unfortunately cannot be assessed here due to data availability issues in the NH. It is thus marked
by large performance differences from one region to another.

In the southwestern U.S. and around Greenland, the MPI models including AWI-ESM-1-1-LR and CMCC-CM 3 main
regions sensitive to reanalysis uncertainty, all model versions assessed in this section consistently thrive towards JRA-55
585 On the contrary, CMCC-CM2-SR5 is in closer agreement with ERA-Interim, reflecting the profound change in the model
components from CMIP5 to 6 (compare Figure 7-8 with the “figs-refjra55/maps/rank” folder in the supplementary material) –

4.7 The joint European and Norwegian model contributions contribution EC-Earth

The EC-Earth consortium is a large collaborative effort made by research institutions from several European countries. Fol-
lowing the idea of seamless prediction (?), the atmospheric component used in the EC-Earth model is based on ECMWF’s
590 Integrated Forecasting System (IFS) complemented by the HTESSEL land-surface model and a new parametrization scheme
for convection, NEMO for the ocean, LIM for the NEMO ocean and LIM sea-ice and OASIS being the coupler models and the
OASIS coupling software (??). Starting from this basic AOGCM configuration, additional components of the extended climate
system climate system components can be optionally added to bring the model to a comprehensive ESM. However, most of the
configurations used to produce augment the complexity of the model. Regarding the historical experiments for CMIP5 and 6 are
595 classical AOGCMs and none of the versions analysed here reaches ESM status since ocean biogeochemistry is missing so far
(see Table 1). A model version incorporating an interactive carbon cycle (, EC-Earth 2.3 (or simply EC-Earth) and 3 are classical
AOGCM configurations, using prescribed vegetation properties and aerosols (in the case of EC-Earth3). EC-Earth3-Veg
comprises interactive vegetation properties and terrestrial carbon cycle processes, whereas aerosols are prescribed. EC-Earth3-AerChem
incorporates the interactive aerosol model TM5 whilst vegetation properties are prescribed. EC-Earth3-CC) was not available
600 at the time of submission and will be included in the final version of the manuscript. The contains interactive vegetation
properties, terrestrial and ocean carbon cycle processes. Aerosols are prescribed in this “Carbon Cycle” model version.

605 Already the model version version used in CMIP5 (EC-Earth2.3~~or simply EC-Earth) already~~) comprises a fine resolution in the atmosphere and ocean (except for the relatively few vertical layers in the ocean) and this configuration was adopted or even improved for what is named “low resolution” in CMIP6 (EC-Earth3-LR, EC-Earth3-Veg-LR). For the other configurations used in CMIP6 (EC-Earth3~~and~~, EC-Earth3-Veg, EC-Earth3-AerChem, EC-Earth3-CC), the atmospheric resolution is further refined in the horizontal and vertical (?).

Results reveal an already very good performance for EC-Earth2.3 in all regions except the North Pacific and subtropical central Atlantic (see Figure 8) ~~which, for the North Atlantic –European sector, 9) which~~ is in line with the ~~results from findings in ? and ?~~. EC-Earth3 performs even better, and does so irrespective of the applied model complexity (~~vegetation dynamics are optionally added in EC-Earth3-Veg~~) or model resolution. These CMIP6 model versions ~~, all run at the Irish Centre for High-End Computing (ICHEC),~~ rank very well in almost any region of the the world, including the central Asian high mountain areas. ~~As a results, if neither model complexity nor reanalysis uncertainty was an argument, then this model family would be claimed “the best one” in the context of the present study. Note that the very favourable results for EC-Earth3 hold for any of the~~

615 When evaluated against JRA-55 instead of ERA-Interim, the ranks for the EC-Earth model family consistently worsen by up to 20 historical runs available from the ESGF, with only slight variations in integers in the southwestern U.S. and around the southern tip of Greenland, but remain roughly constant in the Gobi desert (compare Figure 9 with the “figs-refjra55/maps/rank” folder in the supplementary material). This worsening brings the EC-Earth family to a closer agreement with the HadGEM models. Consequently, when evaluated against JRA-55, HadGEM3-GC31-MM links up with EC-Earth3 in what is considered
620 the “best model”.

4.8 Model contributions from Italy and Norway

The Centro Euro-Mediterraneo per i Cambiamenti Climatici (CMCC) models are mainly built upon component models from MPI, NCAR and IPSL. For CMCC-CM, ECHAM5 is used in conjunction with SILVA, a land-vegetation model developed in Italy (?), and OPA8.2 (note that later OPA versions were integrated into the NEMO framework) plus LIM for ocean and sea-ice dynamics, respectively. The very high horizontal resolution in atmosphere (T159) is achieved at the expense of a low horizontal resolution in the ocean and comparatively few vertical layers in both realms, as well as by the fact that no further climate system components are considered by this model version (?). For the core model contributing to CMIP6 (CMCC-CM2), all of the aforementioned components except the OGCM were substituted by those available from CESM1 (?). For the model version considered here (CMCC-CM2-SR5), CAM5.3 is run in conjunction with CLM4.5. For ocean and sea-ice dynamics, NEMO3.6 (i.e. OPA’s successor) and CICE are applied (?). The coupler changed from OASISv3 to CPLv7 (??) and the interactive aerosol model MAM3 was included. CMCC-ESM2 is the most complex version in this model family, including the aforementioned aerosol model, activated terrestrial biogeochemistry in CLM4.5 and the use of BFM5.1 to simulate ocean biogeochemistry processes. Due to the completely distinct model setups, the error and ranking patterns substantially change from CMIP5 to 6 for this model family (see Figure 10). While CMCC-CM performs relatively weak in northern Canada, Scandinavia and northwestern Russia, CMCC-CM2-SR5 does so in the North Atlantic, particularly to the west of the Strait of Gibraltar. In the

635

remaining regions, very good ranks are obtained by both models. Notably, ~~CMCC-CM2-SR5 is one of the error pattern and magnitude from one member of the initial conditions ensemble to another, meaning that internal climate variability plays a minor role here (see Section 4.9)~~ few models performing well in the central Asian high mountain ranges and also in the Rocky Mountains (except in Alaska). In most of the remaining regions it is likewise one of the best models considered here. Note that this model, due to identical model components for all realms except the ocean, is a good estimator for the performance of CESM1, which unfortunately cannot be assessed here due to data availability issues. The error ranking patterns of CMCC-ESM2 are similar to CMCC-CM2-SR5, yielding fewer regional differences and a much better performance over the central eastern North Atlantic Ocean. Hence, CMCC-ESM2 is not only the most sophisticated but also the best performing model version in this family.

The Norwegian Earth System Model ~~NorESM (NorESM)~~ shares substantial parts of its source code with the NCAR model family (particularly with CCSM and CESM2). NorESM1-M, the standard model version used in CMIP5 (?), comprises the CAM4-Oslo AOGCM —derived from CAM4 and complemented with the ? aerosol module—, CLM4 for land-surface processes, CICE4 for sea-ice dynamics and an ocean model based on the Miami Isopycnic Coordinate Ocean Model (MICOM) originally developed by NASA/GISS (?). CPL7 is used as coupler. ~~Biogeochemical processes can be included, but are not considered in the model version assessed here~~ NorESM1-M contains interactive terrestrial carbon cycle processes and aerosols, whereas vegetation properties are prescribed. From NorESM1 to NorESM2, the model components from CCSM were updated to CESM2.1 (?) whilst keeping the Norwegian aerosol module and modifying a number of parametrization schemes in CAM6-Nor w.r.t. to CAM6 (?). Through the coupling of an updated MICOM version with the ocean biogeochemistry model HAMOCC, combined with the use of the CLM5 land-surface model, ~~both oceanic and terrestrial biogeochemical processes are represented~~ vegetation processes as well as the land and ocean carbon cycles are interactively resolved in NorESM2. ~~Since the Community Ice Sheet Model (CISM) is used in addition (?), NorESM2 pertains to the group of the most sophisticated ESMs considered here (together with MRI-ESM1 MRI-ESM2 and HadGEM2-ES). The~~ Vegetation properties and atmospheric chemistry are prescribed, and the coupler has been updated from CPL7 to CIME, which is also used in CESM2. In the present study, the basic configuration NorESM2-LM is evaluated together with NorESM2-MM, the latter being integrated with using a much finer horizontal resolution in the atmosphere (see Table 1). ~~Otherwise, the two experiments are identical.~~ The corresponding maps in Figure 8-10 reveal a low model performance for NorESM1-M with an error magnitude and spatial pattern similar to CCSM4. When switching to NorESM2-LM, i.e. to updated and extended component models and an almost identical resolution in the atmosphere and ocean, notable performance gains are obtained in most regions of the NH, except in a zonal band extending from Newfoundland to the Urals which, further to the East, re-emerges over the Baikal region. In the higher-resolution version NorESM2-MM, these errors are further reduced to a large degree, with the overall effect of obtaining one of the best models considered here, particularly when its complexity is taken into account.

~~If these two model families are evaluated against~~ In the 3 regions of pronounced reanalysis uncertainties, CMCC-CM is in closer agreement with JRA-55 instead of whereas CMCC-CM2-SR5 and CMCC-ESM2 are more similar to ERA-Interim, the ranks for the EC-Earth model family consistently worsen by up to 20 integers in the southwestern U.S. and around the southern tip of Greenland, but remain roughly constant in the Gobi desert reflecting the profound change in the model components from

CMIP5 to 6 (compare Figure 8-10 with the “figs-refjra55/maps/rank” folder in the supplementary material). This worsening brings the EC-Earth family to a closer agreement with the HadGEM models. Consequently, when evaluated against JRA-55, HadGEM3-GC31-MM links up with EC-Earth3 in what is considered the “best model” if model complexity was not argument (see also “figs-refjra55/as-figure-10-but-wrt-jra55.pdf” in the supplementary material). For the NorESM family, different re-analysis affinities are obtained for the 3 regions. While NorESM1 is closer to JRA-55 in all of them, NorESM2-LM is closer to ERA-Interim in the southwestern U.S., but closer to JRA-55 in the Gobi desert. NorESM2-MM is generally less sensitive to reanalysis uncertainty, with some affinity to ERA-Interim in the southwestern U.S.

4.9 Model contributions from Russia and South Korea

The *Institute of Numerical Mathematics, Russian Academy of Sciences* model INM-CM4 is a classical AOGCM comprising an atmosphere, land-surface, ocean and sea-ice model, all developed by scientists working Russia (?). INM-CM4 contributed to CMIP5 and an updated version (INM-CM4-8) is currently participating in CMIP6, but the 6-hourly SLP data is not available for this version so that it had to be excluded here. The resolution setup of INM-CM4 is comparable to other CMIP5 models, except for the very few vertical layers used in the atmosphere (see Table 1). As shown by Figure 9, INM-CM4 performs well to very well in the eastern North Atlantic, northern Europe and the Gulf of Alaska, regularly over northern China and Korea and poorly over the remaining regions of the NH. It is thus marked by large performance differences from one region to another.

The *Seoul National University Atmosphere Model version 0 with a Unified Convection Scheme* (SAM0-UNICON) contributes for the first time in CMIP6 (?). Its component models are identical to CESM1 in its AOGCM configuration including aerosols (?), with the special feature of using a large number of alternative parametrization schemes involving convection, stratiform clouds, aerosols, radiation, surface fluxes and planetary boundary layer dynamics (?). In spite of its conceptual similarity to CMCC-CM2-SR5 and NorESM2, the error pattern is different in SAM0-UNICON (compare Figure 9 with Figures 8 and 7), which might be due to the ocean model taken from CESM1 (POP is used instead of NEMO or MICOM, see Table 1), or precisely due to the effects of the particular parametrization schemes mentioned above. Although the error magnitude of SAM0-UNICON is similar to CMCC-CM-SR5, SAM0-UNICON exhibits weaker regional performance differences, making it the more balanced model out of the two. In most regions of the NH, SAM0-UNICON yields better results than NorESM2-LM but is outperformed by NorESM2-MM.

While INM-CM4 compares better with JRA-55 in the 3 regions sensitive to reanalysis uncertainty, SAM0-UNICON is in closer agreement with ERA-Interim, there (compare Figure 9 with the “figs-refjra55/maps/rank” folder in the supplementary material).

4.9 Summary boxplot and role of internal model resolution, model complexity and internal variability

For each model version listed in Table 1, the spatial distribution of the pointwise MAE values can also be represented with a boxplot instead of a map, which allows for an overarching performance comparison visible at a glance (see Figure 10-11 for the evaluation against ERA-Interim). Here, the standard configuration of the boxplot is applied. For a given sample of MAE values corresponding to a specific model, the box refers to the interquartile range (IQR) of that sample and the horizontal bar to the

median. Whiskers are drawn at the 75th percentile + $1.5 \times \text{IQR}$ and at the 25th percentile - $1.5 \times \text{IQR}$. All values outside this range are considered outliers (indicated by dots). ~~Additional~~ Four additional boxplots are provided for the joint MAE samples of ~~1) all CMIP5 model versions, 2) all CMIP6 model versions, 3) all model versions considered ESMs (ESM) and 4) all other model versions (AOGCM)~~ the more and the less complex model versions used in CMIP5 and 6. In these 4 cases ~~the~~ outliers are not plotted for the sake of simplicity. The acronyms of the *coupled* model configurations, as well as their participation in either CMIP5 or 6 (indicated by the final integer), are shown below the x-axis. ~~Above~~ Along the x-axis, the names of the coupled models' *atmospheric* components are also shown since some of them are shared by various research institutions (see also Table 1).

Results indicate a performance gain for most model families when switching from CMIP5 to 6 (available model pairs are located next to each other in Figure ~~10~~ 11). The largest improvements are obtained for those models performing relatively poorly in CMIP5. Namely, FGOALS-g2 improves upon FGOALS-g2 (dark brown), NorESM2-LM and NorESM2-MM ~~improve~~ upon NorESM1-M (rose), BCC-CSM1.1 upon BCC-CSM2-MR (orange), MIROC6 ~~improves~~ upon MIROC5 (blue-green) and IPSL-CM6A-LR upon IPSL-CM5A-LR and IPSL-CM5A-MR (grey). GISS-E2-R-5 improves upon GISS-E2-H and GISS-E2-R (green) in terms of *median* performance, but suffers slightly larger spatial performance differences as indicated by the IQR. The MPI (neon green), CMCC (cyan), GFDL (magenta) and MRI (brown) models already performed well in CMIP5 and further improve in CMIP6. Among the MPI models, however, an advantage over the two CMIP5 versions is only obtained when considering the *high-resolution* CMIP6 version (compare MPI-ESM1.2-HR with MPI-ESM-LR and MPI-ESM-MR). Contrary to the remaining models, the performance of the CNRM (red) models does ~~not~~ not improve from CMIP5 to 6, which may be due to the fact that the CMIP5 version (CNRM-CM5) already performed very well. Remarkably, CNRM's high-resolution CMIP6 version (CNRM-CM6-1-HR) is ~~the worst performing one~~ performing worst within this model family. ~~Similarly~~ Likewise, the ACCESS models (blue) do not improve either if ACCESS1.0 instead of ACCESS1.3 is taken as reference CMIP5 model.

The CMCC, HadGEM, and particularly the EC-Earth model families perform overly best and all three exhibit a performance gain from CMIP5 to 6. ~~However, none of the EC-Earth or CMCC model versions is an ESM and neither is HadGEM3-GC31-MM, the latest Hadley Centre model version considered here. So if model complexity matters and only ESMs are taken into account, then NorESM2-MM is the best choice, followed by MRI-ESM2, GFDL-CM4, MPI-ESM1.2-HR and NorESM2-MM also belongs to the best performing models and largely improves upon NorESM2-LM and NorESM1.~~ Remarkably, for four out of five possible comparisons, the more complex model version performs similar to less complex one (compare ACCESS-ESM1.5, as well as the HadGEM2-ES model already used in CMIP5. Given its status as fully comprehensive ESMs, the with ACCESS-CM2, CMCC-ESM2 with CMCC-CM2-SR5, CNRM-ESM2-1 with CNRM-CM6-1-HR and EC-Earth3-CC with EC-Earth3). Only the MIROC family suffers a considerable performance loss when switching from less to more complexity and only in this family the AGCM's resolution is considerably lower in the more complex configurations (compare MIROC-ESM with MIROC5 and MIROC-ES2L with MIROC6 in Figure 11 and Table 1).

A virtual lack of outliers is another remarkable advantage of NorESM2-MM. MRI-ESM2 and GFDL-CM4 are also relatively robust to outliers, but less so than NorESM2-MM. The fewest number of outliers among all models is obtained for EC-Earth, irrespective of the model version.

The model evaluation against JRA-55 reveals similar results (see “figs-refjra55/as-figure-10-but-wrt-jra55.pdf” in the supplementary material), indicating that uncertain reanalysis data in the 3 relevant regions detected above do not substantially affect the hemispheric-wide statistics. What is noteworthy, however, is the slight but nevertheless visible performance loss for the EC-Earth model family, bringing EC-Earth3 approximately to the performance level of HadGEM3-GC31-MM. If evaluated against JRA-55, all EC-Earth model versions also comprise more outlier results. EC-Earth’s affinity to ERA-Interim might be explained by the fact that this reanalysis was also built with ECMWF IFS.

Table 2 provides the rank correlation coefficients between the median MAE w.r.t. to ERA-Interim for each model, corresponding to the horizontal bars within the boxes in Figure 10–11, and various resolution parameters for of the atmosphere and for ocean component models. Correlations are calculated separately for the zonal, meridional and vertical resolution represented by the number of grid-boxes in the corresponding direction (due. Due to the presence of reduced Gaussian grids, longitudinal grid-boxes at the equator are considered). In addition, the 2D mesh defined as the number of longitudinal grid boxes \times number of latitudinal grid boxes, as well as for the 2D (lon \times lat) and the 3D (lon mesh defined as the number of longitudinal grid boxes \times lat-number of latitudinal grid boxes \times layers) meshes, respectively. This is done number of vertical layers, are taken into account in the analysis. Correlations are first calculated separately for the atmosphere and ocean. Due the presence of and, in the last step, the sizes of the atmosphere and ocean 3D meshes are added to obtain the size of the combined atmosphere-ocean mesh. All dimensions are obtained from the source attribute inside the netCDF files from ESGF or directly from the data array stored therein. Note that due to an unstructured grid in one ocean model, the breakdown in zonal and meridional resolution cannot be made in this realm. In a final step, the number of grid-boxes of the 3D meshes from both atmosphere and ocean are added to obtain the size of combined atmosphere-ocean mesh.

As can be seen from Table 2, average model performance is closer related to the *horizontal* than to the vertical resolution applied in the atmosphere. Associations with the ocean resolution are weaker, as expected, but nevertheless significant for both the horizontal and vertical resolution. This is somewhat unexpected, particularly when taking into account that the corresponding link with the vertical resolution in the atmosphere is spurious. Since the resolution increase for most models has gone hand in hand with improvements in the internal parameters (parametrization, model physics, bugs) it is difficult to say which of these two effects is more influential on model performance. However, most of the models undergoing a version change without resolution increase do not experience a clear performance gain either. This is observed for the 3 ACCESS versions using the same AGCM (i.e. GA in 1.3, CM2 and ESM1-5) and also for the 3 model versions from GISS, all comprising the same horizontal resolution in the atmosphere within their respective model family. Likewise, CNRM-CM6-1 and MPI-ESM1-2-LR even perform slightly worse than their predecessors (CNRM-CM5 and MPI-ESM-LR), meaning that the update is counterproductive for their performance (see Figure 10–11). This points to the fact that resolution is likely more influential on performance than model updates as long as the latter are not too substantial. Interestingly, the relationship between the models’ median performance and the horizontal mesh size of their atmospheric component is non-linear ($r_s = -0.72$), with an abrupt shift towards better results at approximately 25,000 grid points (see Figure 13a).

Figure 13b shows the sum of the integer code provided in Table 1, column 7, here used as a summary measure for model complexity, plotted against the models’ median performance. From this two-dimensional decision base for model

775 selection, one can see that the best performing model family (EC-Earth) is not the most complex one, and that some model configurations performing less well are particularly complex (e.g. CNRM-ESM2-1). Also, model performance is generally unrelated to model complexity, which is an argument in favour of the more complex model versions, since they provide a more complete representation of the climate system. Interestingly, for four out of five possible comparisons, the most complex model configuration within a given family performs similar to the less complex ones if the AGCM's horizontal resolution is not reduced (compare ACCESS-ESM1.5 with ACCESS-CM2, CMCC-ESM2 with the CMCC-CM2-SR5, CNRM-ESM2-1
780 with CNRM-CM6-1-HR and CNRM-CM6-1-HR and EC-Earth3-CC with EC-Earth3). Within the MIROC family, this kind of resolution was reduced for the more complex configurations and a systematic performance decrease is observed (compare MIROC5 with and MIROC6 with MIROC-ES2L)

In comparison with the *inter-model* variability discussed above, the *internal* model variability (or “intra-model variability”) is much smaller and only marginally affects the results, which for all runs of a given model version are in close agreement
785 even for the outliers (see Figure 14.12). Albeit the use of alternative model runs might lead to slight shifts in the ranking order at the grid-box scale, ~~which is why a “best model per grid-box map” is intentionally not provided here,~~ a “good” rank would not change into an “average” or even “bad” one. However, while internal model variability ~~does only play~~ only plays a minor role in the context of the present study, some specific models indeed seem to be more sensitive to initial conditions uncertainty (which is where ensemble spread stems from in the experiments considered here) ~~then than~~ others, with NorESM2-LM (the
790 lower resolution version only) and NESM3 seemingly being less stable in this sense. Remarkably, MPI-ESM1.2-HR is found to be stable in spite of the fact that it is considered a more “unstable” configuration by its development team because the carbon cycle had not been run ~~been~~ to equilibrium for this version ~~of MPI-ESM1.2(?)~~. It is also good news that HadGEM2-ES, known to perform well for *r1i1p1* and consequently used as baseline for many downscaling applications and impact studies ~~(???)of the past (???)~~, performs nearly identical for *r2i1p1*. ~~Finally~~ Lastly, the large performance increase from IPSL-CM5A-LR to
795 IPSL-CM6A-LR is likewise robust to the effects of internal ~~model~~-variability.

5 Specific model performance for each Lamb weather type

In Figures ~~12 to 14~~ 14 to 16, the simulated, hemispheric-wide frequency pattern for a given model and LWT is compared with the respective quasi-observed frequency pattern obtained from ERA-Interim by using a normalized Taylor diagram (?). The first thing to note here is that, for most LWTs, the models tend to cluster in a region that would be generally considered a good
800 result. Except for some outlier models and individual LWTs, the pattern correlation lies in between 0.6 and 0.9, the standard deviation ratio is not too far from unity (= best result) and the centred normalized RMSE ranges between 0.25 and 0.75 × the standard deviation of the observed frequency pattern.

It is also ~~becomes evident~~ found that all members of the EC-Earth model family yield best results for *any* LWT (observe the proximity of the yellow cluster to the perfect score indicated by the black half ~~eyele~~). ~~Recall, however, that no EC-Earth~~
805 ~~version actually fulfils the criterion of an ESM since ocean biogeochemistry is not considered.~~ circle). Within the group of ~~ESMs~~ the more complex models, NorESM2-MM (the rose triangle pointing to the left) performs best and actually lies in close

proximity to the EC-Earth Cluster for most LWTs. The Hadley Centre and ACCESS models (filled with orange and dark blue) form another cluster that generally performs very well for most LWTs. However, the spatial standard deviation of the 3 eastern LWTs (cyclonic, anticyclonic and directional) is overestimated by these ~~“Commonwealth” models~~~~(the Commonwealth is here referred to for illustrative purposes and does not reflect any political opinion)~~models, which is indicated by a standard deviation ratio ≈ 1.25 , while values close to unity or below are obtained for the remaining models. It is also worth mentioning that not only ACCESS1.0 but also the other, more independently developed ACCESS versions pertain to ~~the Commonwealth~~this cluster, which indicates the common origin of their atmospheric component (the Met Office Hadley Centre) even at the level of detail of specific weather types. For all other models, the LWT-specific results do not largely deviate from the overall MAE results shown in Section 4, meaning that overall performance is generally also a good indicator of LWT-specific performance. As an example, MIROC-ESM (the blue-green cross), IPSL-CM5A-LR and IPSL-CM5A-LR (the grey cross and grey plus) are located in the “weak” area of the Taylor diagram for *each* of the 27 LWTs, which is in line with the likewise weak *overall* performance obtained for these models in Section 4.

The corresponding results for the model evaluation against JRA-55 are generally in close agreement with those mentioned above, except for the EC-Earth model family performing slightly less favourable (see “figs-refjra55/taylor” folder in the supplementary material to this article).

6 Summary ~~, discussion and conclusions~~Conclusions

In the present study, ~~46–56~~coupled general circulation model versions contributing historical experiments to CMIP5 and 6 have been evaluated in terms of their capability to reproduce the observed frequency of the 27 atmospheric circulation types originally proposed by ?, as represented by the ERA-Interim or JRA-55 reanalyses. The outcome is an objective, regional-scale ranking catalogue that is expected to be of interest for the model development teams themselves, and also for the downscaling and regional climate change community asking for model selection criteria. In this context, the present study is a direct response to the claim for a circulation-based model performance assessment made by ?. In addition, a straightforward method to estimate the complexity of the participating model configurations is proposed that relies on the assumption that complexity is proportional to the number of interactive model components.

On average, the model versions used in CMIP6 perform better than their CMIP5 predecessors and ~~the more complex ESMs are outperformed by the simpler AOGCMs~~this finding holds for the more and the less complex model configurations. Among a number of tested resolution parameters, the ~~closest statistical relationship with model performance is obtained for the~~ horizontal resolution in the atmosphere is closest related to performance, which is in line with ?, with equal contributions from the latitudinal and longitudinal ~~grid distance and no significant relationship for~~ resolution and a weaker relationship with the number of vertical layers. An abrupt shift towards better model results at a horizontal mesh size of approximately 25.000 grid points is observed (see Figure 13a), which might point to the existence of a minimum atmospheric resolution that should be maintained while augmenting the complexity of the coupled model configurations. The corresponding links with the ocean resolution are ~~weak~~weaker but nevertheless significant, ~~even for the number of vertical layers used in this realm.~~

840 Improving the internal model parameters (physics and parametrization schemes) and/or adding more vertical layers to the atmosphere seems to have little effect for most model families if the horizontal resolution is not refined in addition. This is the case for ACCESS-CM2 w.r.t. ACCESS1.3, CNRM-CM6-1 w.r.t. CNRM-CM5, GISS-E2-1-G w.r.t. GISS-ES-R and MPI-ESM1.2-LR w.r.t. MPI-ESM-LR.

For a subgroup of ~~12 out of 46~~ 13 out of 56 models, the impact of internal model variability on the performance was assessed with ~~70 additional historical~~ 72 additional historical model integrations, each one initialized from a unique starting date of the corresponding pre-industrial control run. The thereby created initial conditions uncertainty has little effect on the overall results. Albeit the point-wise ranking order might change by a few integers when alternative runs are evaluated, which is why a “best model” map is intentionally not provided here, a well performing model would not even change to an “intermediate” one or vice versa if another ensemble member was put to the test. A similarly small effect was found for changing the reference reanalysis from ERA-Interim to JRA-55, except in the following 3 problematic regions, where ~~this change can largely~~ reanalysis uncertainties can substantially affect the models’ ranking order: the southwestern United States, the Gobi desert, and Greenland plus the surrounding seas.

~~This study also shows that the models’ complexity, here defined as the number of realms simulated online, should be taken into account for a correct interpretation of the results. Namely, comprehensive ESMs such as HadGEM2-ES, MRI-ESM1, MRI-ESM2 and NorESM2 are by construction more sensitive to model uncertainties than traditional AOGCM configurations. Hence, while the distinct EC-Earth versions considered here are consistently performing “best”, none of them reaches the complexity of an ESM. This specific conclusion will be re-evaluated by inclusion of EC-Earth3-CC during the review phase, which was not available when this manuscript version was submitted. If only ESMs are considered, NorESM2-MM and MRI-ESM2 play a particular role because they are the most complex models and at the same time perform comparatively well, a finding that also holds for the older, well tested, HadGEM2-ES, GFDL-CM4 and MPI-ESM1.2-HR perform similarly well but are less complex than NorESM2-MM, MRI-ESM2 and HadGEM2-ES. Since the inclusion of more component models in a coupled model configuration provides a more realistic representation of the climate system and also yields distinguishable future scenarios (??), it would make sense to consider model complexity as an additional model selection criterion in future studies. The approach proposed here is intended to be a straightforward starting point to measure this criterion. It should be further refined as soon as more detailed model documentation, already provided for some climate system components (?), become available in a systematic way, e.g. via the *Earth System Documentation* project (<https://es-doc.org/>).~~

Since ESMs are in principle preferable to AOGCMs, a discussion about how model complexity should influence the choice of driving GCMs in regional climate studies is needed. A separate ranking of the models pertaining to each group would be a simple solution (see “figs-refinterim-aogem” and “figs-refinterim-esm” folders in the supplementary material to this article). ~~Once the user has decided on whether to use AOGCMs or ESMs, he/she can then select the most favourable model(s) from one of the two groups.~~ As a final remark, the here provided metadata about the participating component models can also be used to estimate the degree of dependence between the numerous coupled model configurations.

Code and data availability. The netCDF files containing the Lamb Weather Type catalogues computed for this study have been permanently archived at <https://doi.org/10.5281/zenodo.4452080>. The underlying Python code was stored at <https://doi.org/10.5281/zenodo.4555367>. A
875 Python function providing metadata about the coupled model configurations and their individual components can be retrieved from https://github.com/SwenBrands/gcm-metadata-for-cmip/blob/main/get_historical_metadata.py.

Author contributions. All working steps were accomplished by SB.

Competing interests. The author declares no competing interests.

Acknowledgements. ~~The author~~ I am grateful to Jesús Fernández (CSIC, Spain) and Joaquín Bedia (UC, Spain) for discussing the manuscript
880 and would like to thank the following model developers for revising the complexity codes provided in Table 1: Jian Cao (NUIST, China), Bin Wang (IPRC, Hawaii), Laurent Li (LMD, France), Tongwen Wu (Beijing Climate Center, China), Evgeny Volodin (INM, Russia), Hiroaki Tatebe (JAMSTEC, Japan), Swapna Panickal (IITM, India), YoungHo Kim (Pukyong National University, Korea), Thorsten Mauritsen (MPI, Germany), Øyvind Seland (Norwegian Meteorological Institute), Seiji Yukimoto (MRI, Japan), Klaus Wyser and Ralf Döscher (SMHI, Sweden), Annalisa Cherchie and Enrico Scoccimarro (CMCC, Italy), Aurore Voltaire and Roland Séférian (CNRM, France), Olivier
885 Boucher (IPSL, France), Peter Gent (NCAR, USA), Tido Semmler (AWI, Germany), Gill Martin (Met Office, UK) and Ina Tegen (TROPOS, Germany). I would also like thank the Agencia para la Modernización Tecnológica de Galicia (AMTEGA) and the Centro de Supercomputación de Galicia (CESGA) for providing the necessary computational resources.

References

- AMS: General Circulation Model, Glossary of Meteorology, https://glossary.ametsoc.org/wiki/General_circulation_model, 2020.
- 890 Bentsen, M., Bethke, I., Debernard, J. B., Iversen, T., Kirkevåg, A., Seland, Ø., Drange, H., Roelandt, C., Seierstad, I. A., Hoose, C., and Kristjánsson, J. E.: The Norwegian Earth System Model, NorESM1-M – Part I: Description and basic evaluation of the physical climate, *Geoscientific Model Development*, 6, 687–720, <https://doi.org/10.5194/gmd-6-687-2013>, <https://gmd.copernicus.org/articles/6/687/2013/>, 2013.
- 895 Bi, D., Dix, M., Marsland, S. J., O’Farrell, S., Rashid, H., Uotila, P., Hirst, A., Kowalczyk, E., Golebiewski, M., Sullivan, A., Yan, H., Hannah, N., Franklin, C., Sun, Z., Vohralik, P., Watterson, I., Zhou, X., Fiedler, R., Collier, M., Ma, Y., Noonan, J., Stevens, L., Uhe, P., Zhu, H., Griffies, S., Hill, R., Harris, C., and Puri, K.: The ACCESS coupled model: description, control climate and evaluation, *Australian Meteorological and Oceanographic Journal*, 63, 41–64, <https://doi.org/0.22499/2.6301.004>, 2013.
- 900 Bi, D., Dix, M., Marsland, S., O’Farrell, S., Sullivan, A., Bodman, R., Law, R., Harman, I., Srbinovsky, J., Rashid, H., Dobrohotoff, P., Mackallah, C., Yan, H., Hirst, A., Savita, A., Dias, F. B., Woodhouse, M., Fiedler, R., and Heerdegen, A.: Configuration and spin-up of ACCESS-CM2, the new generation Australian Community Climate and Earth System Simulator Coupled Model, *Journal of Southern Hemisphere Earth Systems Science*, in press, <https://doi.org/doi:10.1071/ES19040>, 2020.
- Bleck, R. and Smith, L. T.: A wind-driven isopycnic coordinate model of the north and equatorial Atlantic Ocean: 1. Model development and supporting experiments, *Journal of Geophysical Research: Oceans*, 95, 3273–3285, <https://doi.org/10.1029/JC095iC03p03273>, <https://agupubs.onlinelibrary.wiley.com/doi/abs/10.1029/JC095iC03p03273>, 1990.
- 905 Boucher, O., Servonnat, J., Albright, A. L., Aumont, O., Balkanski, Y., Bastrikov, V., Bekki, S., Bonnet, R., Bony, S., Bopp, L., Braconnot, P., Brockmann, P., Cadule, P., Caubel, A., Cheruy, F., Codron, F., Cozic, A., Cugnet, D., D’Andrea, F., Davini, P., de Lavergne, C., Denvil, S., Deshayes, J., Devilliers, M., Ducharne, A., Dufresne, J.-L., Dupont, E., Éthé, C., Fairhead, L., Falletti, L., Flavoni, S., Foujols, M.-A., Gardoll, S., Gastineau, G., Ghattas, J., Grandpeix, J.-Y., Guenet, B., Guez, Lionel, E., Guilyardi, E., Guimberteau, M., Hauglustaine, D., Hourdin, F., Idelkadi, A., Joussaume, S., Kageyama, M., Khodri, M., Krinner, G., Lebas, N., Levavasseur, G., Lévy, C., Li, L., Lott, F., 910 Lurton, T., Luysaert, S., Madec, G., Madeleine, J.-B., Maignan, F., Marchand, M., Marti, O., Mellul, L., Meurdesoif, Y., Mignot, J., Musat, I., Ottlé, C., Peylin, P., Planton, Y., Polcher, J., Rio, C., Rochetin, N., Rousset, C., Sepulchre, P., Sima, A., Swingedouw, D., Thiéblemont, R., Traore, A. K., Vancoppenolle, M., Vial, J., Vialard, J., Viovy, N., and Vuichard, N.: Presentation and Evaluation of the IPSL-CM6A-LR Climate Model, *Journal of Advances in Modeling Earth Systems*, 12, e2019MS002 010, <https://doi.org/10.1029/2019MS002010>, 2020.
- Brands, S.: Which ENSO teleconnections are robust to internal atmospheric variability?, *Geophysical Research Letters*, 44, 1483–1493, 915 <https://doi.org/https://doi.org/10.1002/2016GL071529>, 2017.
- Brands, S., Gutiérrez, J. M., Herrera, S., and Cofiño, A. S.: On the Use of Reanalysis Data for Downscaling, *Journal of Climate*, 25, 2517–2526, <https://doi.org/10.1175/JCLI-D-11-00251.1>, 2012.
- Brands, S., Herrera García, S., Fernández, J., and Gutiérrez, J.: How well do CMIP5 Earth System Models simulate present climate conditions in Europe and Africa? A performance comparison for the downscaling community, *Climate Dynamics*, 41, 803–817, 920 <https://doi.org/10.1007/s00382-013-1742-8>, 2013.
- Brands, S., Herrera, S., and Gutiérrez, J.: Is Eurasian snow cover in October a reliable statistical predictor for the wintertime climate on the Iberian Peninsula?, *International Journal of Climatology*, 34, 1615–1627, <https://doi.org/https://doi.org/10.1002/joc.3788>, 2014.
- Cannon, A.: Reductions in daily continental-scale atmospheric circulation biases between generations of Global Climate Models: CMIP5 to CMIP6, *Environmental Research Letters*, 15, 064 006, <https://doi.org/10.1088/1748-9326/ab7e4f>, 2020.

- 925 Cao, J., Wang, B., Yang, Y.-M., Ma, L., Li, J., Sun, B., Bao, Y., He, J., Zhou, X., and Wu, L.: The NUIST Earth System Model (NESM) version 3: description and preliminary evaluation, *Geoscientific Model Development*, 11, 2975–2993, <https://doi.org/10.5194/gmd-11-2975-2018>, <https://gmd.copernicus.org/articles/11/2975/2018/>, 2018.
- Cherchi, A., Fogli, P. G., Lovato, T., Peano, D., Iovino, D., Gualdi, S., Masina, S., Scoccimarro, E., Materia, S., Bellucci, A., and Navarra, A.: Global Mean Climate and Main Patterns of Variability in the CMCC-CM2 Coupled Model, *Journal of Advances in Modeling Earth*
930 *Systems*, 11, 185–209, <https://doi.org/10.1029/2018MS001369>, 2019.
- Chylek, P., Li, J., Dubey, M. K., Wang, M., and Lesins, G.: Observed and model simulated 20th century Arctic temperature variability: Canadian Earth System Model CanESM2, *Atmospheric Chemistry and Physics Discussions*, 11, 22 893–22 907, <https://doi.org/10.5194/acpd-11-22893-2011>, <https://acp.copernicus.org/preprints/11/22893/2011/>, 2011.
- 935 Collier, M., Jeffrey, S., Rotstayn, L., Wong, K.-H., Dravitzki, S., Moeseneder, C., Hamalainen, C., Syktus, J., Suppiah, R., Antony, J., El Zein, A., and Atif, M.: The CSIRO-Mk3.6.0 Atmosphere-Ocean GCM: participation in CMIP5 and data publication, *Proceedings of MODSIM 2011 International Congress on Modelling and Simulation*, pp. 2691–2697, 2011.
- Collins, W. J., Bellouin, N., Doutriaux-Boucher, M., Gedney, N., Halloran, P., Hinton, T., Hughes, J., Jones, C. D., Joshi, M., Liddicoat, S., Martin, G., O’Connor, F., Rae, J., Senior, C., Sitch, S., Totterdell, I., Wiltshire, A., and Woodward, S.: Development and evaluation of an Earth-System model – HadGEM2, *Geoscientific Model Development*, 4, 1051–1075, <https://doi.org/10.5194/gmd-4-1051-2011>,
940 <https://gmd.copernicus.org/articles/4/1051/2011/>, 2011.
- Craig, A. P., Vertenstein, M., and Jacob, R.: A new flexible coupler for earth system modeling developed for CCSM4 and CESM1, *The International Journal of High Performance Computing Applications*, 26, 31–42, <https://doi.org/10.1177/1094342011428141>, 2012.
- Danabasoglu, G., Lamarque, J.-F., Bacmeister, J., Bailey, D. A., DuVivier, A. K., Edwards, J., Emmons, L. K., Fasullo, J., Garcia, R., Gettelman, A., Hannay, C., Holland, M. M., Large, W. G., Lauritzen, P. H., Lawrence, D. M., Lenaerts, J. T. M., Lindsay, K., Lipscomb,
945 W. H., Mills, M. J., Neale, R., Oleson, K. W., Otto-Bliesner, B., Phillips, A. S., Sacks, W., Tilmes, S., van Kampenhout, L., Vertenstein, M., Bertini, A., Dennis, J., Deser, C., Fischer, C., Fox-Kemper, B., Kay, J. E., Kinnison, D., Kushner, P. J., Larson, V. E., Long, M. C., Mickelson, S., Moore, J. K., Nienhouse, E., Polvani, L., Rasch, P. J., and Strand, W. G.: The Community Earth System Model Version 2 (CESM2), *Journal of Advances in Modeling Earth Systems*, 12, e2019MS001 916, <https://doi.org/10.1029/2019MS001916>, 2020.
- Dee, D. P., Uppala, S. M., Simmons, A. J., Berrisford, P., Poli, P., Kobayashi, S., Andrae, U., Balmaseda, M. A., Balsamo, G., Bauer, P.,
950 Bechtold, P., Beljaars, A. C. M., van de Berg, L., Bidlot, J., Bormann, N., Delsol, C., Dragani, R., Fuentes, M., Geer, A. J., Haimberger, L., Healy, S. B., Hersbach, H., Holm, E. V., Isaksen, L., Kallberg, P., Koehler, M., Matricardi, M., McNally, A. P., Monge-Sanz, B. M., Morcrette, J. J., Park, B. K., Peubey, C., de Rosnay, P., Tavolato, C., Thepaut, J. N., and Vitart, F.: The ERA-Interim reanalysis: configuration and performance of the data assimilation system, *Q. J. R. Meteorol. Soc.*, 137, 553–597, <https://doi.org/10.1002/qj.828>, 2011.
- Deser, C., Simpson, I. R., McKinnon, K. A., and Phillips, A. S.: The Northern Hemisphere Extratropical Atmospheric Circulation Response to ENSO: How Well Do We Know It and How Do We Evaluate Models Accordingly?, *Journal of Climate*, 30, 5059–5082, <https://doi.org/10.1175/JCLI-D-16-0844.1>, <https://doi.org/10.1175/JCLI-D-16-0844.1>, 2017.
- Döscher, R., Acosta, M., Alessandri, A., Anthoni, P., Arneth, A., Arsouze, T., Bergmann, T., Bernadello, R., Boussetta, S., Caron, L.-P., Carver, G., Castrillo, M., Catalano, F., Cvijanovic, I., Davini, P., Dekker, E., Doblas-Reyes, F. J., Docquier, D., Echevarria, P., Fladrich, U., Fuentes-Franco, R., Gröger, M., v. Hardenberg, J., Hieronymus, J., Karami, M. P., Keskinen, J.-P., Koenigk, T., Makkonen, R., Massonnet,
960 F., Ménégos, M., Miller, P. A., Moreno-Chamarro, E., Nieradzick, L., van Noije, T., Nolan, P., O’Donnell, D., Ollinaho, P., van den Oord, G., Ortega, P., Prims, O. T., Ramos, A., Reerink, T., Rousset, C., Ruprich-Robert, Y., Le Sager, P., Schmith, T., Schrödner, R., Serva, F., Sicardi, V., Sloth Madsen, M., Smith, B., Tian, T., Tourigny, E., Uotila, P., Vancoppenolle, M., Wang, S., Wärlind, D., Willén, U., Wyser,

- K., Yang, S., Yepes-Arbós, X., and Zhang, Q.: The EC-Earth3 Earth System Model for the Climate Model Intercomparison Project 6, *Geoscientific Model Development Discussions*, 2021, 1–90, <https://doi.org/10.5194/gmd-2020-446>, <https://gmd.copernicus.org/preprints/gmd-2020-446/>, 2021.
- 965 Dufresne, J.-L., Foujols, M.-A., Denvil, S., Caubel, A., Marti, O., Aumont, O., Balkanski, Y., Bekki, S., Bellenger, H., Benschila, R., Bony, S., Bopp, L., Braconnot, P., Brockmann, P., Cadule, P., Cheruy, F., Codron, F., Cozic, A., Cugnet, D., de Noblet, N., Duvel, J.-P., Etche, C., Fairhead, L., Fichefet, T., Flavoni, S., Friedlingstein, P., Grandpeix, J.-Y., Guez, L., Guilyardi, E., Hauglustaine, D., Hourdin, F., Idelkadi, A., Ghattas, J., Joussaume, S., Kageyama, M., Krinner, G., Labetoulle, S., Lahellec, A., Lefebvre, M.-P., Lefevre, F., Levy, C., Li, Z. X.,
- 970 Lloyd, J., Lott, F., Madec, G., Mancip, M., Marchand, M., Masson, S., Meurdesoif, Y., Mignot, J., Musat, I., Parouty, S., Polcher, J., Rio, C., Schulz, M., Swingedouw, D., Szopa, S., Talandier, C., Terray, P., Viovy, N., and Vuichard, N.: Climate change projections using the IPSL-CM5 Earth System Model: from CMIP3 to CMIP5, *Clim. Dyn.*, 40, 2123–2165, <https://doi.org/10.1007/s00382-012-1636-1>, 2013.
- Eyring, V., Bony, S., Meehl, G. A., Senior, C. A., Stevens, B., Stouffer, R. J., and Taylor, K. E.: Overview of the Coupled Model Intercomparison Project Phase 6 (CMIP6) experimental design and organization, *Geoscientific Model Development*, 9, 1937–1958,
- 975 <https://doi.org/10.5194/gmd-9-1937-2016>, <https://gmd.copernicus.org/articles/9/1937/2016/>, 2016.
- Fogli, P. G., Manzini, E., Vichi, M., Alessandri, A., Patara, L., Gualdi, S., Scoccimarro, E., Masina, S., and Navarra, A.: INGV-CMCC Carbon (ICC): A carbon cycle Earth system model, *SSRN Electronic Journal*, p. 31pp., <https://doi.org/10.2139/ssrn.1517282>, 2009.
- Gates, W.: AMIP - The Atmospheric Model Intercomparison Project, *Bull. Amer. Meteorol. Soc.*, 73, 1962–1970, [https://doi.org/10.1175/1520-0477\(1992\)073<1962:ATAMIP>2.0.CO;2](https://doi.org/10.1175/1520-0477(1992)073<1962:ATAMIP>2.0.CO;2), 1992.
- 980 Gent, P. R., Danabasoglu, G., Donner, L. J., Holland, M. M., Hunke, E. C., Jayne, S. R., Lawrence, D. M., Neale, R. B., Rasch, P. J., Vertenstein, M., Worley, P. H., Yang, Z.-L., and Zhang, M.: The Community Climate System Model Version 4, *Journal of Climate*, 24, 4973–4991, <https://doi.org/10.1175/2011JCLI4083.1>, 2011.
- Giorgetta, M. A., Jungclaus, J., Reick, C. H., Legutke, S., Bader, J., Böttinger, M., Brovkin, V., Crueger, T., Esch, M., Fieg, K., Glushak, K., Gayler, V., Haak, H., Hollweg, H.-D., Ilyina, T., Kinne, S., Kornbluh, L., Matei, D., Mauritsen, T., Mikolajewicz, U., Mueller, W.,
- 985 Notz, D., Pithan, F., Raddatz, T., Rast, S., Redler, R., Roeckner, E., Schmidt, H., Schnur, R., Segschneider, J., Six, K. D., Stockhause, M., Timmreck, C., Wegner, J., Widmann, H., Wieners, K.-H., Claussen, M., Marotzke, J., and Stevens, B.: Climate and carbon cycle changes from 1850 to 2100 in MPI-ESM simulations for the Coupled Model Intercomparison Project phase 5, *Journal of Advances in Modeling Earth Systems*, 5, 572–597, <https://doi.org/10.1002/jame.20038>, <https://agupubs.onlinelibrary.wiley.com/doi/abs/10.1002/jame.20038>, 2013.
- 990 Gourgue, O.: Normalized Taylor diagram Python module (Version 1.0), Zenodo, <https://doi.org/10.5281/zenodo.3715535>, 2020.
- Griffies, S., Winton, M., Donner, L., Horowitz, L., Downes, S., Farneti, R., Gnanadesikan, A., Hurlin, W., Lee, H.-C., Liang, Z., Palter, J., Samuels, B., Wittenberg, A., Wyman, B., Yin, J., and Zadeh, N.: The GFDL-CM3 Coupled Climate Model: Characteristics of the Ocean and Sea Ice Simulations, *Journal of Climate*, 24, 3520–3544, <https://doi.org/10.1175/2011JCLI3964.1>, 2011.
- Grotch, S. and MacCracken, M.: The Use of General Circulation Models to Predict Regional Climatic Change, *Journal of Climate*, 4, 286–
- 995 303, [https://doi.org/10.1175/1520-0442\(1991\)004<0286:TUOGCM>2.0.CO;2](https://doi.org/10.1175/1520-0442(1991)004<0286:TUOGCM>2.0.CO;2), 1991.
- Gutiérrez, J. M., San-Martín, D., Brands, S., Manzananas, R., and Herrera, S.: Reassessing Statistical Downscaling Techniques for Their Robust Application under Climate Change Conditions, *Journal of Climate*, 26, 171–188, <https://doi.org/10.1175/JCLI-D-11-00687.1>, 2013.
- Haarsma, R. J., Roberts, M. J., Vidale, P. L., Senior, C. A., Bellucci, A., Bao, Q., Chang, P., Corti, S., Fučkar, N. S., Guemas, V., von Hardenberg, J., Hazeleger, W., Kodama, C., Koenigk, T., Leung, L. R., Lu, J., Luo, J.-J., Mao, J., Mizielinski, M. S., Mizuta,
- 1000 R., Nobre, P., Satoh, M., Scoccimarro, E., Semmler, T., Small, J., and von Storch, J.-S.: High Resolution Model Intercomparison

- Project (HighResMIP v1.0) for CMIP6, Geoscientific Model Development, 9, 4185–4208, <https://doi.org/10.5194/gmd-9-4185-2016>, <https://gmd.copernicus.org/articles/9/4185/2016/>, 2016.
- 1005 Hajima, T., Watanabe, M., Yamamoto, A., Tatebe, H., Noguchi, M. A., Abe, M., Ohgaito, R., Ito, A., Yamazaki, D., Okajima, H., Ito, A., Takata, K., Ogochi, K., Watanabe, S., and Kawamiya, M.: Development of the MIROC-ES2L Earth system model and the evaluation of biogeochemical processes and feedbacks, Geoscientific Model Development, 13, 2197–2244, <https://doi.org/10.5194/gmd-13-2197-2020>, <https://gmd.copernicus.org/articles/13/2197/2020/>, 2020.
- Harris, C., Millman, K., Walt, S., Gommers, R., Virtanen, P., Cournapeau, D., Wieser, E., Taylor, J., Berg, S., Smith, N., Kern, R., Picus, M., Hoyer, S., Kerkwijk, M., Brett, M., Haldane, A., Río, J., Wiebe, M., Peterson, P., and Oliphant, T.: Array programming with NumPy, Nature, 585, 357–362, <https://doi.org/10.1038/s41586-020-2649-2>, 2020.
- 1010 Hazeleger, W., Severijns, C., Semmler, T., Briceag, S., Yang, S., Wang, X., Wyser, K., Dutra, E., Baldasano, J., Bintanja, R., Bougeault, P., Caballero, R., Ekman, A., Christensen, J., Hurk, B., Jimenez-Guerrero, P., Jones, C., Kallberg, P., Koenigk, T., and Willén, U.: EC-Earth: A Seamless Earth-System Prediction Approach in Action, Bulletin of the American Meteorological Society, 91, 1357–1363, <https://doi.org/10.1175/2010bams2877.1>, 2010.
- 1015 Hazeleger, W., Wang, X., Severijns, C., Briceag, S., Bintanja, R., Sterl, A., Wyser, K., Semmler, T., Yang, S., Hurk, B., Noije, T., Van der Linden, E., and van der Wiel, K.: EC-Earth V2.2: Description and validation of a new seamless Earth system prediction model, Climate Dynamics, 39, 1–19, <https://doi.org/10.1007/s00382-011-1228-5>, 2011.
- 1020 Held, I. M., Guo, H., Adcroft, A., Dunne, J. P., Horowitz, L. W., Krasting, J., Shevliakova, E., Winton, M., Zhao, M., Bushuk, M., Wittenberg, A. T., Wyman, B., Xiang, B., Zhang, R., Anderson, W., Balaji, V., Donner, L., Dunne, K., Durachta, J., Gauthier, P. P. G., Ginoux, P., Golaz, J.-C., Griffies, S. M., Hallberg, R., Harris, L., Harrison, M., Hurlin, W., John, J., Lin, P., Lin, S.-J., Malyshev, S., Menzel, R., Milly, P. C. D., Ming, Y., Naik, V., Paynter, D., Paulot, F., Rammasswamy, V., Reichl, B., Robinson, T., Rosati, A., Seman, C., Silvers, L. G., Underwood, S., and Zadeh, N.: Structure and Performance of GFDL's CM4.0 Climate Model, Journal of Advances in Modeling Earth Systems, 11, 3691–3727, <https://doi.org/10.1029/2019MS001829>, 2019.
- 1025 Hourdin, F., Rio, C., Grandpeix, J.-Y., Madeleine, J.-B., Cheruy, F., Rochetin, N., Jam, A., Musat, I., Idelkadi, A., Fairhead, L., Foujols, M.-A., Mellul, L., Traore, A.-K., Dufresne, J.-L., Boucher, O., Lefebvre, M.-P., Millour, E., Vignon, E., Jouhaud, J., Diallo, F. B., Lott, F., Gastineau, G., Caubel, A., Meurdesoif, Y., and Ghattas, J.: LMDZ6A: The Atmospheric Component of the IPSL Climate Model With Improved and Better Tuned Physics, Journal of Advances in Modeling Earth Systems, 12, e2019MS001892, <https://doi.org/https://doi.org/10.1029/2019MS001892>, <https://agupubs.onlinelibrary.wiley.com/doi/abs/10.1029/2019MS001892>, e2019MS001892 10.1029/2019MS001892, 2020.
- 1030 Hoyer, S. and Hamman, J.: xarray: N-D labeled Arrays and Datasets in Python, Journal of Open Research Software, 5, 10pp., <https://doi.org/10.5334/jors.148>, 2017.
- Hulme, M., Briffal, K., Jones, P., and Senior, C.: Validation of GCM control simulations using indices of daily airflow types over British Isles, Climate Dynamics, 9, 95–105, <https://doi.org/10.1007/BF00210012>, 1993.
- Hunter, J. D.: Matplotlib: A 2D graphics environment, Computing in Science & Engineering, 9, 90–95, <https://doi.org/10.1109/MCSE.2007.55>, 2007.
- 1035 Hurrell, J. W., Holland, M. M., Gent, P. R., Ghan, S., Kay, J. E., Kushner, P. J., Lamarque, J.-F., Large, W. G., Lawrence, D., Lindsay, K., Lipscomb, W. H., Long, M. C., Mahowald, N., Marsh, D. R., Neale, R. B., Rasch, P., Vavrus, S., Vertenstein, M., Bader, D., Collins, W. D., Hack, J. J., Kiehl, J., and Marshall, S.: The Community Earth System Model: A Framework for Collabora-

- tive Research, *Bulletin of the American Meteorological Society*, 94, 1339–1360, <https://doi.org/10.1175/BAMS-D-12-00121.1>, <https://doi.org/10.1175/BAMS-D-12-00121.1>, 2013.
- 1040 Jacob, D., Petersen, J., Eggert, B., Alias, A., Christensen, O., Bouwer, L., Braun, A., Colette, A., Déqué, M., Georgievski, G., Georgopoulou, E., Gobiet, A., Menut, L., Nikulin, G., Haensler, A., Hempelmann, N., Jones, C., Keuler, K., Kovats, S., and Yiou, P.: EURO-CORDEX: New high-resolution climate change projections for European impact research, *Regional Environmental Change*, 14, 563–578, <https://doi.org/10.1007/s10113-013-0499-2>, 2014.
- Jenkinson, A. and Collison, F.: *An Initial Climatology of Gales over the North Sea*, Synoptic Climatology Branch Memorandum, 1977.
- 1045 Jinjun, J.: A Climate-Vegetation Interaction Model: Simulating Physical and Biological Processes at the Surface, *Journal of Biogeography*, 22, 445–451, 1995.
- Jones, C. D.: So What Is in an Earth System Model?, *Journal of Advances in Modeling Earth Systems*, 12, e2019MS001967, <https://doi.org/https://doi.org/10.1029/2019MS001967>, <https://agupubs.onlinelibrary.wiley.com/doi/abs/10.1029/2019MS001967>, e2019MS001967 2019MS001967, 2020.
- 1050 Jones, P. D., Hulme, M., and Briffa, K. R.: A comparison of Lamb circulation types with an objective classification scheme, *International Journal of Climatology*, 13, 655–663, <https://doi.org/10.1002/joc.3370130606>, <https://rmets.onlinelibrary.wiley.com/doi/abs/10.1002/joc.3370130606>, 1993.
- Jones, P. D., Harpham, C., and Briffa, K. R.: Lamb weather types derived from reanalysis products, *International Journal of Climatology*, 33, 1129–1139, <https://doi.org/10.1002/joc.3498>, <https://rmets.onlinelibrary.wiley.com/doi/abs/10.1002/joc.3498>, 2013.
- 1055 Jungclaus, J. H., Fischer, N., Haak, H., Lohmann, K., Marotzke, J., Matei, D., Mikolajewicz, U., Notz, D., and von Storch, J. S.: Characteristics of the ocean simulations in the Max Planck Institute Ocean Model (MPIOM) the ocean component of the MPI-Earth system model, *Journal of Advances in Modeling Earth Systems*, 5, 422–446, <https://doi.org/10.1002/jame.20023>, 2013.
- Kelley, M., Schmidt, G. A., Nazarenko, L. S., Bauer, S. E., Ruedy, R., Russell, G. L., Ackerman, A. S., Aleinov, I., Bauer, M., Bleck, R., Canuto, V., Cesana, G., Cheng, Y., Clune, T. L., Cook, B. I., Cruz, C. A., Del Genio, A. D., Elsaesser, G. S., Faluvegi, G., Kiang, N. Y., 1060 Kim, D., Lacs, A. A., Leboissetier, A., LeGrande, A. N., Lo, K. K., Marshall, J., Matthews, E. E., McDermid, S., Mezuman, K., Miller, R. L., Murray, L. T., Oinas, V., Orbe, C., García-Pando, C. P., Perlwitz, J. P., Puma, M. J., Rind, D., Romanou, A., Shindell, D. T., Sun, S., Tausnev, N., Tsigaridis, K., Tselioudis, G., Weng, E., Wu, J., and Yao, M.-S.: GISS-E2.1: Configurations and Climatology, *Journal of Advances in Modeling Earth Systems*, 12, e2019MS002025, <https://doi.org/10.1029/2019MS002025>, 2020.
- Kirkevåg, A., Iversen, T., Øyvind Seland, Debernard, J. B., Storelvmo, T., and Kristjánsson, J. E.: Aerosol-cloud-climate interactions in the climate model CAM-Oslo, *Tellus A: Dynamic Meteorology and Oceanography*, 60, 492–512, <https://doi.org/10.1111/j.1600-0870.2007.00313.x>, 2008.
- Knutti, R., Sedláček, J., Sanderson, B. M., Lorenz, R., Fischer, E. M., and Eyring, V.: A climate model projection weighting scheme accounting for performance and interdependence, *Geophysical Research Letters*, 44, 1909–1918, <https://doi.org/https://doi.org/10.1002/2016GL072012>, <https://agupubs.onlinelibrary.wiley.com/doi/abs/10.1002/2016GL072012>, 2017.
- 1070 Kobayashi, S., Ota, Y., Harada, Y., Ebata, A., Moriya, M., Onoda, H., Onogi, K., Kamahori, H., Kobayashi, C., Endo, H., Miyaoka, K., and Takahashi, K.: The JRA-55 Reanalysis: General Specifications and Basic Characteristics, *Journal of the Meteorological Society of Japan*. Ser. II, 93, 5–48, <https://doi.org/10.2151/jmsj.2015-001>, 2015.
- Lamb, H.: British Isles Weather types and a register of daily sequence of circulation patterns, 1861-1971, *Geophysical Memoir*, 116, 85pp., HMSO, 1972.

- 1075 Lee, W.-L., Wang, Y.-C., Shiu, C.-J., Tsai, I., Tu, C.-Y., Lan, Y.-Y., Chen, J.-P., Pan, H.-L., and Hsu, H.-H.: Taiwan Earth System Model Version 1: description and evaluation of mean state, *Geoscientific Model Development*, 13, 3887–3904, <https://doi.org/10.5194/gmd-13-3887-2020>, 2020.
- Li, L., Lin, P., Yu, Y.-Q., Zhou, T., Liu, L., Liu, J., Bao, Q., Xu, S., Huang, W., Xia, K., Pu, Y., Dong, L., Shen, S., Liu, Y., Hu, N., Liu, M., Sun, W., Shi, X., and Qiao, F.-L.: The flexible global ocean-atmosphere-land system model, Grid-point Version 2: FGOALS-g2, *Advances in Atmospheric Sciences*, 30, 543–560, <https://doi.org/10.1007/s00376-012-2140-6>, 2013.
- 1080 Li, L., Yu, Y., Tang, Y., Lin, P., Xie, J., Song, M., Dong, L., Zhou, T., Liu, L., Wang, L., Pu, Y., Chen, X., Chen, L., Xie, Z., Liu, H., Zhang, L., Huang, X., Feng, T., Zheng, W., Xia, K., Liu, H., Liu, J., Wang, Y., Wang, L., Jia, B., Xie, F., Wang, B., Zhao, S., Yu, Z., Zhao, B., and Wei, J.: The Flexible Global Ocean-Atmosphere-Land System Model Grid-Point Version 3 (FGOALS-g3): Description and Evaluation, *Journal of Advances in Modeling Earth Systems*, 12, e2019MS002012, <https://doi.org/https://doi.org/10.1029/2019MS002012>, <https://agupubs.onlinelibrary.wiley.com/doi/abs/10.1029/2019MS002012>, e2019MS002012 2019MS002012, 2020.
- 1085 Lipscomb, W. H., Price, S. F., Hoffman, M. J., Leguy, G. R., Bennett, A. R., Bradley, S. L., Evans, K. J., Fyke, J. G., Kennedy, J. H., Perego, M., Ranken, D. M., Sacks, W. J., Salinger, A. G., Vargo, L. J., and Worley, P. H.: Description and evaluation of the Community Ice Sheet Model (CISM) v2.1, *Geoscientific Model Development*, 12, 387–424, <https://doi.org/10.5194/gmd-12-387-2019>, <https://gmd.copernicus.org/articles/12/387/2019/>, 2019.
- 1090 Lorenzo, M. N., Taboada, J. J., and Gimeno, L.: Links between circulation weather types and teleconnection patterns and their influence on precipitation patterns in Galicia (NW Spain), *International Journal of Climatology*, 28, 1493–1505, <https://doi.org/10.1002/joc.1646>, 2008.
- Lurton, T., Balkanski, Y., Bastrikov, V., Bekki, S., Bopp, L., Braconnot, P., Brockmann, P., Cadule, P., Contoux, C., Cozic, A., Cugnet, D., Dufresne, J.-L., Éthé, C., Foujols, M.-A., Ghattas, J., Hauglustaine, D., Hu, R.-M., Kageyama, M., Khodri, M., Lebas, N., Levavasseur, G., Marchand, M., Ottlé, C., Peylin, P., Sima, A., Szopa, S., Thiéblemont, R., Vuichard, N., and Boucher, O.: Implementation of the CMIP6 Forcing Data in the IPSL-CM6A-LR Model, *Journal of Advances in Modeling Earth Systems*, 12, e2019MS001940, <https://doi.org/https://doi.org/10.1029/2019MS001940>, <https://agupubs.onlinelibrary.wiley.com/doi/abs/10.1029/2019MS001940>, e2019MS001940 10.1029/2019MS001940, 2020.
- 1095 Madec, G.: NEMO ocean engine, Note du Pôle de modélisation, Institut Pierre-Simon Laplace (IPSL), France, No 27, ISSN No 1288-1619, 2008.
- 1100 Madec, G., Delécluse, P., Imbard, M., and Lévy, C.: OPA 8.1 Ocean General Circulation Model reference manual, Notes du pôle de modélisation, laboratoire d'océanographie dynamique et de climatologie, Institut Pierre Simon Laplace des sciences de l'environnement global, 11, 91pp., 1998.
- Maraun, D., Wetterhall, F., Ireson, A. M., Chandler, R. E., Kendon, E. J., Widmann, M., Brienen, S., Rust, H. W., Sauter, T., Themeßl, M., Venema, V. K. C., Chun, K. P., Goodess, C. M., Jones, R. G., Onof, C., Vrac, M., and Thiele-Eich, I.: Precipitation downscaling under climate change: Recent developments to bridge the gap between dynamical models and the end user, *Reviews of Geophysics*, 48, RG3003, <https://doi.org/10.1029/2009RG000314>, 2010.
- 1105 Maraun, D., Shepherd, T., Widmann, M., Zappa, G., Walton, D., Gutiérrez, J., Hagemann, S., Richter, I., Soares, P., Hall, A., and Mearns, L.: Towards process-informed bias correction of climate change simulations, *Nature Climate Change*, 7, 764–773, <https://doi.org/10.1038/nclimate3418>, 2017.
- 1110 Martin, T. H. D. T. G. M., Bellouin, N., Collins, W. J., Culverwell, I. D., Halloran, P. R., Hardiman, S. C., Hinton, T. J., Jones, C. D., McDonald, R. E., McLaren, A. J., O'Connor, F. M., Roberts, M. J., Rodriguez, J. M., Woodward, S., Best, M. J., Brooks, M. E., Brown,

- 1115 A. R., Butchart, N., Dearden, C., Derbyshire, S. H., Dharssi, I., Doutriaux-Boucher, M., Edwards, J. M., Falloon, P. D., Gedney, N., Gray, L. J., Hewitt, H. T., Hobson, M., Huddleston, M. R., Hughes, J., Ineson, S., Ingram, W. J., James, P. M., Johns, T. C., Johnson, C. E., Jones, A., Jones, C. P., Joshi, M. M., Keen, A. B., Liddicoat, S., Lock, A. P., Maidens, A. V., Manners, J. C., Milton, S. F., Rae, J. G. L., Ridley, J. K., Sellar, A., Senior, C. A., Totterdell, I. J., Verhoef, A., Vidale, P. L., and Wiltshire, A.: The HadGEM2 family of Met Office Unified Model climate configurations, *Geoscientific Model Development*, 4, 723–757, <https://doi.org/10.5194/gmd-4-723-2011>, <https://gmd.copernicus.org/articles/4/723/2011/>, 2011.
- 1120 Mauritsen, T., Bader, J., Becker, T., Behrens, J., Bittner, M., Brokopf, R., Brovkin, V., Claussen, M., Crueger, T., Esch, M., Fast, I., Fiedler, S., Fläschner, D., Gayler, V., Giorgetta, M., Goll, D. S., Haak, H., Hagemann, S., Hedemann, C., Hohenegger, C., Ilyina, T., Jahns, T., Jimenéz-de-la Cuesta, D., Jungclaus, J., Kleinen, T., Kloster, S., Kracher, D., Kinne, S., Kleberg, D., Lasslop, G., Kornblueh, L., Marotzke, J., Matei, D., Meraner, K., Mikolajewicz, U., Modali, K., Möbis, B., Müller, W. A., Nabel, J. E. M. S., Nam, C. C. W., Notz, D., Nyawira, S.-S., Paulsen, H., Peters, K., Pincus, R., Pohlmann, H., Pongratz, J., Popp, M., Raddatz, T. J., Rast, S., Redler, R., Reick, C. H., Rohrschneider, T., Schemann, V., Schmidt, H., Schnur, R., Schulzweida, U., Six, K. D., Stein, L., Stemmler, I., Stevens, B., von
- 1125 Storch, J.-S., Tian, F., Voigt, A., Vrese, P., Wieners, K.-H., Wilkenskjeld, S., Winkler, A., and Roeckner, E.: Developments in the MPI-M Earth System Model version 1.2 (MPI-ESM1.2) and Its Response to Increasing CO₂, *Journal of Advances in Modeling Earth Systems*, 11, 998–1038, <https://doi.org/10.1029/2018MS001400>, 2019.
- McKinney, W.: Data Structures for Statistical Computing in Python, in: *Proceedings of the 9th Python in Science Conference*, edited by Stéfan van der Walt and Jarrod Millman, pp. 56 – 61, <https://doi.org/10.25080/Majora-92bf1922-00a>, 2010.
- 1130 Mearns, L., Giorgi, F., Whetton, P., Pabón Caicedo, J. D., Hulme, M., and Lal, M.: Guidelines for Use of Climate Scenarios Developed from Regional Climate Model Experiments (version 1.0.0), p. 38pp., <https://doi.org/10.5281/zenodo.1421091>, http://www.ipcc-data.org/guidelines/dgm_no1_v1_10-2003.pdf, 2003.
- 1135 Müller, W. A., Jungclaus, J. H., Mauritsen, T., Baehr, J., Bittner, M., Budich, R., Bunzel, F., Esch, M., Ghosh, R., Haak, H., Ilyina, T., Kleine, T., Kornblueh, L., Li, H., Modali, K., Notz, D., Pohlmann, H., Roeckner, E., Stemmler, I., Tian, F., and Marotzke, J.: A Higher-resolution Version of the Max Planck Institute Earth System Model (MPI-ESM1.2-HR), *Journal of Advances in Modeling Earth Systems*, 10, 1383–1413, <https://doi.org/10.1029/2017MS001217>, <https://agupubs.onlinelibrary.wiley.com/doi/abs/10.1029/2017MS001217>, 2018.
- Osborn, T., Conway, D., Hulme, M., Gregory, J., and Jones, P.: Air flow influences on local climate: Observed and simulated mean relationships for the United Kingdom, *Climate Research*, 13, 173–191, <https://doi.org/10.3354/cr013173>, 1999.
- 1140 Otero, N., Sillmann, J., and Butler, T.: Assessment of an extended version of the Jenkinson-Collision classification on CMIP5 models over Europe, *Climate Dynamics*, p. 1559–1579, <https://doi.org/10.1007/s00382-017-3705-y>, 2017.
- Pak, G., Noh, Y., Lee, M.-I., Yeh, S.-W., Kim, D., Kim, S.-Y., Lee, J.-L., Lee, H. J., Hyun, S.-H., Lee, K.-Y., Lee, J.-H., Park, Y.-G., Jin, H., Park, H., and Kim, Y. H.: Korea Institute of Ocean Science and Technology Earth System Model and Its Simulation Characteristics, *Ocean Science Journal*, 56, 18–45, <https://doi.org/10.1007/s12601-021-00001-7>, 2021.
- 1145 Palmer, T. and Stevens, B.: The scientific challenge of understanding and estimating climate change, *Proceedings of the National Academy of Sciences*, 116, 24 390–24 395, <https://doi.org/10.1073/pnas.1906691116>, <https://www.pnas.org/content/116/49/24390>, 2019.
- Palmer, T. N., Doblas-Reyes, F. J., Weisheimer, A., and Rodwell, M. J.: Toward Seamless Prediction: Calibration of Climate Change Projections Using Seasonal Forecasts, *Bulletin of the American Meteorological Society*, 89, 459–470, <https://doi.org/10.1175/BAMS-89-4-459>, 2008.

- 1150 Park, S., Shin, J., Kim, S., Oh, E., and Kim, Y.: Global Climate Simulated by the Seoul National University Atmosphere Model Version 0 with a Unified Convection Scheme (SAM0-UNICON), *Journal of Climate*, 32, 2917–2949, <https://doi.org/10.1175/JCLI-D-18-0796.1>, 2019.
- Perez, J., Menendez, M., Mendez, F., and Losada, I.: Evaluating the performance of CMIP3 and CMIP5 global climate models over the north-east Atlantic region, *Climate Dynamics*, p. 2663–2680, <https://doi.org/10.1007/s00382-014-2078-8>, 2014.
- 1155 Perry, A. and Mayes, J.: The Lamb weather type catalogue, *Weather*, 53, 222–229, <https://doi.org/10.1002/j.1477-8696.1998.tb06387.x>, <https://rmets.onlinelibrary.wiley.com/doi/abs/10.1002/j.1477-8696.1998.tb06387.x>, 1998.
- Prein, A. F., Bukovsky, M. S., Mearns, L. O., Bruyère, C. L., and Done, J. M.: Simulating North American Weather Types With Regional Climate Models, *Frontiers in Environmental Science*, 7, 36, <https://doi.org/10.3389/fenvs.2019.00036>, 2019.
- 1160 Roberts, M., Baker, A., Blockley, E., Calvert, D., Coward, A., Hewitt, H., Jackson, L., Kuhlbrodt, T., Mathiot, P., Roberts, C., Schiemann, R., Seddon, J., Vannièrè, B., and Vidale, P.: Description of the resolution hierarchy of the global coupled HadGEM3-GC3.1 model as used in CMIP6 HighResMIP experiments, *Geoscientific Model Development Discussions*, pp. 1–47, <https://doi.org/10.5194/gmd-2019-148>, 2019.
- San-Martín, D., Manzananas, R., Brands, S., Herrera, S., and Gutiérrez, J. M.: Reassessing Model Uncertainty for Regional Projections of Precipitation with an Ensemble of Statistical Downscaling Methods, *Journal of Climate*, 30, 203–223, <https://doi.org/10.1175/JCLI-D-16-0366.1>, 2016.
- 1165 Schmidt, G. A., Kelley, M., Nazarenko, L., Ruedy, R., Russell, G. L., Aleinov, I., Bauer, M., Bauer, S. E., Bhat, M. K., Bleck, R., Canuto, V., Chen, Y.-H., Cheng, Y., Clune, T. L., Del Genio, A., de Fainchtein, R., Faluvegi, G., Hansen, J. E., Healy, R. J., Kiang, N. Y., Koch, D., Laxis, A. A., LeGrande, A. N., Lerner, J., Lo, K. K., Matthews, E. E., Menon, S., Miller, R. L., Oinas, V., Olosio, A. O., Perlwitz, J. P., Puma, M. J., Putman, W. M., Rind, D., Romanou, A., Sato, M., Shindell, D. T., Sun, S., Syed, R. A., Tausnev, N., Tsigaridis, K., Unger, N., Voulgarakis, A., Yao, M.-S., and Zhang, J.: Configuration and assessment of the GISS ModelE2 contributions to the CMIP5 archive, *Journal of Advances in Modeling Earth Systems*, 6, 141–184, <https://doi.org/10.1002/2013MS000265>, <https://agupubs.onlinelibrary.wiley.com/doi/abs/10.1002/2013MS000265>, 2014.
- 1170 Schubert, S. D., Stewart, R. E., Wang, H., Barlow, M., Berbery, E. H., Cai, W., Hoerling, M. P., Kanikicharla, K. K., Koster, R. D., Lyon, B., Mariotti, A., Mechoso, C. R., Müller, O. V., Rodriguez-Fonseca, B., Seager, R., Seneviratne, S. I., Zhang, L., and Zhou, T.: Global Meteorological Drought: A Synthesis of Current Understanding with a Focus on SST Drivers of Precipitation Deficits, *Journal of Climate*, 29, 3989–4019, <https://doi.org/10.1175/JCLI-D-15-0452.1>, <https://doi.org/10.1175/JCLI-D-15-0452.1>, 2016.
- Scoccimarro, E., Gualdi, S., Bellucci, A., Sanna, A., Giuseppe Fogli, P., Manzini, E., Vichi, M., Oddo, P., and Navarra, A.: Effects of Tropical Cyclones on Ocean Heat Transport in a High-Resolution Coupled General Circulation Model, *Journal of Climate*, 24, 4368–4384, <https://doi.org/10.1175/2011JCLI4104.1>, 2011.
- 1180 Seland, Ø., Bentsen, M., Seland Graff, L., Olivíe, D., Toniazzo, T., Gjermundsen, A., Debernard, J. B., Gupta, A. K., He, Y., Kirkevåg, A., Schwinger, J., Tjiputra, J., Schancke Aas, K., Bethke, I., Fan, Y., Griesfeller, J., Grini, A., Guo, C., Ilicak, M., Hafsaht Karset, I. H., Landgren, O., Liakka, J., Onsum Moseid, K., Nummelin, A., Spensberger, C., Tang, H., Zhang, Z., Heinze, C., Iverson, T., and Schulz, M.: The Norwegian Earth System Model, NorESM2 – Evaluation of theCMIP6 DECK and historical simulations, *Geoscientific Model Development*, 2020, 1–68, <https://doi.org/10.5194/gmd-2019-378>, <https://gmd.copernicus.org/preprints/gmd-2019-378/>, 2020.
- 1185 Semmler, T., Danilov, S., Gierz, P., Goessling, H. F., Hegewald, J., Hinrichs, C., Koldunov, N., Khosravi, N., Mu, L., Rackow, T., Sein, D. V., Sidorenko, D., Wang, Q., and Jung, T.: Simulations for CMIP6 With the AWI Climate Model AWI-CM-1-1, *Journal of Advances in Modeling Earth Systems*, 12, e2019MS002009, <https://doi.org/10.1029/2019MS002009>, 2020.

- Soares, P. M. M., Maraun, D., Brands, S., Jury, M. W., Gutiérrez, J. M., San-Martín, D., Hertig, E., Huth, R., Belušić Vozila, A., Cardoso, R. M., Kotlarski, S., Drobinski, P., and Obermann-Hellhund, A.: Process-based evaluation of the VALUE perfect predictor experiment of statistical downscaling methods, *International Journal of Climatology*, 39, 3868–3893, <https://doi.org/10.1002/joc.5911>, 2019.
- 1190 Spellman, G.: An assessment of the Jenkinson and Collison synoptic classification to a continental mid-latitude location, *Theoretical and Applied Climatology*, 128, 731–744, <https://doi.org/10.1007/s00704-015-1711-8>, 2016.
- Stainforth, D. A., Allen, M. R., Tredger, E. R., and Smith, L. A.: Confidence, uncertainty and decision-support relevance in climate predictions, *Philos. Trans. R. Soc. A-Math. Phys. Eng. Sci.*, 365, 2145–2161, <https://doi.org/10.1098/rsta.2007.2074>, 2007.
- Sterl, A.: On the (In)Homogeneity of Reanalysis Products, *Journal of Climate*, 17, 3866 – 3873, [https://doi.org/10.1175/1520-0442\(2004\)017<3866:OTIORP>2.0.CO;2](https://doi.org/10.1175/1520-0442(2004)017<3866:OTIORP>2.0.CO;2), 2004.
- 1195 Stryhal, J. and Huth, R.: Classifications of winter atmospheric circulation patterns: validation of CMIP5 GCMs over Europe and the North Atlantic, *Climate Dynamics*, 52, 3575–3598, <https://doi.org/10.1007/s00382-018-4344-7>, 2018.
- Swapna, P., Koll, R., Aparna, K., Kulkarni, K., Ag, P., Ashok, K., Raghavan, K., Moorthi, S., Kumar, A., and Goswami, B. N.: The IITM Earth System Model: Transformation of a Seasonal Prediction Model to a Long Term Climate Model, *Bulletin of the American Meteorological Society*, 96, 1351–1367, <https://doi.org/10.1175/BAMS-D-13-00276.1>, 2015.
- 1200 Swart, N. C., Cole, J. N. S., Kharin, V. V., Lazare, M., Scinocca, J. F., Gillett, N. P., Anstey, J., Arora, V., Christian, J. R., Hanna, S., Jiao, Y., Lee, W. G., Majaess, F., Saenko, O. A., Seiler, C., Seinen, C., Shao, A., Sigmond, M., Solheim, L., von Salzen, K., Yang, D., and Winter, B.: The Canadian Earth System Model version 5 (CanESM5.0.3), *Geoscientific Model Development*, 12, 4823–4873, <https://doi.org/10.5194/gmd-12-4823-2019>, <https://gmd.copernicus.org/articles/12/4823/2019/>, 2019.
- 1205 Sférian, R., Nabat, P., Michou, M., Saint-Martin, D., Voldoire, A., Colin, J., Decharme, B., Delire, C., Berthet, S., Chevallier, M., Sénési, S., Franchisteguy, L., Vial, J., Mallet, M., Joetzjer, E., Geoffroy, O., Guérémy, J.-F., Moine, M.-P., Msadek, R., Ribes, A., Rocher, M., Roehrig, R., Salas-y Mélia, D., Sanchez, E., Terray, L., Valcke, S., Waldman, R., Aumont, O., Bopp, L., Deshayes, J., Éthé, C., and Madec, G.: Evaluation of CNRM Earth System Model, CNRM-ESM2-1: Role of Earth System Processes in Present-Day and Future Climate, *Journal of Advances in Modeling Earth Systems*, 11, 4182–4227, <https://doi.org/10.1029/2019MS001791>, 2019.
- 1210 Sférian, R., Berthet, S., Yool, A., Palmiéri, J., Bopp, L., Tagliabue, A., Kwiatkowski, L., Aumont, O., Christian, J., Dunne, J., Gehlen, M., Ilyina, T., John, J., Li, H., Long, M., Luo, J., Nakano, H., Romanou, A., Schwinger, J., and Yamamoto, A.: Tracking Improvement in Simulated Marine Biogeochemistry Between CMIP5 and CMIP6, *Current Climate Change Reports*, 6, 95–119, <https://doi.org/10.1007/s40641-020-00160-0>, 2020.
- Tatebe, H., Ogura, T., Nitta, T., Komuro, Y., Ogochi, K., Takemura, T., Sudo, K., Sekiguchi, M., Abe, M., Saito, F., Chikira, M., Watanabe, S., Mori, M., Hirota, N., Kawatani, Y., Mochizuki, T., Yoshimura, K., Takata, K., O’ishi, R., Yamazaki, D., Suzuki, T., Kurogi, M., Kataoka, T., Watanabe, M., and Kimoto, M.: Description and basic evaluation of simulated mean state, internal variability, and climate sensitivity in MIROC6, *Geoscientific Model Development*, 12, 2727–2765, <https://doi.org/10.5194/gmd-12-2727-2019>, 2019.
- 1215 Taylor, K. E.: Summarizing multiple aspects of model performance in a single diagram, *Journal of Geophysical Research: Atmospheres*, 106, 7183–7192, <https://doi.org/10.1029/2000JD900719>, <https://agupubs.onlinelibrary.wiley.com/doi/abs/10.1029/2000JD900719>, 2001.
- 1220 Tegen, I., Neubauer, D., Ferrachat, S., Siegenthaler-Le Drian, C., Bey, I., Schutgens, N., Stier, P., Watson-Parris, D., Stanelle, T., Schmidt, H., Rast, S., Kokkola, H., Schultz, M., Schroeder, S., Daskalakis, N., Barthel, S., Heinold, B., and Lohmann, U.: The global aerosol–climate model ECHAM6.3–HAM2.3 – Part 1: Aerosol evaluation, *Geoscientific Model Development*, 12, 1643–1677, <https://doi.org/10.5194/gmd-12-1643-2019>, <https://gmd.copernicus.org/articles/12/1643/2019/>, 2019.

- 1225 Trigo, R. M. and DaCamara, C. C.: Circulation weather types and their influence on the precipitation regime in Portugal, *International Journal of Climatology*, 20, 1559–1581, <https://doi.org/10.1002/1097-0088>, 2000.
- Turco, M., Quintana-Seguí, P., Llasat, M. C., Herrera, S., and Gutiérrez, J. M.: Testing MOS precipitation down-scaling for ENSEMBLES regional climate models over Spain, *Journal of Geophysical Research: Atmospheres*, 116, <https://doi.org/https://doi.org/10.1029/2011JD016166>, <https://agupubs.onlinelibrary.wiley.com/doi/abs/10.1029/2011JD016166>, 2011.
- Valcke, S.: OASIS3 user guide, PRISM Support Initiative Report, 3, 68pp., 2006.
- 1230 Virtanen, P., Gommers, R., Oliphant, T., Haberland, M., Reddy, T., Cournapeau, D., Burovski, E., Peterson, P., Weckesser, W., Bright, J., Walt, S., Brett, M., Wilson, J., Millman, K., Mayorov, N., Nelson, A., Jones, E., Kern, R., and Larson, E.: SciPy 1.0: fundamental algorithms for scientific computing in Python, *Nature Methods*, 17, 1–12, <https://doi.org/10.1038/s41592-019-0686-2>, 2020.
- 1235 Voldoire, A., Sanchez-Gomez, E., Salas y Melia, D., Decharme, B., Cassou, C., Senesi, S., Valcke, S., Beau, I., Alias, A., Chevallier, M., Deque, M., Deshayes, J., Douville, H., Fernandez, E., Madec, G., Maisonnave, E., Moine, M.-P., Planton, S., Saint-Martin, D., Szopa, S., Tyteca, S., Alkama, R., Belamari, S., Braun, A., Coquart, L., and Chauvin, F.: The CNRM-CM5.1 global climate model: description and basic evaluation, *Clim. Dyn.*, 40, 2091–2121, <https://doi.org/10.1007/s00382-011-1259-y>, 2013.
- 1240 Voldoire, A., Saint-Martin, D., Sénési, S., Decharme, B., Alias, A., Chevallier, M., Colin, J., Guérémy, J.-F., Michou, M., Moine, M.-P., Nabat, P., Roehrig, R., Salas y Méliá, D., Séférian, R., Valcke, S., Beau, I., Belamari, S., Berthet, S., Cassou, C., Cattiaux, J., Deshayes, J., Douville, H., Ethé, C., Franchistéguy, L., Geoffroy, O., Lévy, C., Madec, G., Meurdesoif, Y., Msadek, R., Ribes, A., Sanchez-Gomez, E., Terray, L., and Waldman, R.: Evaluation of CMIP6 DECK Experiments With CNRM-CM6-1, *Journal of Advances in Modeling Earth Systems*, 11, 2177–2213, <https://doi.org/10.1029/2019MS001683>, 2019.
- Volodin, E., Diansky, N., and Gusev, A.: Simulating present-day climate with the INMCM4.0 coupled model of the atmospheric and oceanic general circulations, *Izvestiya, Atmospheric and Oceanic Physics*, 46, 414–431, <https://doi.org/10.1134/S000143381004002X>, 2010.
- 1245 Waliser, D., Gleckler, P. J., Ferraro, R., Taylor, K. E., Ames, S., Biard, J., Bosilovich, M. G., Brown, O., Chepfer, H., Cinquini, L., Durack, P. J., Eyring, V., Mathieu, P.-P., Lee, T., Pinnock, S., Potter, G. L., Rixen, M., Saunders, R., Schulz, J., Thépaut, J.-N., and Tuma, M.: Observations for Model Intercomparison Project (Obs4MIPs): status for CMIP6, *Geoscientific Model Development*, 13, 2945–2958, <https://doi.org/10.5194/gmd-13-2945-2020>, <https://gmd.copernicus.org/articles/13/2945/2020/>, 2020.
- 1250 Walters, D., Baran, A. J., Boutle, I., Brooks, M., Earnshaw, P., Edwards, J., Furtado, K., Hill, P., Lock, A., Manners, J., Morcrette, C., Mulcahy, J., Sanchez, C., Smith, C., Stratton, R., Tennant, W., Tomassini, L., Van Weverberg, K., Vosper, S., Willett, M., Browse, J., Bushell, A., Carslaw, K., Dalvi, M., Essery, R., Gedney, N., Hardiman, S., Johnson, B., Johnson, C., Jones, A., Jones, C., Mann, G., Milton, S., Rumbold, H., Sellar, A., Ujiie, M., Whittall, M., Williams, K., and Zerroukat, M.: The Met Office Unified Model Global Atmosphere 7.0/7.1 and JULES Global Land 7.0 configurations, *Geoscientific Model Development*, 12, 1909–1963, <https://doi.org/10.5194/gmd-12-1909-2019>, <https://gmd.copernicus.org/articles/12/1909/2019/>, 2019.
- 1255 Wang, N., Zhu, L., Yang, H., and Han, L.: Classification of Synoptic Circulation Patterns for Fog in the Urumqi Airport, *Atmospheric and Climate Sciences*, 07, 352–366, <https://doi.org/10.4236/acs.2017.73026>, 2017.
- Watanabe, M., Suzuki, T., O’ishi, R., Komuro, Y., Watanabe, S., Emori, S., Takemura, T., Chikira, M., Ogura, T., Sekiguchi, M., Takata, K., Yamazaki, D., Yokohata, T., Nozawa, T., Hasumi, H., Tatebe, H., and Kimoto, M.: Improved Climate Simulation by MIROC5: Mean States, Variability, and Climate Sensitivity, *Journal of Climate*, 23, 6312–6335, <https://doi.org/10.1175/2010JCLI3679.1>, 2010.
- 1260 Watanabe, S., Hajima, T., Sudo, K., Nagashima, T., Takemura, T., Okajima, H., Nozawa, T., Kawase, H., Abe, M., Yokohata, T., Ise, T., Sato, H., Kato, E., Takata, K., Emori, S., and Kawamiya, M.: MIROC-ESM 2010: model description and basic results of CMIP5-20c3m experiments, *Geoscientific Model Development*, 4, 845–872, <https://doi.org/10.5194/gmd-4-845-2011>, 2011.

- Wilby, R. L. and Quinn, N. W.: Reconstructing multi-decadal variations in fluvial flood risk using atmospheric circulation patterns, *Journal of Hydrology*, 487, 109 – 121, <https://doi.org/https://doi.org/10.1016/j.jhydrol.2013.02.038>, 2013.
- 1265 Wu, T., Yu, R., and Zhang, F.: A Modified Dynamic Framework for the Atmospheric Spectral Model and Its Application, *Journal of the Atmospheric Sciences*, 65, 2235–2253, <https://doi.org/10.1175/2007JAS2514.1>, 2008.
- Wu, T., Li, W., Ji, J., Xin, X., Li, L., Wang, Z., Zhang, Y., Li, J., Zhang, F., Wei, M., Shi, X., Wu, F., Zhang, L., Chu, M., Jie, W., Liu, Y., Wang, F., Liu, X., Li, Q., Dong, M., Liang, X., Gao, Y., and Zhang, J.: Global carbon budgets simulated by the Beijing Climate Center Climate System Model for the last century, *Journal of Geophysical Research: Atmospheres*, 118, 4326–4347, <https://doi.org/https://doi.org/10.1002/jgrd.50320>, <https://agupubs.onlinelibrary.wiley.com/doi/abs/10.1002/jgrd.50320>, 2013.
- 1270 Wu, T., Song, L., Li, W., Wang, Z., Zhang, H., Xin, X., Zhang, Y., Zhang, L., Li, J., Wu, F., Liu, Y., Zhang, F., Shi, X., Chu, M., Zhang, J., Fang, Y., Wang, F., Lu, Y., Liu, X., and Zhou, M.: An Overview of BCC Climate System Model Development and Application for Climate Change Studies, *Acta Meteorologica Sinica*, 28, <https://doi.org/10.1007/s13351-014-3041-7>, 2014.
- Wu, T., Lu, Y., Fang, Y., Xin, X., Li, L., Li, W., Jie, W., Zhang, J., Liu, Y., Zhang, L., Zhang, F., Zhang, Y., Wu, F., Li, J., Chu, M., Wang, Z., Shi, X., Liu, X., Wei, M., Huang, A., Zhang, Y., and Liu, X.: The Beijing Climate Center Climate System Model (BCC-CSM): the 1275 main progress from CMIP5 to CMIP6, *Geoscientific Model Development*, 12, 1573–1600, <https://doi.org/10.5194/gmd-12-1573-2019>, <https://gmd.copernicus.org/articles/12/1573/2019/>, 2019.
- Yukimoto, S., Yoshimura, H., Hosaka, M., Sakami, T., Tsujino, H., Hirabara, M., Tanaka, T., Deushi, M., Obata, A., Nakano, H., Adachi, Y., Shindo, E., Yabu, S., Ose, T., and Kitoh, A.: Meteorological Research Institute-Earth System Model Version 1 (MRI-ESM1) — Model Description —, *Technical Reports of the Meteorological Research Institute*, 64, 1–96, 2011.
- 1280 Yukimoto, S., Kawai, H., Koshiro, T., Oshima, N., Yoshida, K., Urakawa, S., Tsujino, H., Deushi, M., Tanaka, T., Hosaka, M., Yabu, S., Yoshimura, H., Shindo, E., Mizuta, R., Obata, A., Adachi, Y., and Ishii, M.: The Meteorological Research Institute Earth System Model Version 2.0, MRI-ESM2.0: Description and Basic Evaluation of the Physical Component, *Journal of the Meteorological Society of Japan. Ser. II*, 97, 931–965, <https://doi.org/10.2151/jmsj.2019-051>, 2019.
- Ziehn, T., Chamberlain, M. A., Law, R. M., Lenton, A., Bodman, R. W., Dix, M., Stevens, L., Wang, Y.-P., and Sribnovsky, 1285 J.: The Australian Earth System Model: ACCESS-ESM1.5, *Journal of Southern Hemisphere Earth Systems Science*, in press, <https://doi.org/https://doi.org/10.1071/ES19035>, 2020.

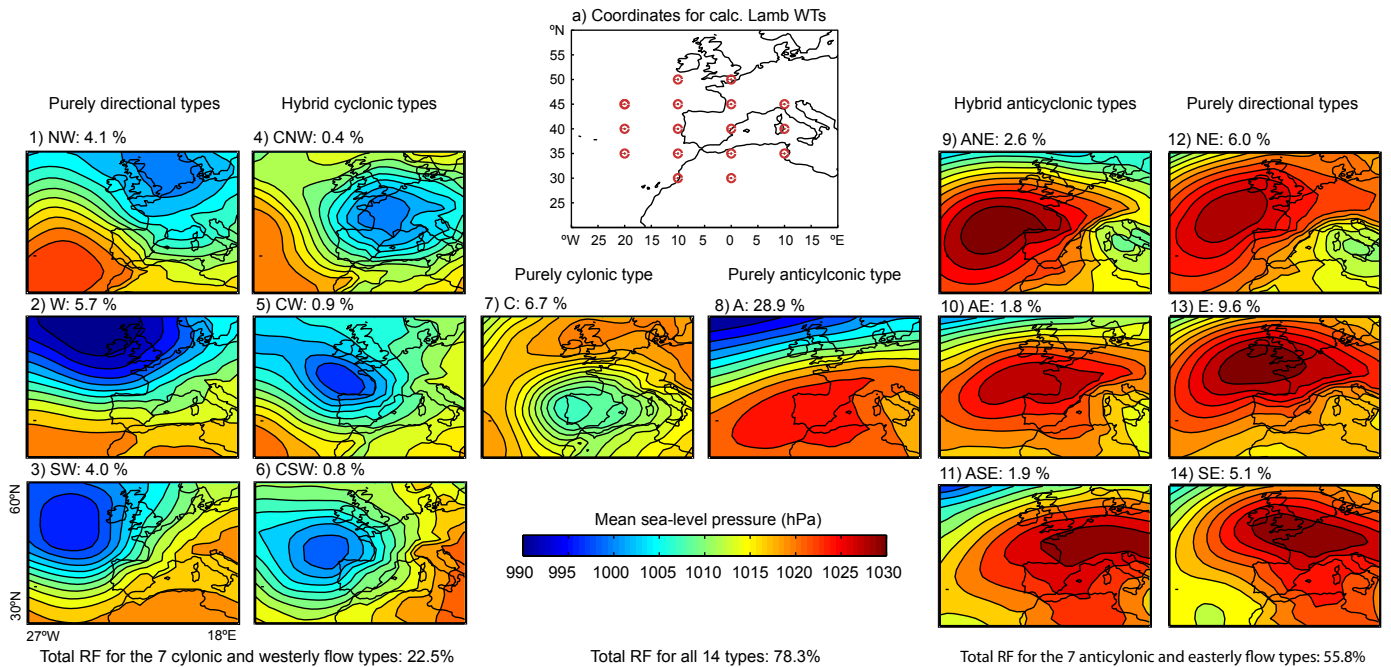


Figure 1. Illustrative example for the usage of the Lamb weather types approach over the central Iberian Peninsula. Shown is the coordinate system configured for this region and a subset of 14 types as well as their relative occurrence frequencies. Note that in the present study, all 27 types originally defined in ? are being used. The figure is taken from ?, courtesy to John Wiley and Sons.

	Ocean Model	Hist
, 38 lv	NOAA/GFDL MOM4p1, 360 × 300, 50 lv	r1il
192 × 144, 38 lv	NOAA/GFDL MOM4p1, 360 × 300, 50 lv	r1il
144, 85 lv	ACCESS-OM2 (GFDL-MOM5), 360 × 300, 50 lv	r1il
192 × 145, 38 lv	ACCESS-OM2 (GFDL-MOM5), 360 × 300, 50 lv	r1il
× 96, 47 lv	FESOM 1.4, 126859 wet nodes (unstructured mesh), 46 lv	r1il
< 64 (T42), 26 lv	GFDL-MOM4, 360 × 232, 40 lv	r1il
0 × 160, 46 lv	GFDL-MOM4, 360 × 232, 40 lv	r1il
5 lv	CanOM4, 256 × 192, 40 lv	r1il
lv	POPv2, 384 × 320, 60 lv	r6il
T159, 31 lv	OPA8.2-ORCA2, 31 lv	r1il
0 lv	NEMO3.6-ORCA1, 50 lv	r1il
0 lv	NEMO3.6-ORCA1, 50 lv	r1il
1 256 × 128, 31 lv	NEMO3.2-ORCA1, 42 lv	r1il
8, 91 lv, T127 Gauss-red-Gr 24572 grid-points-gb	NEMO3.6-ORCA1, 75 lv	r1il
60, 91 lv, T359 Gauss-red-Gr 181724 grid-points-gb	NEMO3.6-ORCA025, 75 lv	r1il
60, T127 Gauss-red-Gr 24572 grid-points-gb, 91 lv	NEMO3.6-ORCA1, 75 lv	r1il
6, T63 spectral, 18 lv	GFDL MOM2.2, 192 × 189, 31 lv	r1il

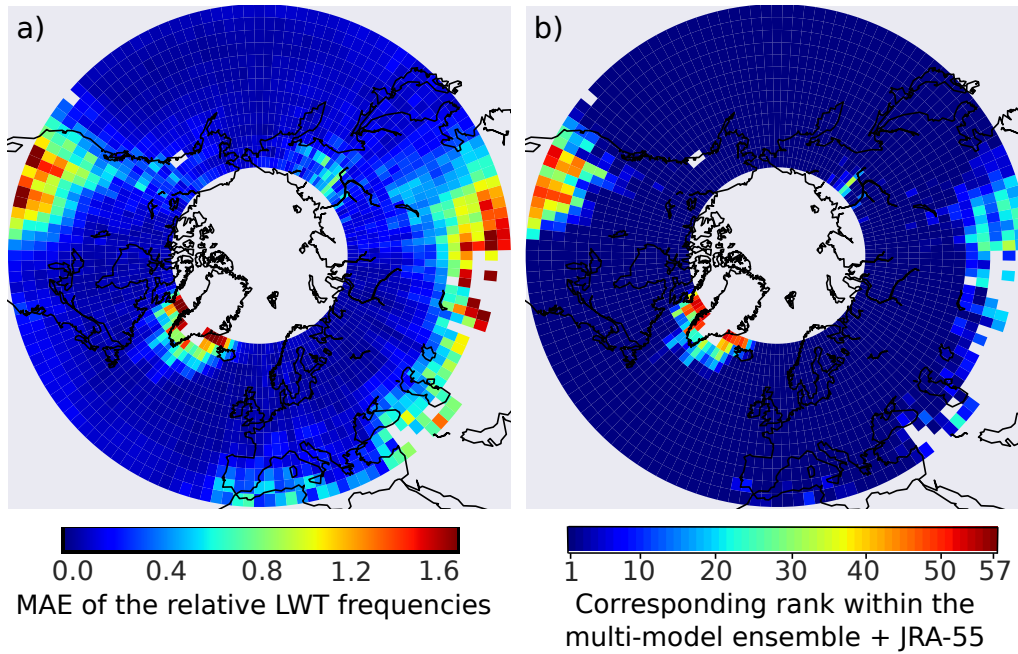


Figure 2. Mean Absolute Error of the relative Lamb weather type frequencies from JRA-55 w.r.t. to ERA-Interim (a), as well as the respective rank within the multi-model ensemble plus JRA-55 (b). The lower the rank, the lower the MAE and the closer the agreement between JRA-55 and ERA-Interim.

Table 2. Rank correlation coefficients between the median MAE values of the 46–56 models and various resolution parameters of the atmosphere or/and ocean component models. A significant relationship is indicated by an asterisk ($\alpha = 0.01$, two-tailed t-test, $H_0 =$ zero correlation). See text for more details.

Realm	Zonal	Meridional	Vertical	2D	3D
atmosphere	<u>-0.63-0.70*</u>	<u>-0.65-0.70*</u>	<u>-0.21-0.35*</u>	<u>-0.64-0.72*</u>	<u>-0.65-0.72*</u>
ocean	-	-	<u>-0.38-0.49*</u>	<u>-0.39-0.46*</u>	<u>-0.45-0.55*</u>
atmosphere + ocean	-	-	-	-	<u>-0.55-0.65*</u>

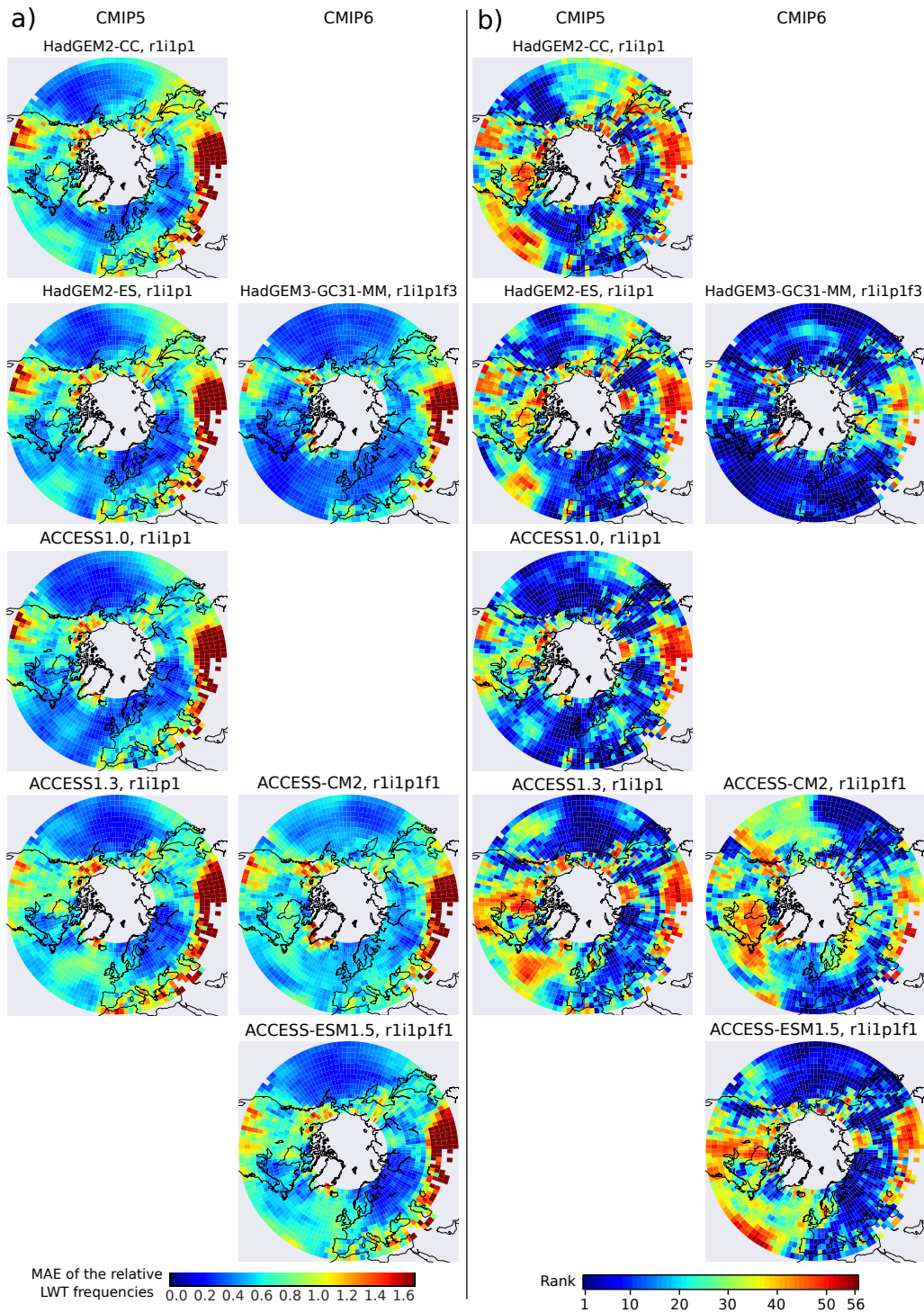


Figure 3. Mean Absolute Error of the relative Lamb weather type frequencies from the historical CMIP experiments w.r.t. to ERA-Interim (column a), as well as the respective rank within the 46-56 distinct model versions outlined in Table 1 (column b). The lower the rank, the lower the MAE and the better the model. Results are for the *Met Office Hadley Centre* and *ACCESS* model families. Model pairs from CMIP5 and 6 are plotted next to each other. Results are for the 1979-2005 period.

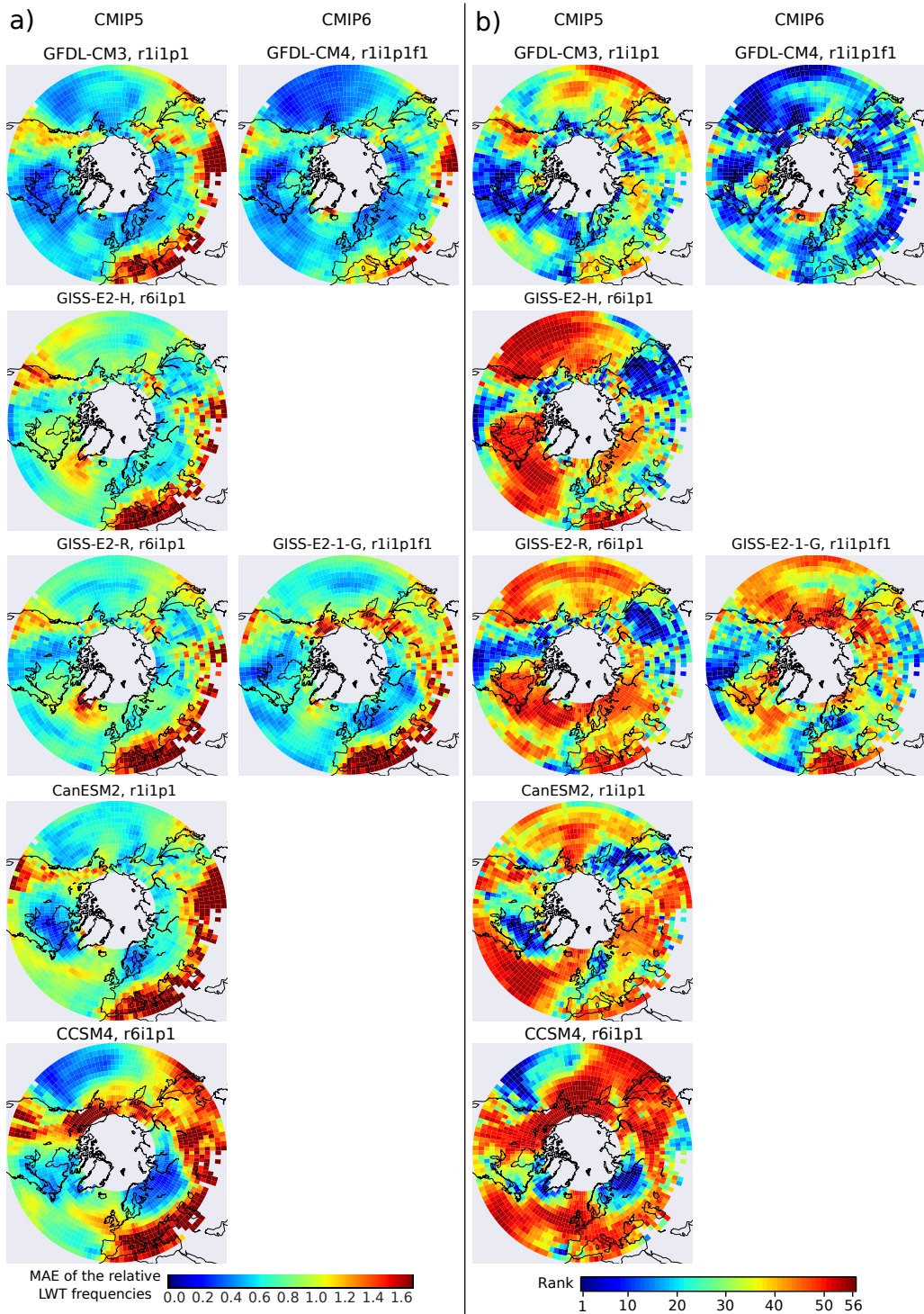


Figure 4. As Figure 23, but for the GFDL, GISS, CCCma and NCAR models.

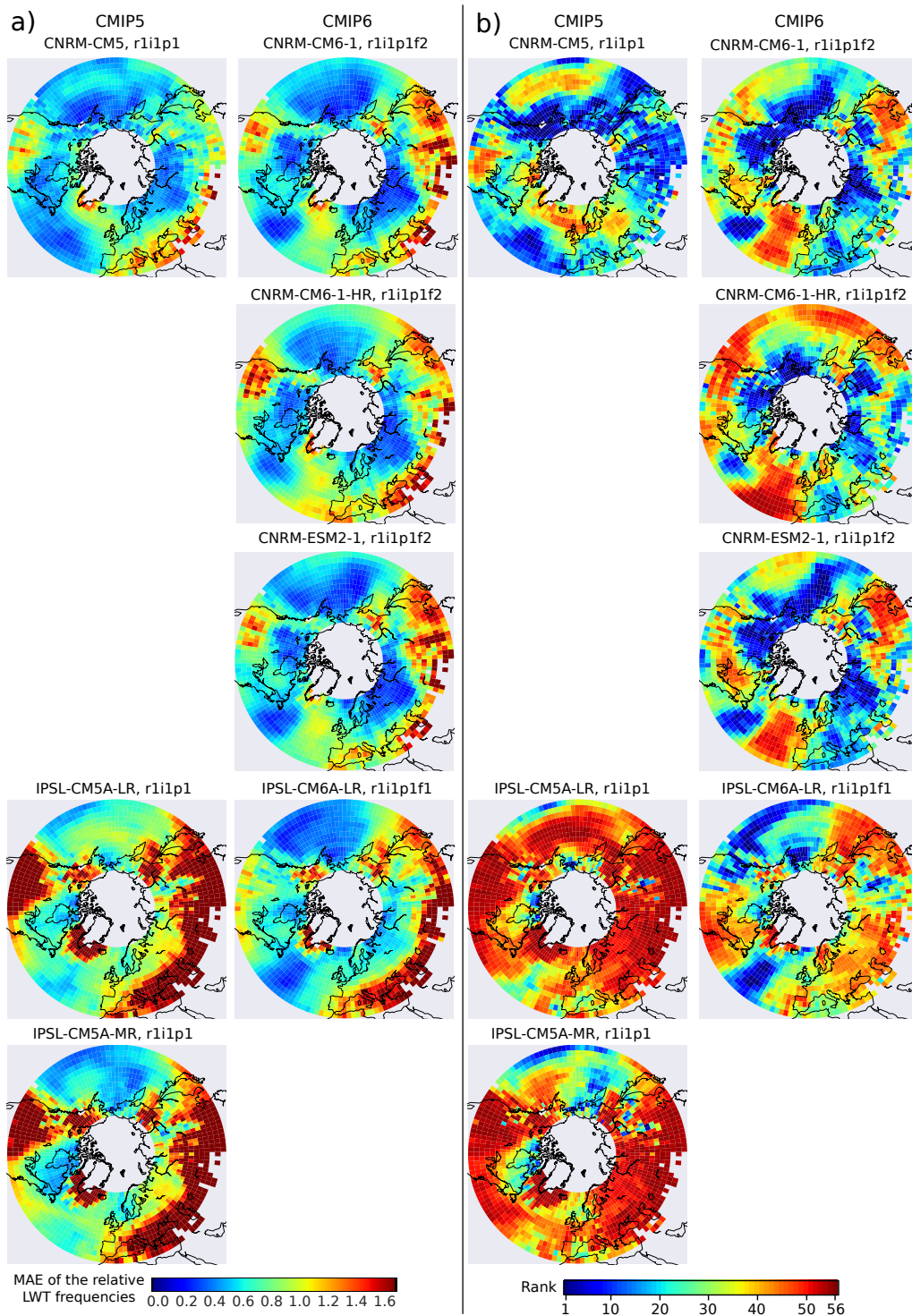


Figure 5. As Figure 23, but for the CNRM and IPSL models

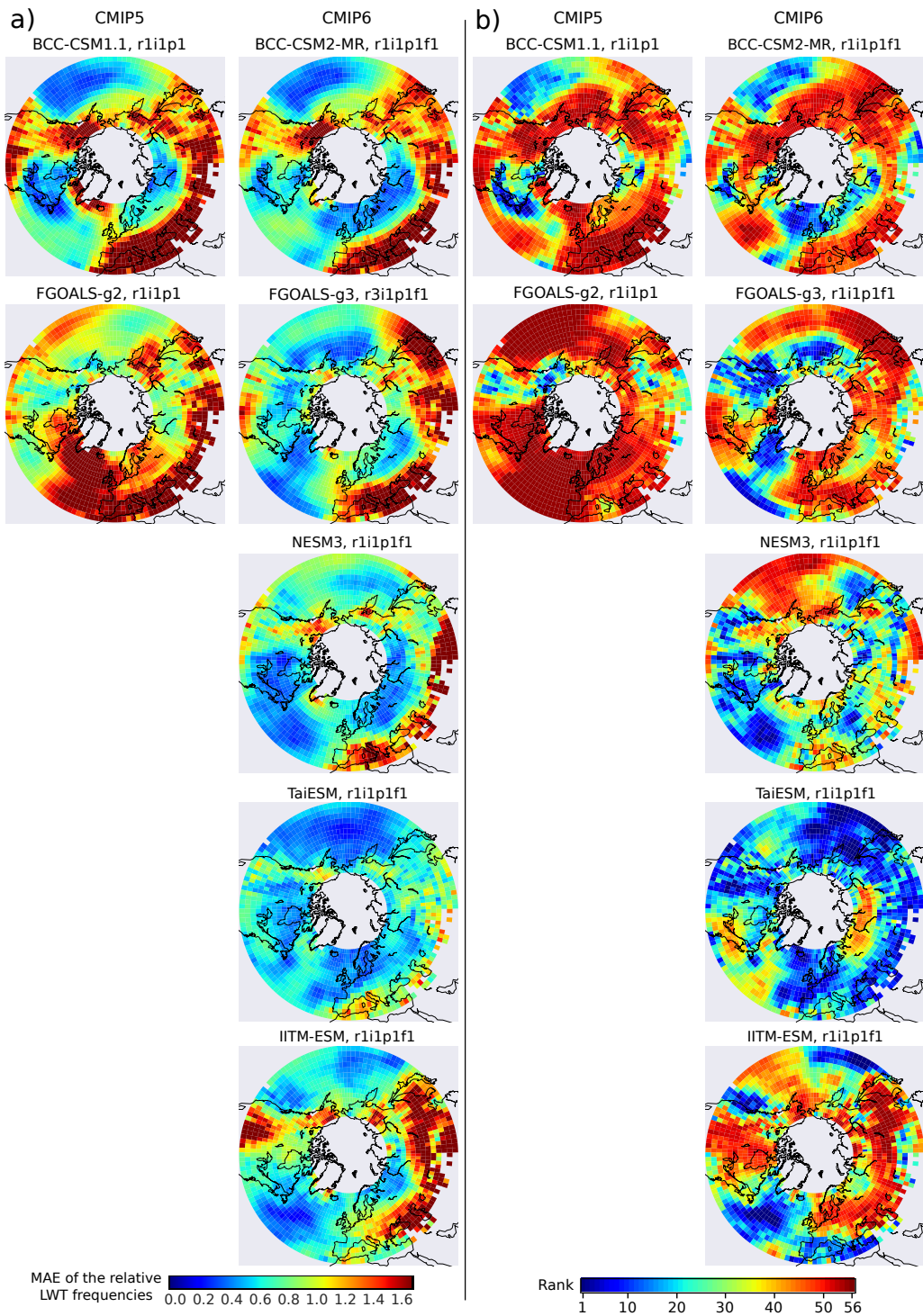


Figure 6. As Figure 23, but for the BCCR and FGOALS models, NESM as well as for NESM3, TaiESM and IITM-ESM

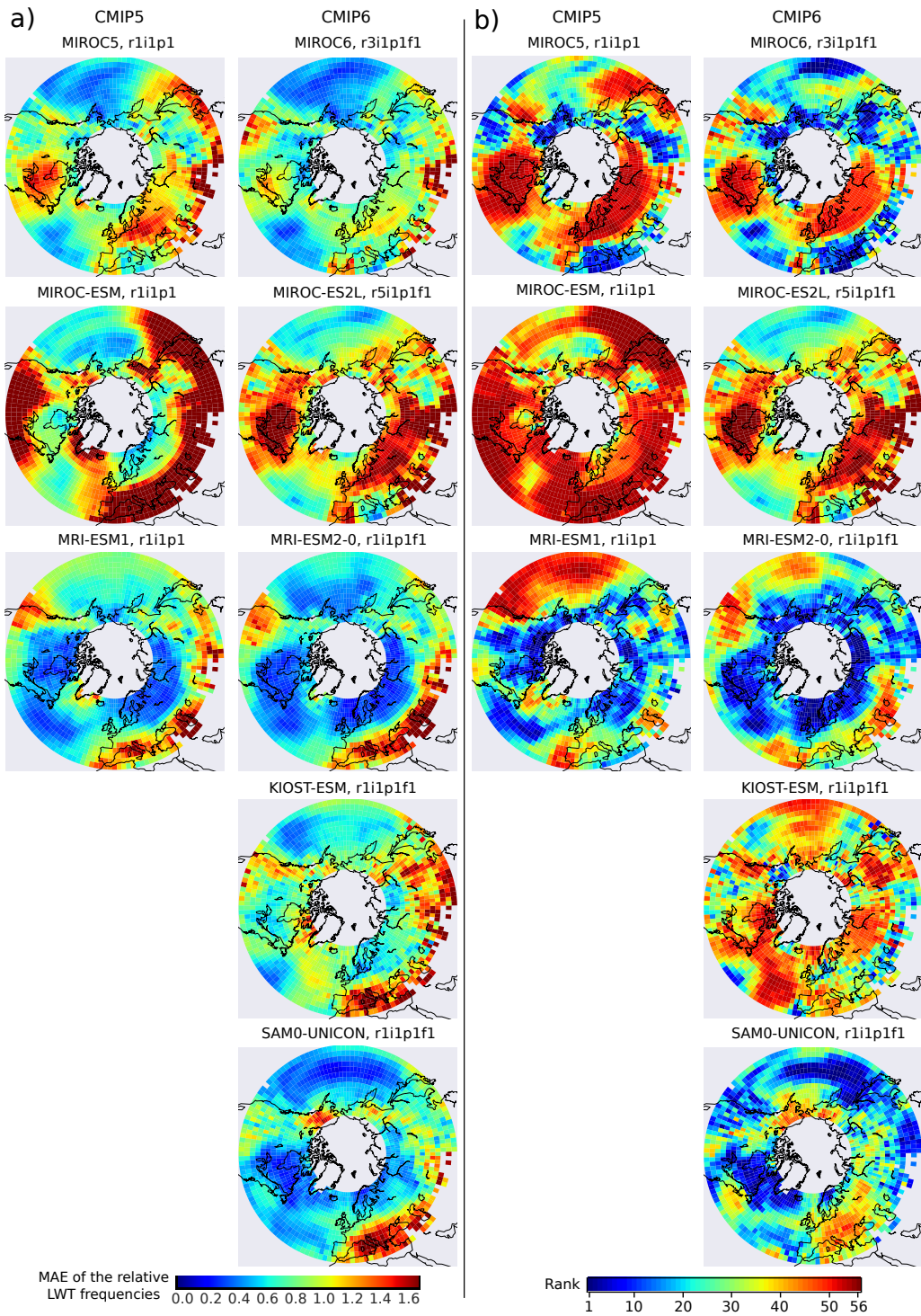


Figure 7. As Figure 3, but for the MIROC and MRI models, as well as KIOST-ESM and SAM0-UNICON.

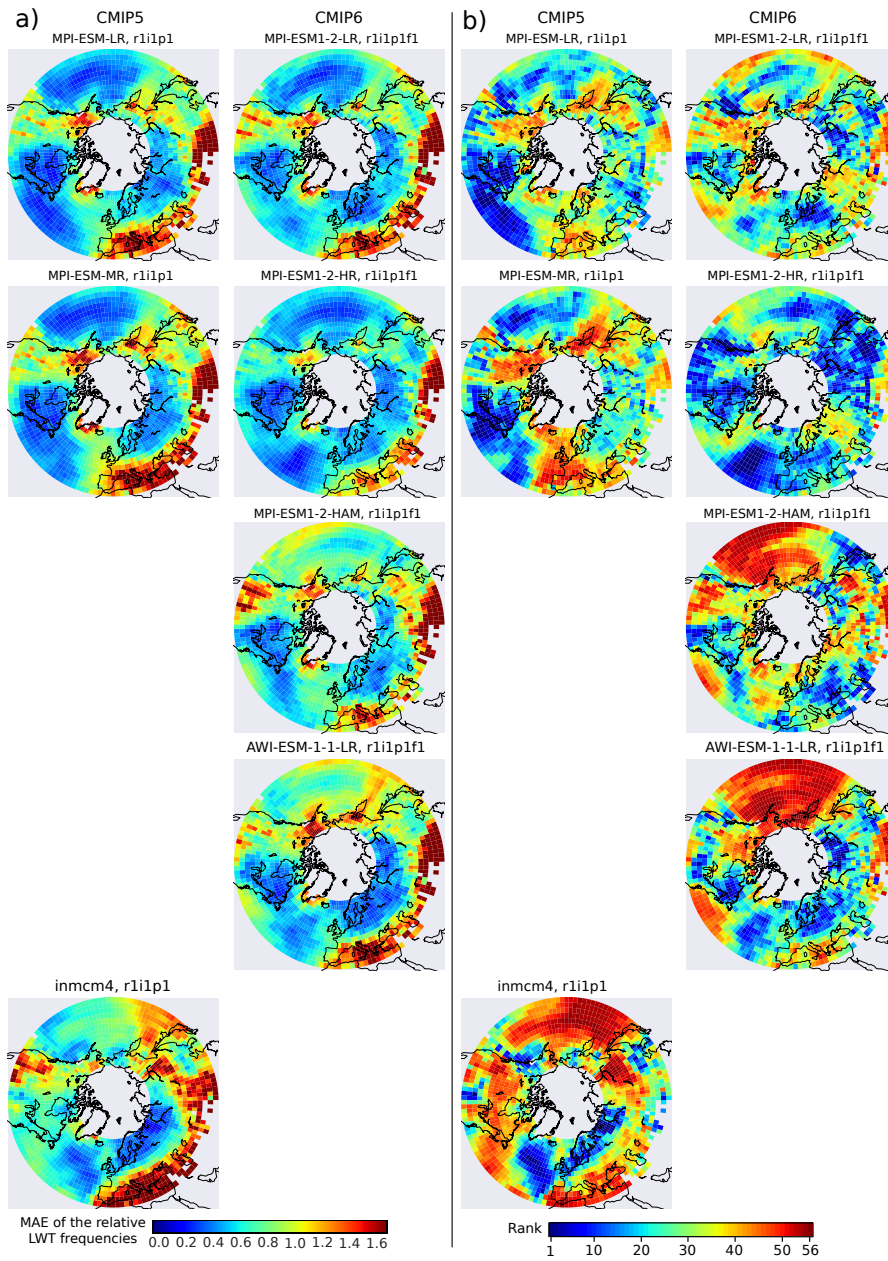


Figure 8. As Figure 23, but for the MPI, AWI and CMCC-INM models

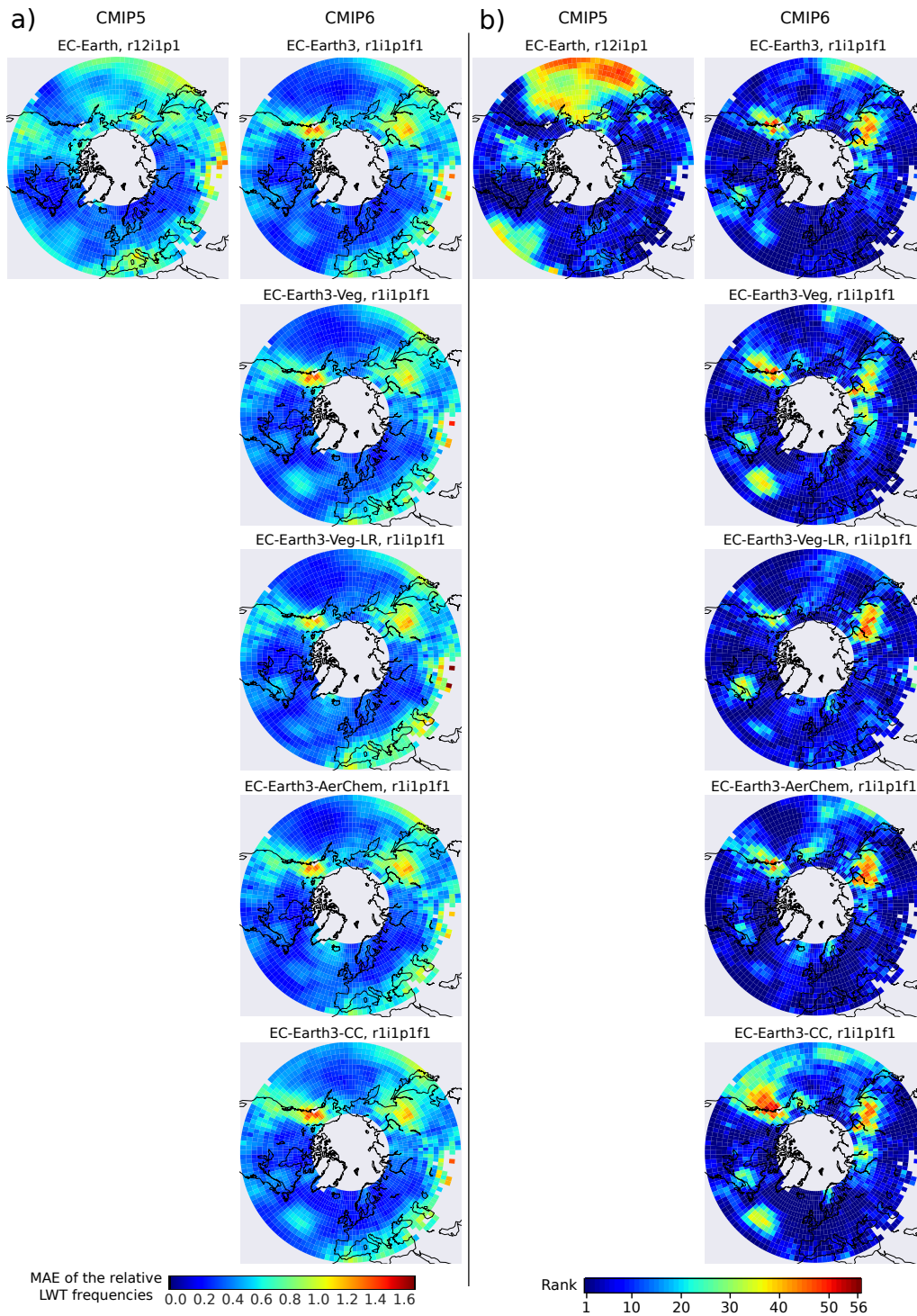
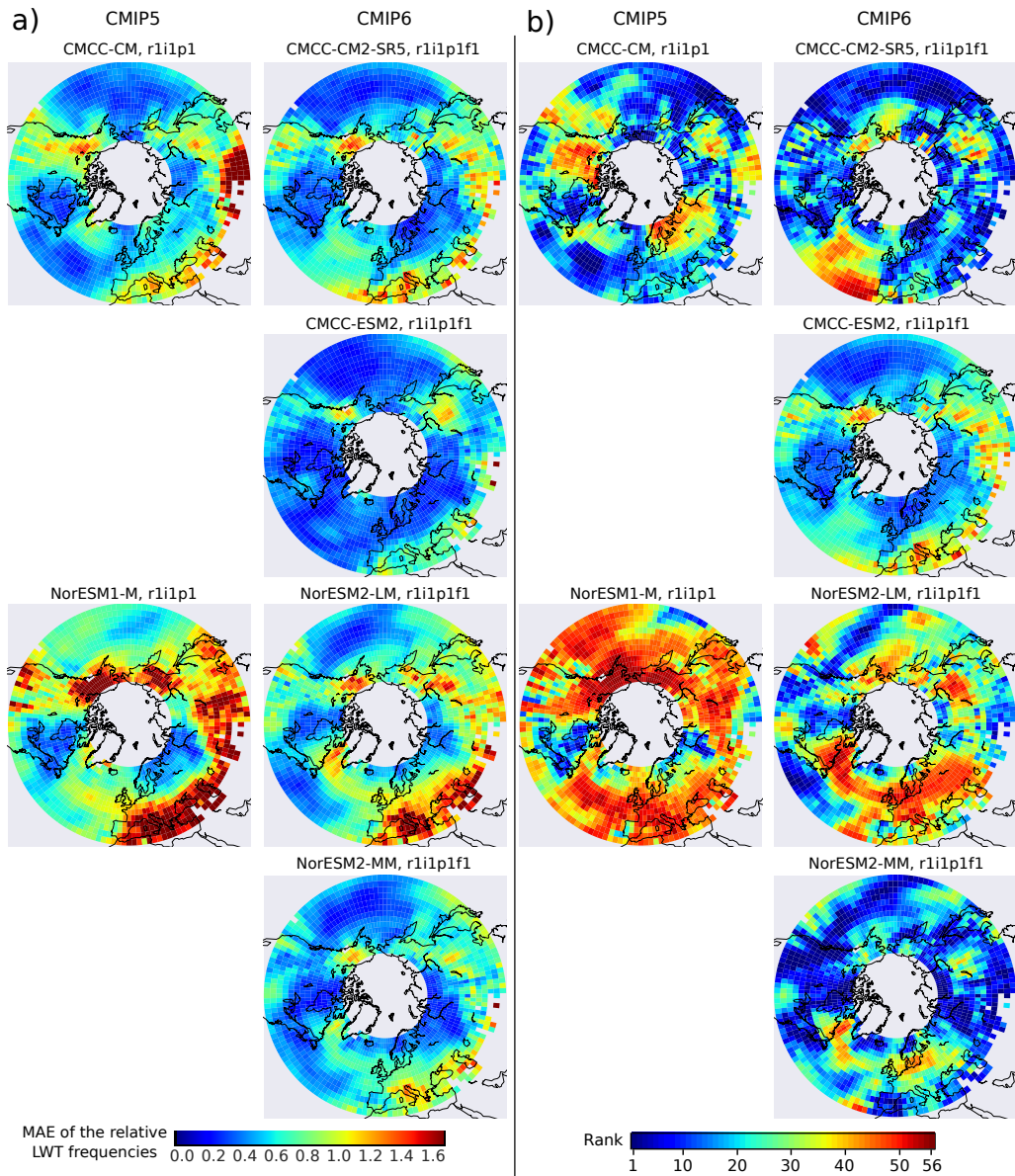


Figure 9. As Figure 23, but for the EC-Earth and NorESM models



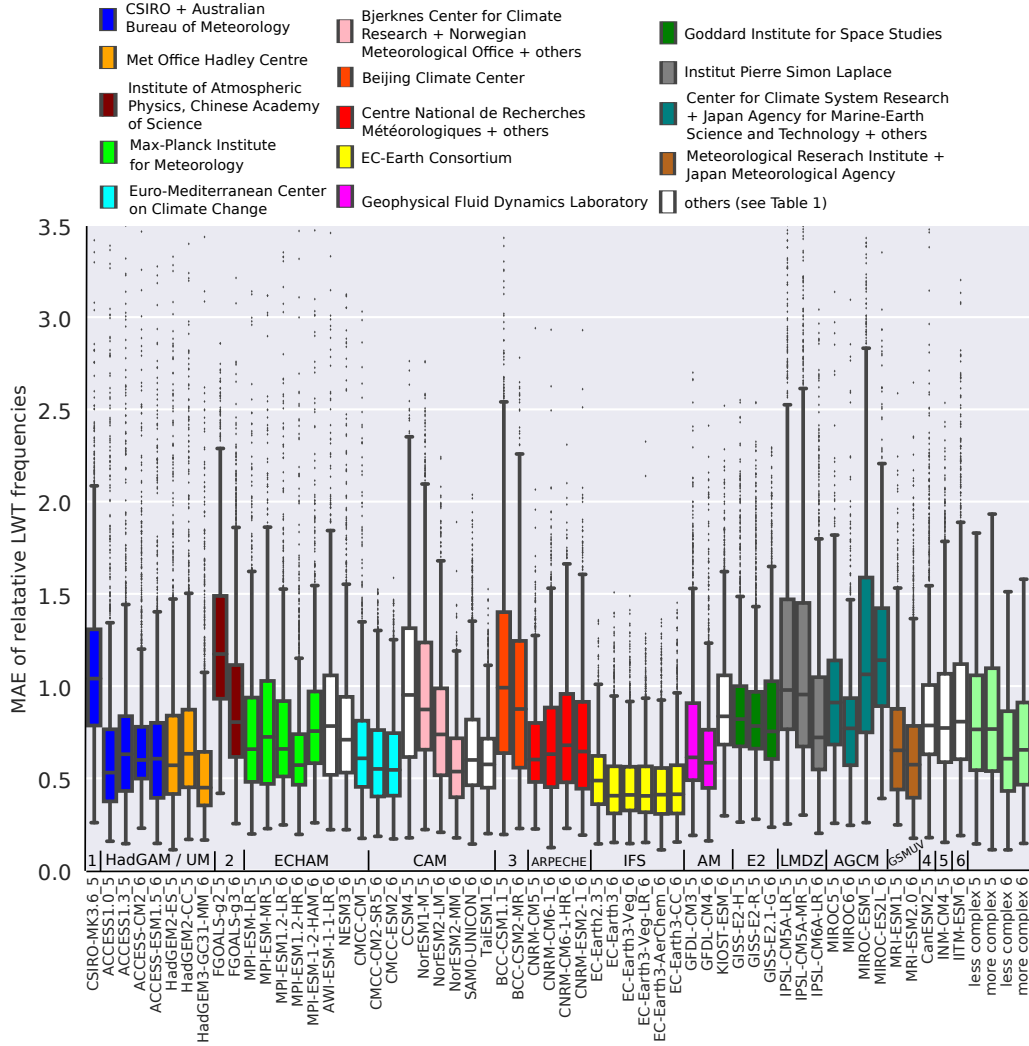


Figure 11. Summary model performance plot based on the MAE. For each model version listed in Table 1 the distribution of the pointwise MAE values is drawn with a boxplot instead of using a map (see text for details). Additional four additional boxplots are provided for 1) all CMIP5 model versions, 2) all CMIP6 the less and the more complex model versions 3) all Earth System Models (ESMs) used in CMIP5 and 4) the remaining models 6, respectively (AOGCM see text for details). Colours are assigned to the distinct coordinating research institutes, as indicated in the legend. The acronyms of the coupled models, as well as their participation in either CMIP5 or 6 (indicated by the final integer) are shown below the x-axis. Above the x-axis, the atmospheric component of each coupled model is shown in addition. Results are for the 1979-2005 period. AGCM abbreviations along the x-axis are as defined as follows: 1) MK3 AGCM, 2) GAMIL, 3) BCC-AGCM, 4) CanAM4, 5) unnamed and 6) IITM-GFSv1; the names of the remaining AGCMs are indicated in the figure.

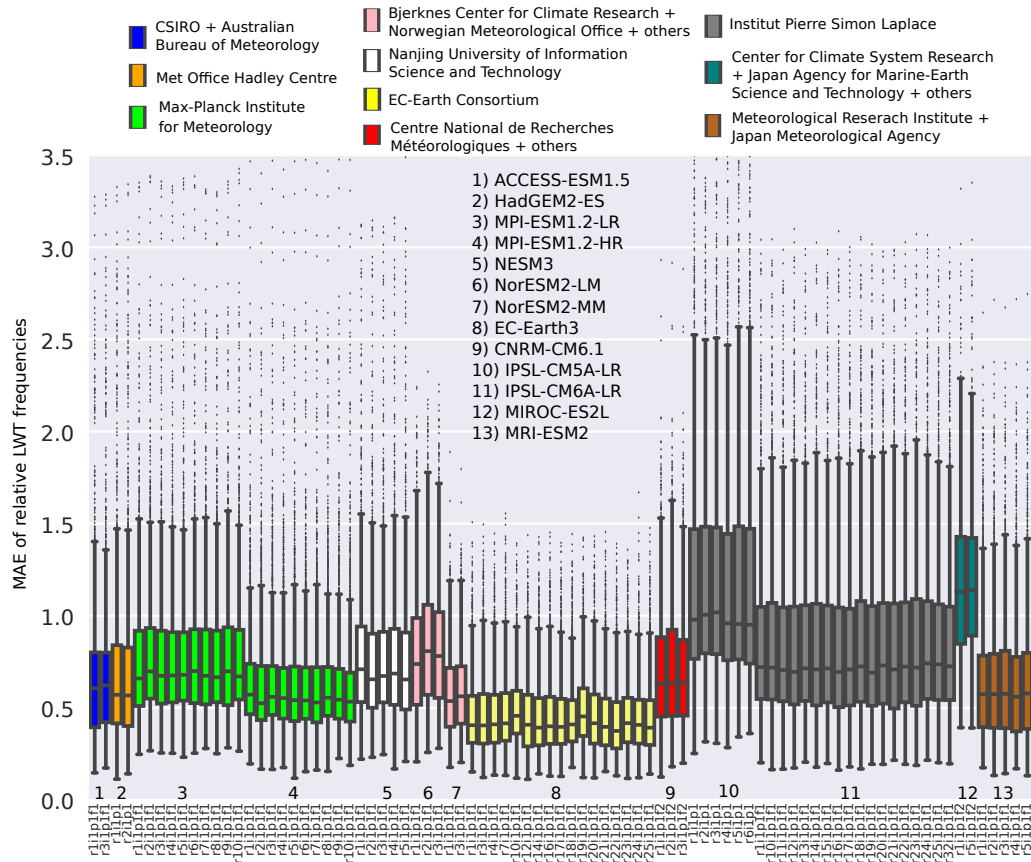


Figure 12. As Figure 10, but considering ~~70-72~~ additional runs for a subset of ~~12-13~~ distinct coupled models. All available runs per model are taken into account, except for IPSL-CM6A-LR for which the analyses were stopped after considering 17 additional ensemble members. Colours indicating the coordinating research institute are identical to Figure 9, except for the *Nanjing University of Information Science and Technology* painted white. Up to 2 ensembles per institute are shown and the acronyms of the individual coupled models are indicated by numbers. The exact run specifications are provided along the x-axis.

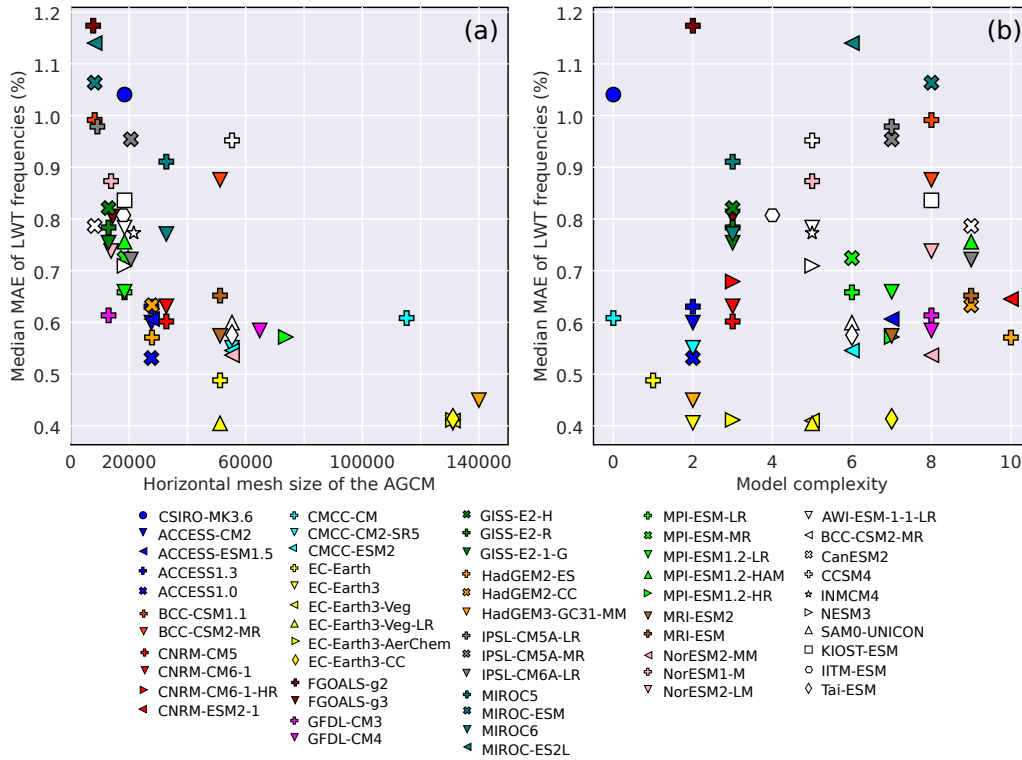


Figure 13. (a) Relationship between the horizontal mesh size of the atmospheric model component and the median model performance of the coupled configuration; (b) Two dimensional summary plot showing the complexity of the coupled model configuration vs. the median model performance. Model performance is w.r.t. ERA-Interim

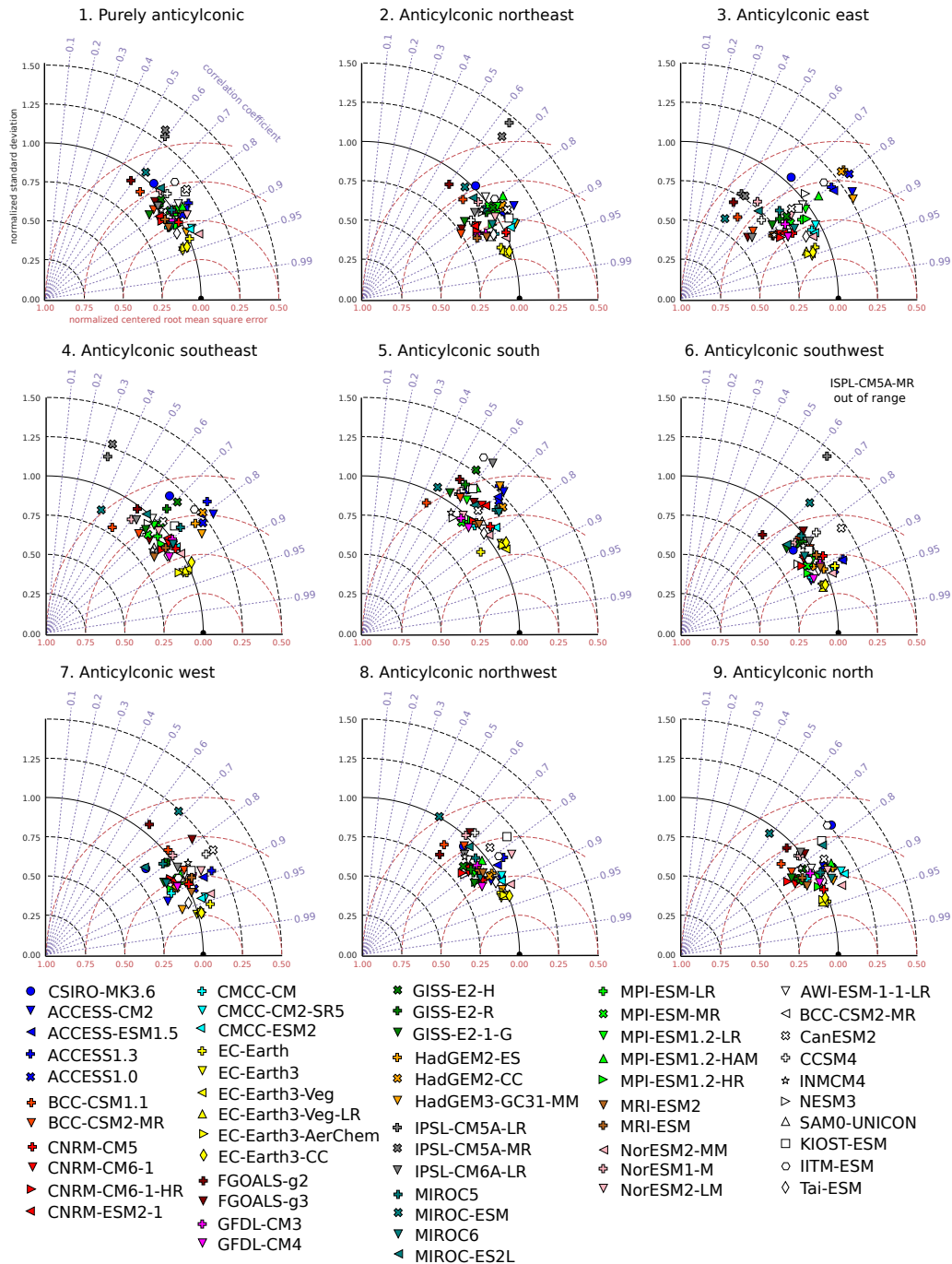
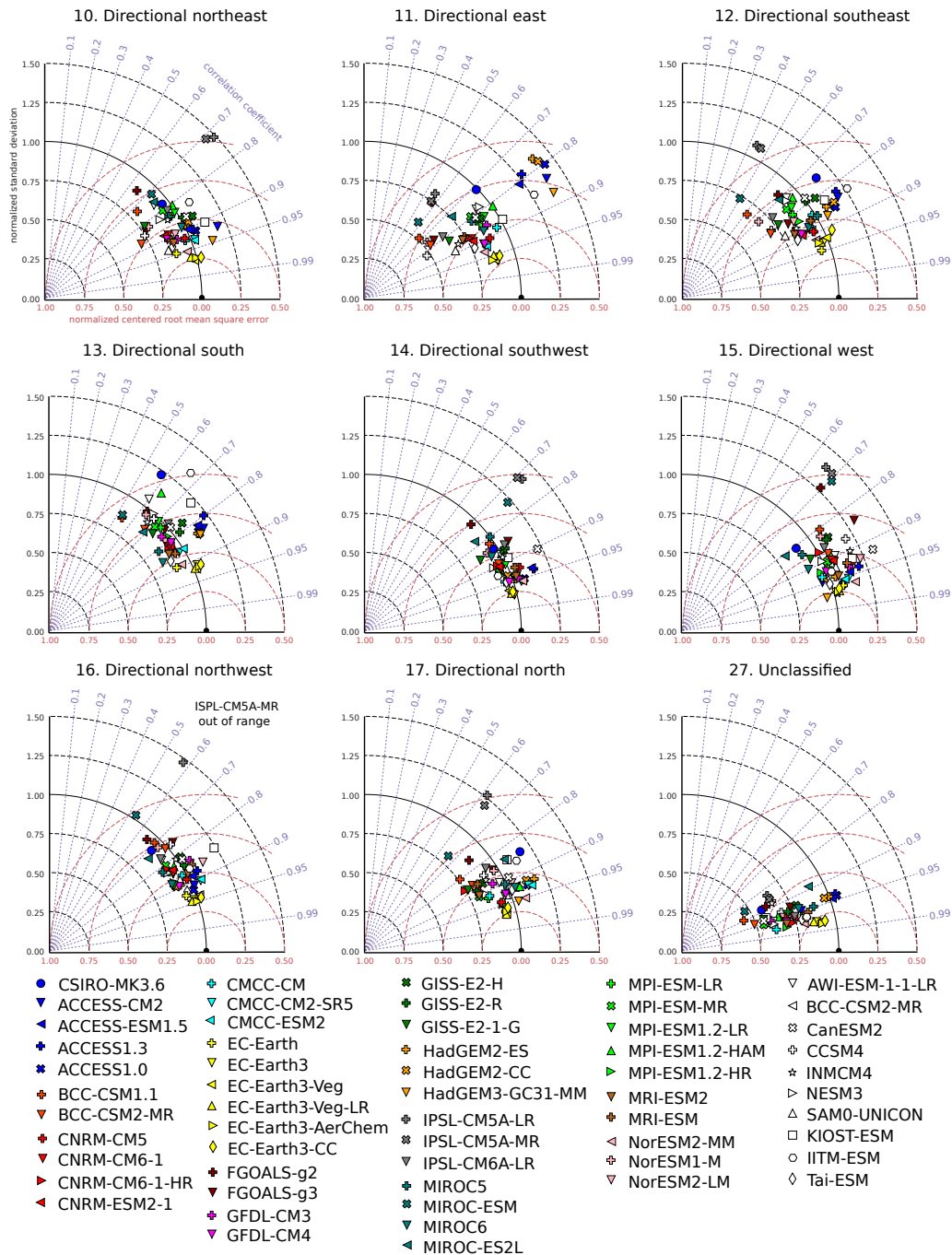
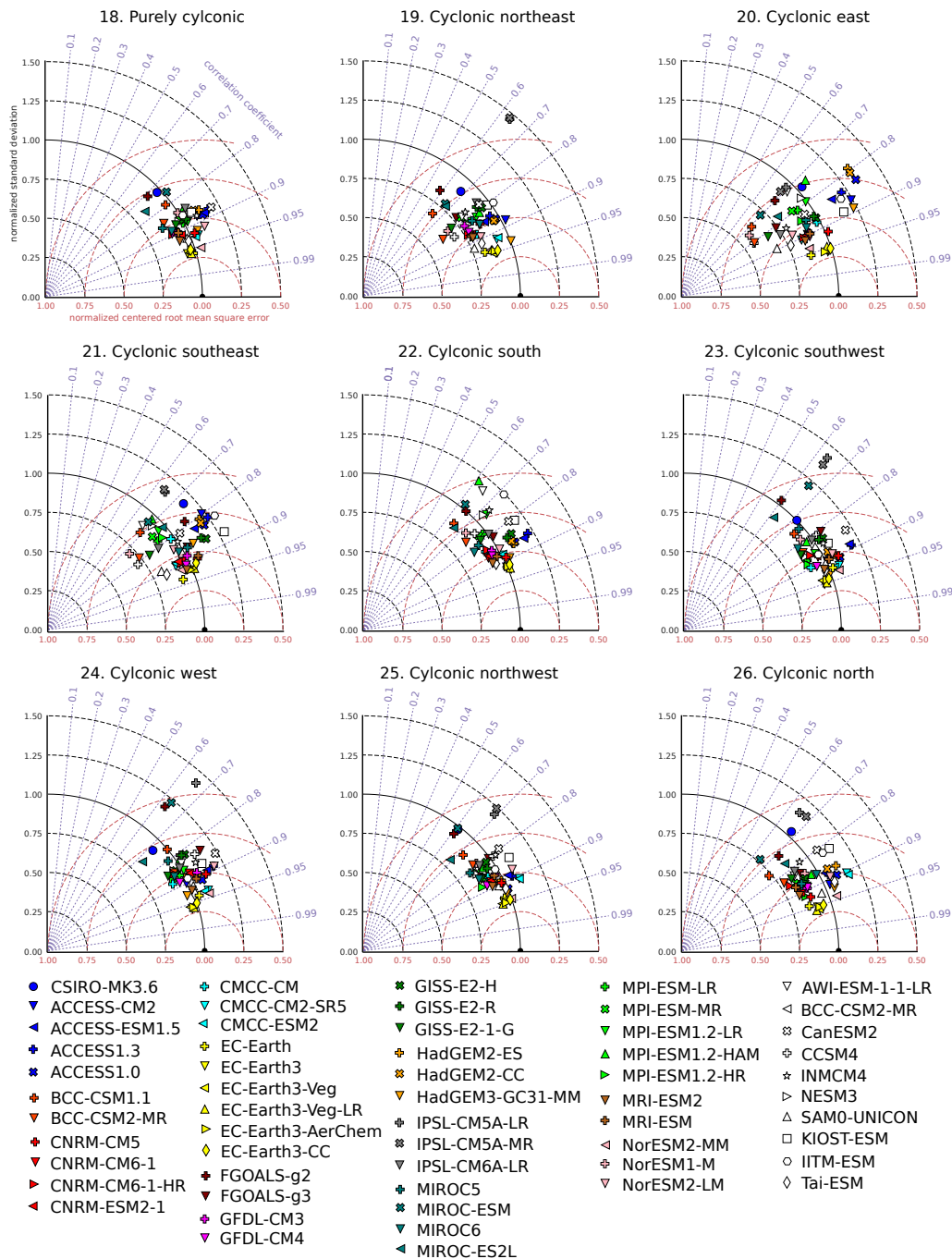


Figure 14. Normalized Taylor diagram for the simulated vs. quasi-observed (from ERA-Interim) hemispheric-wide frequency pattern of a given Lamb weather type. Each panel corresponds to a specific LWT and each of the 46-56 considered models can be identified by a specific marker and colour, as indicated in the legend. Models pertaining to the same coordinating institution have the same colour. Shown are the results for the 9 *anticyclonic* Lamb weather types.



As Figure 11, but for the 8 purely directional Lamb weather types and the unclassified type.

Figure 15. As Figure 14, but for the 8 purely directional Lamb weather types and the unclassified type.



As Figure 11, but for the 9 cyclonic Lamb weather types.

Figure 16. As Figure 14, but for the 9 cyclonic Lamb weather types.